

# Surface Chemistry Study of Low Salinity Waterflood

Jeelaja Kaliyugarasan

Master thesis  
Petroleum Technology – Reservoir Chemistry



Centre for Integrated Petroleum Research (Uni CIPR)

Department of Chemistry

University of Bergen, June 2013

## **Acknowledgement**

All experiments in this thesis have been performed at Centre for Integrated Petroleum Research (Uni CIPR).

I would like to thank my supervisor Professor Arne Skauge for his support, advice and assistance throughout this work.

I would like to thank Edin Alagic, Sverre Hetland and Tore Skodvin for their assistance and advice at the laboratory during the experimental work and Jonas Solbakken for his advice during the writing process.

Thanks to all my co-students and friends at CIPR, especially Elise Kvåle Perttamo, Ragnhild Østensen, Nikou Fazel and Hanne Halstensrud for their support and encouragement.

Last, but not least, I would like to thank my dearest husband Sanjeevan Shanmuganathan, parents Jayanthi Kaliyugarasan and Kaliyugarasan Thirunavukkarasu, brothers Thinesh Kaliyugarasan and Sathiesh Kaliyugarasan and my best friend Tanja Kolnes Snåre for their support, encouragement and trust on me throughout this work.

The simple word **Thank You...** cannot describe how thankful I am for every one of you.

## **Abstract**

There is increasing evidence that injecting low salinity brines has a significant impact on the amount of oil recovered, but the exact mechanism by which this occurs is an unsettled issue, and is supposed to be a cause of the complex interactions occurring between the phases in-situ.

In this thesis, surface chemistry of low salinity brines has been investigated. Fluid/solid and fluid/fluid interactions for two North Sea crude oils in the presence of high salinity brine and a set of dilutions of this have been studied and compared.

Fluid/solid interactions were investigated through wettability studies. Impact of ionic strength, pH and zeta potential on this interaction was measured through contact angle measurements and adhesion test. Microscopic glass slides made of quartz were used to simulate water-wet sandstone.

Fluid/fluid interactions were studied by interfacial tension measurements between crude oils and brines using the drop-volume method.

Further, one of the crudes was mixed with organic liquids to study the impact of these chemicals on crude oil properties.

The main findings from this study showed that crude oil and brine composition to be of major importance for the observed trends. One of the crudes was more sensitive to reduction in brine salinity than the other, and showed more water-wet behaviour with reduction in salinity.

Adhesion mapping and zeta potential measurement showed that a combination of low salinity and low pH brines will make it easier to alter the wettability to more oil-wet.

The most favourable interfacial tension was obtained with high salinity brine and interfacial activity dominated by ionized acidic species.

The combined impact of the organic liquids did not change the crude oil property significantly.

## Symbols and Abbreviations

$\rho$	Density (g/cm <sup>3</sup> )
$\sigma$	Interfacial tension (mN/m)
$\theta$	Contact angle measured through water phase (°Degrees)
$\theta_E$	Equilibrium contact angle (°Degrees)
$\theta_a$	Water advancing contact angle (°Degrees)
$\theta_r$	Water receding contact angle (°Degrees)
pH	$-\log_{10} [\text{H}_3\text{O}^+]$
$\mu$	Viscosity (Pa.s)
$P_c$	Capillary pressure (Psi)
$P_o$	Oil pressure (Psi)
$P_w$	Water pressure (Psi)
$p_{c_{\text{cri}}}$	Critical Capillary pressure (Psi)
$\Pi$	Disjoining pressure (Pa)
$\psi_o$	Electric potential (mV)
$\kappa^{-1}$	Debye length (m)
$K_a$	Acid – Dissociation constant
$K_b$	Base – Dissociation constant
$K_w$	Water Dissociation constant ( $1 \times 10^{-14}$ )
$pK_a$	$-\log_{10} K_a$
$\zeta$	Zeta potential (mV)
$I$	Ionic strength ( mol/l )

$z$	Ion valence
$c$	Concentration ( mol/l )
$m$	Mass of fluid (g)
$V$	Volume (cm <sup>3</sup> )
$g$	Gravity (m/s <sup>2</sup> )
$r$	Radius of the inverted needle (m)
$F$	Empirical correlation coefficient (dimensionless)
$U_E$	Electrophoretic mobility (μmcm/Vs)
$\epsilon$	Dielectric constant
$A$	Apparatus constant
$T$	Period
$P$	Air pressure (mmHg)
$F$	Air humidity in (%)
$T$	Temperature (°C or K)

CAG	Contact angle goniometer
CEC	Cation exchange capacity
CF	Capillary force
COBR	Crude oil/brine/rock
DLVO	Derjaguin, Landau, Verrvey, Overbeek
EOR	Enhanced oil recovery
EL-A	Electrostatic attraction
EL-R	Electrostatic repulsion
FW	Fractional-wet
GF	Gravity force
HC	Hydrocarbon
HS	High salinity
HSW	High salinity water
IEP	Isoelectric point
IFT	Interfacial tension
ISFET	Ion sensitive field effect transistor
ISG	Ionizable site group
LS	Low salinity
LSW	Low salinity water
LSE	Low salinity effect
MIE	Multicomponent ionic exchange
MWL	Mixed-wet large
MWL	Mixed-wet small
NSO atoms	Nitrogen, Oxygen and Sulphur atoms
OOIP	Original oil in place
ppm	Parts per million

PZC	Point of zero charge
SARA	Saturates, Aromatics, Resins and Asphaltenes
SCAL	Special core analysis data
SSW	Synthetic sea water
Sor	Residual oil saturation
ST	Surface tension
SWCTT	Single well chemical tracer test
TDS	Total dissolved solid
USBM	U.S.Bureau of Mines
VF	Viscous force
WW	Water-wet

## TABLE OF CONTENT

<b>Acknowledgement</b> .....	<b>i</b>
<b>Abstract</b> .....	<b>ii</b>
<b>Symbols and Abbreviations</b> .....	<b>iii</b>
<b>1. Introduction</b> .....	<b>1</b>
<b>2. Wettability</b> .....	<b>6</b>
<b>2.1. Introduction Wettability</b> .....	<b>6</b>
<b>2.2. Measurement Methods and Wettability Classes</b> .....	<b>7</b>
<b>2.3. Contact Angle Hysteresis</b> .....	<b>8</b>
<b>3. Low Salinity Water (LSW)</b> .....	<b>11</b>
<b>3.1. Lab Scale and Field Scale LSW Recovery Data</b> .....	<b>11</b>
<b>3.2. Proposed Low Salinity Mechanisms</b> .....	<b>13</b>
3.2.1. Fines Migration .....	14
3.2.2. pH Effects .....	15
3.2.3. Multicomponent Ionic Exchange (MIE) .....	17
3.2.4. Double Layer Expansion .....	20
3.2.5. Wettability Alteration .....	20
<b>4. Fluids/Solid Impact on Wettability Alteration</b> .....	<b>24</b>
<b>4.1. Four Identified Mechanisms by which Wetting can be Altered</b> .....	<b>24</b>
<b>4.2. The Oil Phase</b> .....	<b>26</b>
4.2.1. Crude Oil Composition .....	28
4.2.2. Polar Organic Compounds in Crude Oil .....	29
4.2.3. Acid/Base Properties of Crude Oil Components .....	30



4.2.4. Physical Adsorption through Weak Polar Interactions and Precipitation of Asphaltenes .....	30
<b>4.3. The Brine Phase .....</b>	<b>32</b>
4.3.1. Acid/Base Reactions at Crude Oil/Brine Interface .....	33
4.3.2. Interaction with Divalent/Multivalent Ions present in the Brine Phase .....	35
<b>4.4. The Solid Phase .....</b>	<b>36</b>
<b>5. Fundamental Surface Forces .....</b>	<b>38</b>
<b>5.1. The Stability of the Water-film .....</b>	<b>38</b>
<b>5.2. Disjoining Pressure – Contribution Forces .....</b>	<b>39</b>
5.2.1. Van der Waal Interactions .....	39
5.2.2. Electrostatic Interactions between Electrical Double Layers .....	40
5.2.3. Structural Forces .....	41
5.2.4. Schematic Illustration of Disjoining Pressure – Summary of Force Contribution .....	42
<b>5.3. Zeta Potential Measurement .....</b>	<b>43</b>
<b>5.4. Adhesion .....</b>	<b>48</b>
5.4.1. Adhesion Test .....	48
5.4.2. Relationship between Adhesion/non-Adhesion and Contact Angles .....	51
5.4.3. Adhesion in Mixed Brine .....	51
<b>5.5. Oil/Water Interfacial Tension .....</b>	<b>52</b>
5.5.1. Salinity Effect on IFT .....	54
<b>6. Experimental Work .....</b>	<b>58</b>
<b>6.1. Fluids, Solid and Chemicals .....</b>	<b>58</b>
6.1.1. Crude Oils .....	58
6.1.2. Brines .....	60

6.1.3. Solid .....	61
6.1.4. Chemicals for pH Adjustment .....	62
6.1.5. Chemicals for Washing Procedures of Equipment .....	62
<b>6.2. Experimental Apparatus, Equipment and Procedures .....</b>	<b>63</b>
6.2.1. IFT Measurements-Drop-Volume Method .....	63
6.2.2. Contact Angle Measurements – Sessile Drop Method .....	67
6.2.3. Adhesion Test by using Sessile Drop Method .....	70
6.2.4. Measurement of Electrophoretic Mobility (Zeta Potential) – Zetasizer .....	72
6.2.5. pH Meter .....	77
6.2.6. Digital Temperature Meter .....	78
6.2.7. Digital Density Meter .....	79
<b>7. Main Results and Discussion .....</b>	<b>82</b>
<b>7.1. Contact Angel Measurement .....</b>	<b>82</b>
7.1.1. Contact Angle for Crude Oils, A-12, Exp-12 and Exp-12-D .....	84
7.1.2. Individual Impact of Xylene and Iododecane on Exp-12 Contact Angle .....	87
<b>7.2. Adhesion Test .....</b>	<b>89</b>
<b>7.3. Zeta Potential .....</b>	<b>96</b>
7.3.1. Adhesion Results Discussed based on Zeta Potential Results .....	99
<b>7.4. Interfacial tension (IFT) .....</b>	<b>105</b>
7.4.1. IFT – Crude Oils A-12, Exp-12 and Exp 12-D .....	105
7.4.2. Individual Impact of Xylene and Iododecane on Exp-12 IFT .....	108
7.4.3. IFT as Function of Brine Salinity with varying pH .....	110
<b>7.5. Wettability Results and Previous Studies .....</b>	<b>112</b>
<b>8. Conclusion .....</b>	<b>116</b>
<b>9. Further Work .....</b>	<b>118</b>

<b>10. References</b> .....	<b>119</b>
<b>Appendix</b> .....	<b>131</b>
A.1 Density Data .....	131
A.2 IFT Data .....	132
A.3 Zeta Potential Data .....	135
A.4 Contact Angle Data .....	138
A.5 pH Data .....	143

# 1 Introduction

Waterflooding is a secondary recovery method widely used for oil recovery from petroleum reservoirs, where the main purpose is to give pressure support to the reservoir and to displace the oil from the injector to the producer.<sup>[1]</sup> The efficiency of oil recovery by waterflooding and the amount of oil left behind in this recovery process is strongly dependent on the complex interaction between fluids/solid in-situ, and the balance of capillary, viscous and gravitational forces (CF, VF, GF), and whether each of these work for or against the displacement of oil toward the production well.<sup>[2]</sup>

CF acting in the interface region between oil and water are forces acting against the flow of oil in the displacement process, and the magnitude of the force is proportional to the interfacial tension (IFT) reflecting fluid/fluid interactions in-situ.

VF acting in the fluids can either stabilize or destabilize the interface between oil and water dependent on the viscosity,  $\mu$ , of the fluids. Destabilized interface results in fingering of the displacing fluid into the displaced fluid, which results in poor sweep efficiency.

GF does also lead to instability phenomena such as segregated flow and gravity fingering.

The stability of the flow under the influence of this force is dependent on the injection direction.<sup>[1]</sup>

For a typical waterflood the average oil recovery is close to fifty percent or less dependent on the in-situ interactions. This implies that after a secondary process a significant amount of oil remains in the reservoir, either as un-swept or as immobile oil.<sup>[1]</sup>

To improve and increase the oil recovery after a secondary process several enhanced oil recovery (EOR) methods have been developed, where the purpose of these tertiary recovery methods involves their influence in changing the impact of the viscous forces, fluid/fluid interactions (IFT) and fluid/solids interactions (wettability) in a way that is favourable for the recovery.<sup>[3]</sup>

A broad range of studies concerning the brine phase have shown that altering the chemistry of the injecting water contributes to improved and increased oil recovery, and have thus lead to development of several EOR methods concerning the brine phase.

One such attention has concerned reducing the salinity of the injecting water.

Conventional waterflood brines are aquifer water and sea water. Aquifer water salinity varies from fresh water to saline water with more than 300.000 parts per million (ppm) of total dissolved solids

(TDS), while sea water salinity is close to 35.000 ppm.<sup>[5]</sup> The reduced saline water salt concentration is typically in the range of 500 to 5000 ppm and no more than 6000 ppm.<sup>[4]</sup> This reduced salinity water is named low salinity water (LSW).

The first research works of low salinity brine effects on oil recovery dates back to Martin<sup>[6]</sup> in 1959 and Bernard in 1967.<sup>[7]</sup> After them the interest for LSW injection studies increased gradually but slowly. It was first from the late 1990's with the results of the study performed by Tang and Morrow<sup>[8]</sup> presenting increased oil recovery with only modest increase in resistance to flow, the interest for LSW recovery increased rapidly. A numerous of laboratory coreflood experiments with LSW conducted on outcrop and reservoir cores both in secondary and tertiary recovery modes have been performed. The investigations have mostly shown potential oil recovery, but also no LSW potential has been reported.<sup>[8, 9, 10, 11, 12, 30]</sup> Lab scale success has also provided field scale success in tertiary low saline field tests.<sup>[11, 13]</sup>

Although improve in oil recovery with LSW is proved, mechanisms behind the low salinity effect (LSE) have been debated in the literature for the last decade. Several mechanisms both physical and chemical mechanisms have been proposed, but none of the suggested mechanisms have been accepted as the primary mechanism of LSE, and might be result of the proposed mechanisms also have contradicting evidence. However, some mechanisms are more accepted than others, and for the most accepted proposed mechanisms found in the literature, wettability is considered as a key factor in achieving potential LSE. <sup>[ 8, 9, 11, 30, 34, 37]</sup>

The traditional scenario of the reservoir development is an initial 100% water-wet reservoir rock. Then with migration/accumulation process of oil from source rock to reservoir rock, wettability alteration might has occurred due to adsorption and deposition of organic material from the oil, as a result of the interactions occurring between the phases over geological time.<sup>[2, 14]</sup>

This is the general explanation for classification of most sandstone reservoirs as neither strongly oil-wet nor strongly water-wet, but rather falls into the classes of intermediate-wet state.<sup>[15]</sup>

One of the first publications concerning mixed-wettability to exist in reservoirs was the study performed by Salathiel.<sup>[16]</sup> He described mixed wettability as a system that developed when some pores became oil-wet, and suggested the wettability alteration occurred where the water-film thickness between crude oil and rock surface was minimal. According to the proposed low salinity (LS) mechanisms, further wettability alteration from this mixed-wet state toward more water-wet state during the course of LSW is the suggested cause of increased oil recovery. Thus, for these

proposed mechanisms establishing weakly oil-wet to intermediate-wet conditions is a necessary condition for LSE. Most of the proposed LS mechanisms are based on hypothesis regarding mechanisms happening in a core, and have concluded wettability alteration toward more water-wet state based on imbibition tests and waterfloods that are more characterised as wettability indicators, and are thereby very weak evidence to confirm wettability shift. But wettability alteration toward more water-wet state has also been proved with the most accepted wettability measurement methods that exist.<sup>[37, 60]</sup>

Adhesion test is a simple test developed by Buckley et al.<sup>[17]</sup> to study the water-film stability bounded by the interface of oil/water and water/solid. Whether or not the thin brine film (1-100 nm) ruptures or not is determined by disjoining pressure, a force per unit area acting in the water-film.<sup>[2, 17, 18]</sup> This test shows generally an opposite wettability trend with more water-wet state at high salinity (HS) regions and more oil-wet state at LS regions.

A combined study of electrokinetic charges at crude oil/brine interface, contact angle measurement and adhesion test will provide an explanation for the observed wettability trends. Such static LSW studies prior to LSW dynamic coreflood experiments will also provide useful knowledge and contribute to a better understanding of the observed results. Publications concerning both static LSW and dynamic LSW coreflood studies can be found in the literature, but compared with coreflood studies there are fewer publications concerning static studies. (Static studies can include dynamic measurement methods) Thus, this work has been performed to be an additional contribution to more static LSW data.

Crude oil/brine/rock (COBR) interaction studies are complicated due to the complex interactions occurring between the phases. The interactions are strongly dependent on the individual composition of the phases interacting with each other.<sup>[2]</sup> The role of brine phase is of major importance in this interaction due to the fact that crude oil/brine and mineral/brine interfaces are electrically charged in presence of water.<sup>[2, 12]</sup> The magnitude of the electrical interaction between crude oil and rock are in addition to brine composition function of their own compositions.

The electrostatic forces acting between the interfaces are one of the main contribution forces for disjoining pressure.<sup>[18]</sup> Zeta potential measurement of emulsified crude oil droplets in brines of different compositions, and zeta potential measurements of suspended particles of the solid phase representing the reservoir rock in brines of different compositions, demonstrates the net surface

charge distribution at the surfaces of crude oil and rock.<sup>[2, 60, 61]</sup> This kind of measurements contribute to strength the observed wettability results. In this study, zeta potential measurements were only performed for crude oil/brine system, but based on literature reported zeta potential data for quartz in brines containing monovalent ions, hypothetical values for quartz in presence of brine containing divalent ions have been used to explain the observed wettability results with adhesion test.

In addition to zeta potential measurement that evidence the charging character of crude oil surface in contact with water, IFT measurement evidences the surfactant properties of these charged species at crude oil/brine interface, and the influence on this character by changing ionic strength and pH of the aqueous medium. Based on the results obtained in this study and results of previous studies, it seems like an unique concentration relationship between the surface active species and salinity of the brine phase is required to achieve a positive contribution of IFT to LSE.<sup>[50, 68, 69, 70, 71]</sup>

Both crude oils used in this study had very high viscosities under ambient conditions compared with water viscosity. For laboratory experiments e.g. dynamic coreflooding, favourable low mobility ratio of the displaced and displacing fluids are of great importance as mentioned previously, to avoid fingering effects. One method to achieve favourable mobility ratios is by diluting the crude oil.

One of the crudes used in coreflood experiments conducted at our laboratory are mixed with Xylene and Iododecane. The purpose of Xylene is to dilute the oil, while Iododecane is added for x-ray contrast. An x-ray scanner is normally used to scan the core to see visually what happen with the in-situ saturations in a core during the flooding experiment. Iododecane added to the crude oil has the ability to adsorb x-radiations and thereby contribute fewer radiations to be emitted. The difference between the emitted compared with the transmitted radiations gives a clue about the in-situ saturations. As a support study to LSW dynamic coreflooding experiments, wettability and IFT measurements have been conducted on Xylene and Iododecane mixed crude oil, where the purpose was to investigate the impact of these chemicals on crude oil properties.

This thesis starts with general wettability aspects presented in Chapter 2, and are required to understand the wettability terms used in the further chapters. In Chapter 3, the observed potential of LSW on lab-scale and field scale are presented based on data from a recently study.

The chapter continues with presenting the five proposed LS mechanisms, and the contradicting evidence for these mechanisms. Chapter 4 and 5 will provide a background for understanding the experimental results of this thesis and are linked to each other. Chapter 4 introduces four identified

mechanisms of wettability alteration, with main focus in the chapter being on the individual phase impact on these alteration mechanisms. Detailed description of the stability of the water-film between crude oil and rock, which has impact on two of the mechanisms in Chapter 4, will be presented in Chapter 5 presenting fundamental surface forces, which governs the water-film stability. Introduction to adhesion test and previous adhesion studies will be presented further in Chapter 5, finally followed by a presentation of IFT properties between crude oil and brines of different compositions, focused on both past and recently studies and observations.

The next Chapter 6 will be about the materials used in the experiment and the experimental procedure, with main results and discussion continued in Chapter 7. Conclusion and suggestions for further work are given in Chapter 8 and 9, respectively. All the data used for presentation of experimental results in Chapter 7, are listed in tables in Appendices at the end of this thesis.



## 2 Wettability

### 2.1 Introduction Wettability

Oil recovery efficiency by water flooding in a COBR system is strongly influenced by reservoir rock wettability. Wettability is a major factor dominating location, flow and distribution of the fluids in-situ.<sup>[20]</sup>

Craig<sup>[21]</sup> defined the wettability of a reservoir rock as the tendency of one fluid to spread on or adhere to a solid surface in presence of another immiscible fluid.

For two immiscible fluids such as oil and water in presence of a smooth homogenous surface as shown in Figure 2.1, the wettability of the surface is thermodynamically defined in terms of contact angle derived from a force balance between the interfacial tensions that act in the three-phase system. Young's equation presents this relationship and is given as:<sup>[1, 14]</sup>

$$\cos\theta_{ow} = \frac{\sigma_{os} - \sigma_{ws}}{\sigma_{ow}} \quad (2.1)$$

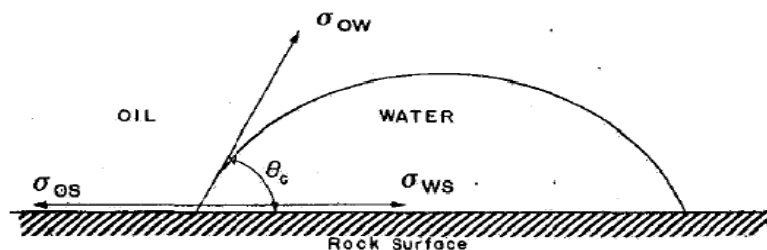
Where:

$\theta_{ow}$  = contact angle oil/water interface creates with the solid surface

$\sigma_{ws}$  = interfacial tension between water/solid

$\sigma_{os}$  = interfacial tension between oil/solid

$\sigma_{ow}$  = interfacial tension between oil/water



**Figure 2.1:** Oil/water/rock system at thermodynamic equilibrium state.<sup>[22]</sup>

## 2.2 Measurement Methods and Wettability Classes

In-situ measurement of reservoir wettability is not available, thus the knowledge of reservoir wettability is based on laboratory experiments and theoretical evaluations.

The literature distinguishes between quantitative and qualitative wettability measurement methods. Among them the widely used quantitative methods: Contact angle method, Amott Harvey method and U.S Bureau of Mines (USBM) method gives physical measured values for the wettability state of the system, while qualitative methods such as imbibition rates, permeability curves, permeability saturation relationship etc. are more characterized as wettability indicators providing a rough idea of the wettability state, and are therefore very thin basis for wettability conclusions.<sup>[22]</sup>

Dependent on the interaction between fluids and rock, three types of wettability classes are characterized to reflect the core (reservoir) wettability, with respect to the measured values of the quantitative methods: Contact angle values and USBM and Amott wettability indices.

These wettability classes are classified as water-wet, oil-wet and intermediate-wet systems.

Anderson presents in his literature review following relationship as presented in Table 2.1 between the wettability classes and the measured values.<sup>[22]</sup>

Method	Water-wet	Intermediate-wet	Oil-wet
<b>Contact angle</b>			
<b>Min <math>\theta</math></b>	0°	60°-75°	105°-120°
<b>Max <math>\theta</math></b>	60°-75°	105°-120°	180°
<b>USBM Index</b>	$I_{USBM} \sim 1$	$I_{USBM} \sim 0$	$I_{USBM} \sim -1$
<b>Amott-Harvey Index</b>	$+0.3 \leq I_{AH} \leq 1.0$	$-0.3 < I < 0.3$	$-1.0 \leq I \leq -0.3$

**Table 2.1:** Three types of wettability classes defined in terms of contact angle, USBM index and Amott wettability index.<sup>[22]</sup>

Contact angles close or equal to 0° for a water-wet system and 180° for an oil-wet system, classifies them as strongly water-wet or strongly oil-wet. In the literature this region can be found defined as 0° – 30° for water-wet systems, and 150° – 180° for oil-wet systems.<sup>[23]</sup> Higher  $\theta$  values for water-wet and lower  $\theta$  values for oil-wet systems classify them as preferential water-wet or preferential oil-wet.<sup>[14]</sup>

The intermediate wettability class can further be divided into three sub-classes dependent on fluid distribution pattern within the porous medium, and are known as mixed-wet-large (MWL: larger pores oil-wet and smaller pores water-wet), mixed-wet-small (MWS: smaller pores oil-wet and larger pores water-wet) and fractional-wet (FW: large and small pores are oil-wet and water-wet) systems.<sup>[24]</sup>

Amott test measures the average wettability of a core based on spontaneous fluid displacement or spontaneous imbibition process, meaning wetting fluid displaces the non-wetting fluid, e.g. water injection into water-wet pores to displace oil. USBM test measures the average wettability of the core based on forced imbibition or drainage process, where non-wetting fluid displaces the wetting fluid, e.g. oil displacement by water in oil-wet pores. Both methods reflect the core wettability in terms of wettability indices.<sup>[22, 23]</sup> Detail description of these methods is beyond the scope of this thesis, as the methods have not been used in this study, for more see reference.<sup>[22, 23]</sup>

Contact angle measurement methods are divided into optical methods and force methods.<sup>[82]</sup>

In this thesis the optical contact angle method using a goniometer system, that capture the profile of an oil droplet placed in contact with a solid mineral surface covered by brine has been used to measure the contact angles oil/brine interface creates with the solid surface.

### 2.3 Contact Angle Hysteresis

All the wettability classes defined in Table 2.1 are defined through the equilibrium contact angle,  $\theta_E$ . However, the condition for measurement of the thermodynamic equilibrium contact angle is never met, because of contact angle hysteresis observed for crude oil and brine on a mineral surface.<sup>[2, 25]</sup>

The initial angle measured after an oil droplet has been placed on the solid surface covered by water, illustrated in Figure 2.1 above, is referred as receding contact angle,  $\theta_r$ . When the oil droplet is being placed on this surface it pushes away the water such as it recedes, thus the angle measured is receding angle. In the opposite case when oil is pulled back as the water advances over the previously oil contacted surface, the angle is referred as advancing contact angle,  $\theta_a$ .

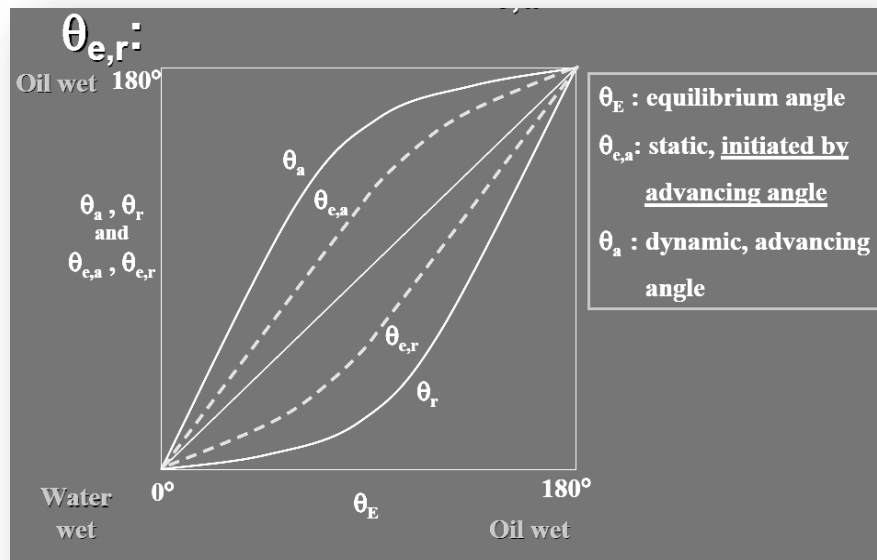
Generally  $\theta_a > \theta_E > \theta_r$ , thereby there exists a hysteresis between the two contact angle values.<sup>[23]</sup>

The magnitude of hysteresis is given as:

$$\theta_a - \theta_r = \text{hysteresis} \quad (2.2)$$

and the higher the hysteresis the more far from equilibrium contact angle, advancing and receding values are.<sup>[23]</sup> The reason for contact angle hysteresis on smooth solid surface is related to adsorption of surface active components from the oil-phase at the solid surface. These components can alter the wettability towards more oil-wet as the oil/solid interface ages. Consequently the oil drop deforms when it is pulled back and forms a new and a higher contact angle with the solid surface.<sup>[22]</sup> Surface active components and their ability for wettability alteration will be discussed in Chapter 4.

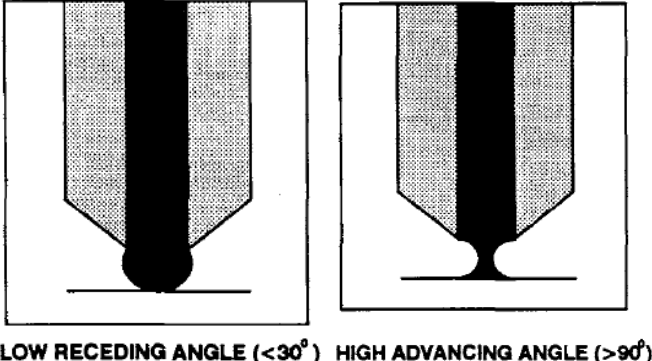
Morrow<sup>[26]</sup> measured dynamic  $\theta_r$  and  $\theta_a$  angles for rough surfaces, and presented them as function of  $\theta_E$  angle. In addition to his results, recently studies have shown that static angles initiated by  $\theta_r$  and  $\theta_a$  angles reduce the degree of hysteresis to a lesser extent compared with dynamic angles. Figure 2.2 illustrate this relationship and are in the literature found to be used as a common graph for describing crude oils hysteresis.<sup>[23]</sup>



**Figure 2.2:** Dynamic advancing and receding contact angles,  $\theta_r$ ,  $\theta_a$ , and static equilibrium advancing and receding contact angles,  $\theta_{e,a}$ ,  $\theta_{e,r}$ , as function of  $\theta_E$  representing the real wettability of a given system. <sup>[23]</sup>

Sessile drop or captive drop method is an optical contact angle method used to measure both dynamic and static  $\theta_a$  and  $\theta_r$  angles. The method is based on measuring contact angles by using a syringe filled with crude oil to expand and contract the volume of the crude oil droplet at the tip of a capillary needle, which is placed in contact with the solid surface immersed in brine.<sup>[22]</sup>

Figure 2.3 presents an example of the hysteresis effect observed during a sessile drop measurement.<sup>[25]</sup> This method has been developed further by Buckley et al.<sup>[17]</sup> to investigate COBR interactions, a test named adhesion test and is discussed about in Chapter 5.



**Figure 2.3:** Illustration of a very large contact angle hysteresis.<sup>[25]</sup>

Receding and advancing angles are also used to describe drainage and imbibition processes in a reservoir. The situation is similar as for contact angle measurements. When oil displaces water the contact angle of the process is in receding form, and when water displaces oil in advancing form.

## 3 Low Salinity Water (LSW)

### 3.1 Lab Scale and Field Scale LSW Recovery Data

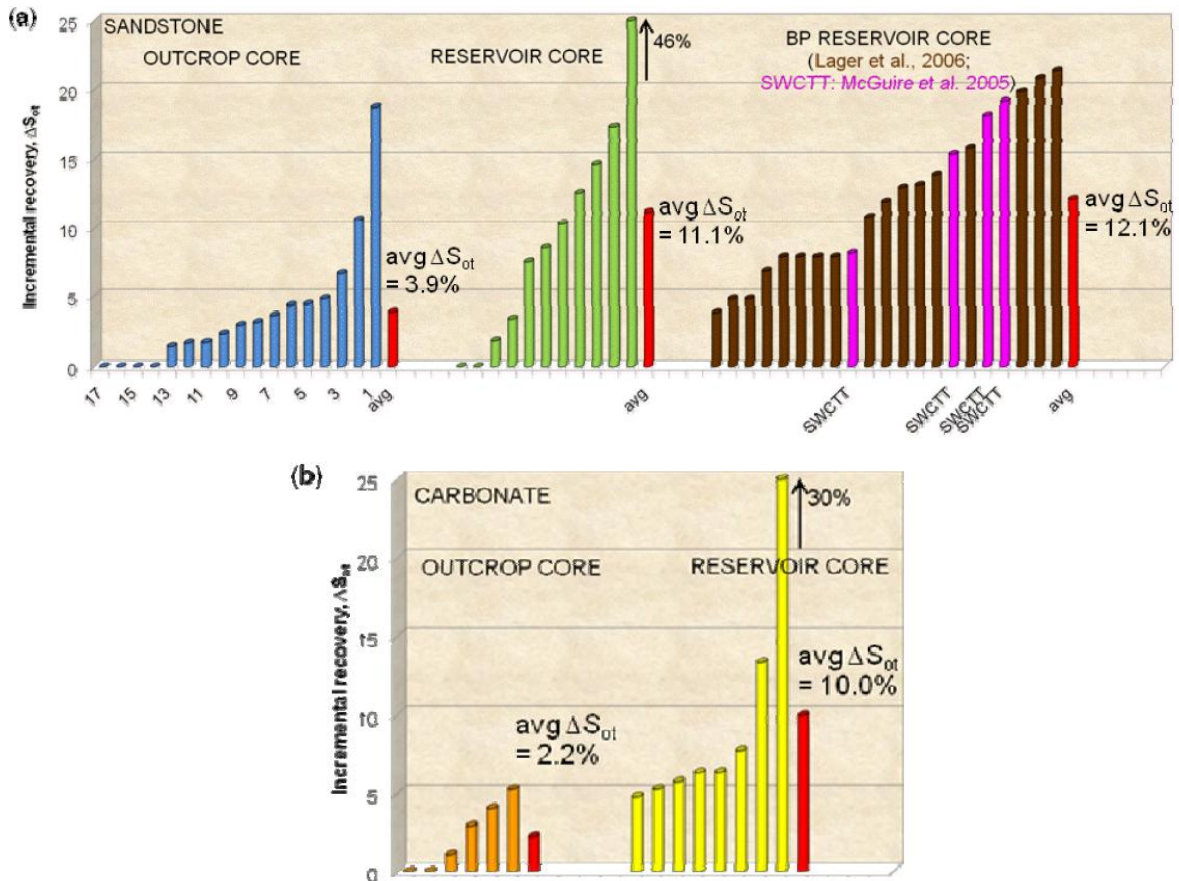
Several laboratory LS waterflood studies both in secondary and tertiary recovery modes using both outcrop and reservoir cores have been performed, and the potential of the recovery has shown both increasing, decreasing or no additional production compared with high salinity water (HSW).<sup>[8, 9, 10, 11, 12, 30, 31, 32, 37]</sup>

The recently study performed by Winoto et al.<sup>[10]</sup> provides a nice overview of this observed trend. They compared LS waterflood recovery in tertiary mode, for a wide range of outcrop and reservoir cores for both sandstones and carbonates. Among these, 6 sandstone and 3 carbonate outcrop cores were also tested in secondary recovery using LSW as both connate (irreducible water saturation) and invading brine to compare the recovery with HSW injection for the same cores. Tertiary recovery was conducted by changing the invading brine salinity to LSW which was the SSW diluted by a factor of 20, after waterflooding down to residual oil saturation,  $S_{or}$ , with SSW was reached. WP crude oil was used for the outcrop tests while the corresponding reservoir crude oils for the reservoir core tests.

For secondary recoveries their results showed no clear trend by comparing HSW and LSW recoveries, and the net differences ranged from higher to even lesser recoveries. The highest net difference with LSW for sandstone cores was increase in original oil initially in place (OOIP) with 10% and lesser LSW recovery with 6% OOIP. For the carbonates the highest net difference was 16% OOIP and lesser LSW recovery with 6% OOIP.

Figure 3.1 a) and b) presents the incremental recovery,  $\Delta S_{o_{tot}}$ , in tertiary mode, which is the additional oil recovery expressed as a percentage of recovery given by the secondary flooding with SSW. In addition to their results, the results of LS waterflood performed on BP reservoir cores and well tests are presented in Figure 3.1.a). The average incremental recovery of the 17 outcrop sandstones was 3.9% compared to 11.1% for the 11 reservoir sandstone cores, and 12.1% for reservoir cores and well tests performed at BP. For outcrop carbonate the average was 2.2% compared to 10% for reservoir cores. The overall result indicates higher waterflood recovery for reservoir cores compared to outcrop cores, for both sandstones and carbonates, but also cores

showing no LSE are observable. No special link between the amount of oil recovered in the secondary recovery and tertiary recovery was observable in their study.



**Figure 3.1:** Schematic illustration of increase in tertiary recovery ( $\Delta S_{ot}$ ) by low salinity waterflooding performed on outcrop and reservoir cores for a) sandstone cores b) carbonate cores.<sup>[10]</sup>

As illustrated in Figure 3.1 a), lab scale success has also provided field scale success in tertiary low saline field tests. The SWCTT results presented in Figure 3.1 a), presents the results obtained by tertiary LS waterfloods in four different single well chemical tracers-test (SWCTT) field pilots, after high salinity SWCTT was performed at Western operating area, Northwest Eileen field, Borealis field, and Endicott field in the North slope of Alaska operated by BP. Increase in oil recovery by LS waterflooding for these well tests was respectively, 8%, 15%, 18% and 19%, which can also be seen from Figure 3.1 a).<sup>[11]</sup>

SWCTT is a method of measuring  $S_{or}$  in reservoir intervals following a waterflood. The test is performed by first injecting a volume of brine with chemical tracers into the test zone, and shut in of well for a one to ten day period dependent on the reservoir temperature.

By doing this, the injected tracers can react with the reservoir water and produce a secondary tracer. During the production of the well, the produced water is analysed for tracer content, and the separation between the reaction product and the chemical tracer is used calculate  $S_{or}$ .<sup>[11, 12]</sup>

However, field tests have also resulted in low LSE potential, an example is the SWCTT field pilot performed at Snorre field located in North Sea, which resulted in very low potential of LSE both in laboratory reservoir core floods and field test.<sup>[13]</sup> The results of BP and Snorre field test indicate that laboratory reservoir core floods results have shown consistency with field pilot tests.

### **3.2 Proposed Low Salinity Mechanisms**

The most accepted proposed LSW mechanisms are listed below and are all related to wettability alteration from weakly oil-wet to more water-wet state. The first four proposed mechanisms suggest wettability alteration to be a consequence of physical and chemical processes taking place in-situ in a core, while the last proposed mechanism is not a consequence of any processes, but suggest pure wettability alteration to be the cause of LSE.

- Fines migration
- pH effects
- Multicomponent ionic exchange
- Double layer effects
- Wettability alteration



### 3.2.1 Fines Migration

Tang and Morrow<sup>[27]</sup> proposed a low salinity mechanism based on migration of clay fragments or fines. LS waterflood studies was performed on outcrop Berea (high clay content) and Bentheimer (low clay content) cores, and their results showed there was a relationship between amount of clay present in the cores, fines migration and amount of oil recovered with LSW. The almost clay free sandstone showed less increase in oil recovery with decreasing salinity than the clay containing sandstone. The release and migration of fines, especially kaolinite, was explained through DLVO<sup>[19]</sup> (Derjaguin, Landau, Verrvey, Overbeek) theory of colloids as follows: When the salinity of the brine phase is reduced, the double layer between the individual clay particles expand, and the initial stabilized flocculated state of the clay particles in presence of HSW is disturbed, and as a result fines migration takes place. Electrical double layer forces are discussed in detail in Chapter 5.

Fines migration has been proposed lead to increased oil recovery due to:

- 1) Wettability alteration<sup>[27]</sup>
- 2) Diversion of flow.<sup>[6, 7, 28]</sup>

The first proposed case is from the study by Tang and Morrow.<sup>[27]</sup> In this case it is assumed that the clay particles are initially mixed-wet, and as low salinity water is injected the release of these mixed wet clay fragments results in exposure of new underlying surfaces, which increase the water wetness of the system and thus leading to increase in oil recovery. Another suggestion was that these mixed-wet clay fragments will mobilize previously adsorbed oil clusters to these clay particles that will give an additional recovery.

But more important is the suggested case two, where release of clay particles can block pore throats and divert the flow of water into new un-swept regions, and thereby improve the microscopic sweep efficiency. Increased oil recovery due to this technique was proposed by Martin already in 1959<sup>[6]</sup> and Bernard in 1967,<sup>[7]</sup> and more recently Skauge<sup>[28, 29]</sup> has also explained log-jamming or bridging process which is the blocking process of pore throat entry by colloids in solution to be an important EOR contribution, by giving both microscopic diversion flow and sweep improvement.

He explained the increased recovery related to acceleration of particles which will be slower than water due to differences in their mass, thereby when the particles reach the pore throat water has

already swept the pore throat the particles will start blocking. Figure 3.2 illustrate the log-jamming process at pore throat entry.



**Figure 3.2:** *Reduced salinity of invading brine causes release of clay fines from pore walls that results in blocking of pore throat entry, a process called log-jamming.<sup>[5]</sup>*

Although the experiments performed by Tang and Morrow<sup>[27]</sup> showed fines being eluted during LSW injection, the BP researches Lager et al.<sup>[30]</sup> argue that BP has conducted a set of coreflood experiments with LSW injection resulting in increased oil recovery, where neither permeability reduction nor fines migration were observed.

Cissokho et al.<sup>[31]</sup> showed through their study additional recovery with LSW, even when no significant production of fines in the effluent was observed. The sandstone core was also a kaolinite free core. Boussour et al.<sup>[32]</sup> performed LS waterflooding on a sandstone core with no increased production of oil, despite a significant amount of fines production. Thus, these observations question the link between oil recovery and fines migration.

### 3.2.2 pH Effects

Tang and Morrow<sup>[27]</sup> observed an increase in effluent pH with LS injection in Berea cores, and McGuire et al.<sup>[11]</sup> observed pH increase in the effluent on North slope field samples.

Based on their observations, McGuire et al. concluded the increased oil recovery with LS waterflooding to behave in the same way as an alkaline flooding, with reduced IFT between oil and water due to generation of surfactants in crude oil and wettability alteration toward more water-wet state. The presence of surfactants in crude oil, are described in detail in Chapter 4.

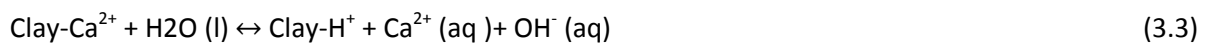
Lager et al.<sup>[30]</sup> suggested the rise in pH can be caused by carbonate dissolution and cation exchange. They explained that the dissolution of carbonate results in an excess of  $\text{OH}^-$  ions, according to Equation 3.1 and 3.2.



Initially solubility equilibrium exists between  $\text{CaCO}_3$  in solid form and the solution of that compound as shown in the Equation 3.1. The decrease in concentration of these ions in the reduced saline brine will disturb the established chemical equilibrium. Consequently the equilibrium in Equation 3.1 shifts toward right according to Le chatelier's principle, which says that any change in a chemical equilibrium caused by the surroundings will shift the reaction in the direction that tries to offset the effect of change.<sup>[33]</sup> As a result of this shift in equilibrium, more carbonate dissolution is promoted.  $\text{CO}_3^{-2}$  is the corresponding base of the second stage ionization of  $\text{H}_2\text{CO}_3$ . These ions can react with water molecules and initiate acid/base equilibrium reactions as shown in Equation 3.2. Shift in equilibrium toward right in Equation 3.1 will shift the equilibrium of reaction 3.2 toward right, and thereby contribute to an increase in pH of the solution due to increase in  $\text{OH}^{-}$  ions.

Carbonate dissolution reactions are reported to be relatively slow and depends on the amount of carbonate material present in the rock.<sup>[30]</sup> Limestone is mainly composed of carbonate minerals, but cementing material in sandstone reservoirs contains calcite.<sup>[5]</sup>

Further they explained that cation exchange process occurring on the surface of clay minerals was much faster reactions. This is an exchange mechanism which occurs between the cation initially adsorbed at the mineral surface and  $\text{H}^{+}$  ions in the invading water, which leads to decrease in  $\text{H}^{+}$  ions in the solution and can thereby also contribute to increase in pH of the pore water. Equation 3.3 illustrates this reaction with  $\text{Ca}^{2+}$  as example.<sup>[34]</sup> Cation exchange mechanism is described further in multicomponent ionic exchange (MIE)



More recently Austad et al.<sup>[34]</sup> proposed a LSE in tertiary mode based on the effect of pH on adsorption and desorption reactions of organic materials with the surface of clay minerals.

He suggested that initially both acidic and basic species are adsorbed at the clay surface together with cations from the pore water. It is the pH of the pore water even below pH 5 due to dissolved  $\text{CO}_2$  and  $\text{H}_2\text{S}$  that made it possible for both acidic and basic species to be adsorbed at different clay minerals.

He explained that according to Equation 3.3, a local increase in pH near the clay surface causes concomitant reaction between OH<sup>-</sup> ions and the adsorbed acidic and basic organic species, which promotes desorption of adsorbed species and increase the oil recovery as the water wetness of the rock surface is improved. The acid/base reactions are shown in Equation 3.4 and 3.5.



However, conflicting evidence to the suggestions of McGuire et al.<sup>[11]</sup> is the parameters in alkaline flooding. According to the literature, for an alkaline flooding to succeed an oil with high acid number (AN > 0,2) is required to generate sufficient surfactants and thereby induce wettability reversal and IFT reduction.<sup>[30]</sup> But Lager et al.<sup>[30]</sup> reports that LS waterflooding has shown positive results for oils with very low acid number, (AN <0,05) and also for systems with increase in pH with 1 unit and even below pH 7. Cissokho et al.<sup>[31]</sup> reported increase in pH with LSW, but no increase in oil recovery. These results create a doubt if there is any relationship between measured pH in the effluent and increased oil recovery with LSW.

### 3.2.3 Multicomponent Ionic Exchange (MIE)

Clay minerals are normally reactive because of their large surface area and because they commonly carry a permanent negative charge. The permanent charge is due to isomorphic substitution processes occurring in clay minerals during crystallization. In this process, the basic building stone Silicon (Si) and Aluminium (Al) atoms of clay minerals are replaced by other clay composing atoms with lower cation valence, which contributes the clay minerals to carry a permanent net negative charge. The clay minerals can adsorb cations to the naturally negative charged external surface and between the Al and Si sheets building the clay minerals. This ability of clay minerals to hold on these cations is called the cation exchange capacity (CEC).<sup>[81]</sup>

Multicomponent ionic exchange (MIE) involves the competition of all the ions present in pore water for the mineral matrix exchange sites of the minerals composing the rock.<sup>[12]</sup> Early studies performed by Hydrogeologist have shown the best application of this theory. When an aqueous solution with different composition and lower salinity than connate brine was injected, ion exchange occurring

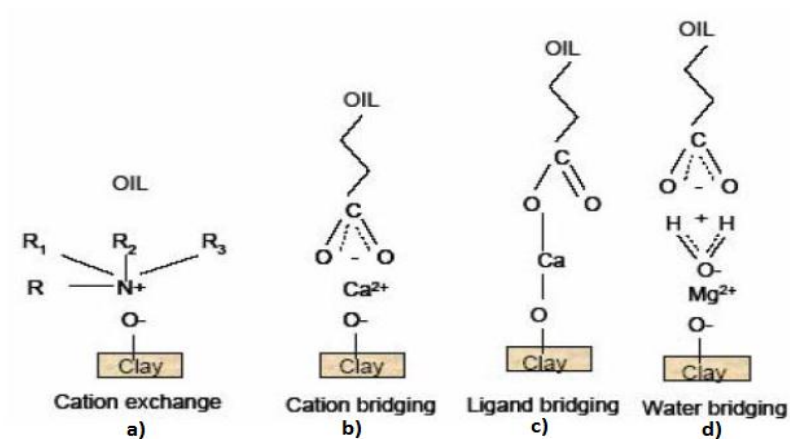
between the mineral surface and the injected brine resulted in observable change in the chemistry of the effluent water. In LS waterflood experiments conducted at BP and Heriot Watt University, they observed decrease in the concentration of  $\text{Ca}^{2+}$  and  $\text{Mg}^{2+}$  ions in the effluent relative to the concentration initially present in connate water and injected brine. According to the authors this indicated to be a result of strong adsorption of these ions to the rock matrix.<sup>[30]</sup>

The BP researchers Lager et al.<sup>[30]</sup> proposed MIE as a mechanism responsible for the increased oil recovery during LS injection, since cation exchange mechanisms occurring during LS waterflooding will affect some of the mechanisms which cause organic matter adsorption at the mineral surface.

Sposito et al.<sup>[35, 30]</sup> proposed eight different possible mechanisms of organic matter adsorption onto clay minerals. Lager et al. classified four of them as mechanisms affected by cation exchange capacity in LS waterflooding. The affected mechanisms are:

- 1) Cation exchange
- 3) Cation bridging
- 3) Ligand bonding
- 4) Water bridging.

Figure 3.3 illustrates these four mechanisms.



**Figure 3.3** Different ways crude oil components are attached to the mineral surface directly or by divalent cations.<sup>[36]</sup>

Cation exchange mechanism, illustrated in Figure 3.3 a) is the primary mechanism and occurs when molecules containing nitrogen, ring NH or heterocyclic N rings, replace exchangeable metal cations initially bound to the clay surface. Cation bridging shown in Figure 3.3 b) is an adsorption mechanism

between polar functional groups as carboxylate, amines, carbonyl or alcoholic OH and exchangeable cations at the surface of the clay. The direct bond formation between a multivalent cation and a carboxylate group is referred as ligand bonding, which forms organo-metallic complexes (RCOO-Ca). Figure 3.3 c) represents this type of binding. Ligand bonds are much stronger compared with cation exchange and cation bridging bonds. When the exchangeable cation is strongly solvated, water bridging may occur. This mechanism involves the complexions between the water molecules solvating the exchangeable cation and the polar functional group of the organic molecule as amino, carbonyl and carboxyl. Figure 3.3 d) illustrates this interaction mechanism.

Organo-metallic complexes formed at the clay surface promote oil wetness in reservoirs. The organic materials may also adsorb directly to the mineral surface by displacing the most labile cations present at the mineral surface and thus enhance the wettability alteration toward more oil-wet according to the proposed mechanisms. Further, the BP researchers suggested that when LSW is injected, MIE results in removing the organo-metallic complexes and polar components from the surface by replacing them with uncomplexed cations. As a result, the reservoir becomes more water-wet, and oil recovery increases.

To test and to confirm MIE mechanism in LS waterflooding, Lager et al.<sup>[30]</sup> conducted a coreflooding experiment where they replaced all the divalent cations present on the mineral surface with Na<sup>+</sup>, by flush the core sample with NaCl brine until the effluent contained only traces of the Mg<sup>2+</sup> and Ca<sup>2+</sup>. After aging the core sample with crude oil up to connate water saturation with pure NaCl composition, primary injection with high salinity NaCl was performed and resulted in production up to nearly 50% OOIP. Injection with LSW, NaCl solution did not produce any oil since all the mobile oil was produced in the primary injection, and nor did the injection followed by LS brine containing Ca<sup>2+</sup> and Mg<sup>2+</sup>. They explained this was due to only non-complexable monovalent cations i.e. Na<sup>+</sup> will be desorbed from the mineral surface by the divalent ions present in the injection brine. From this result, they suggested that the presence of divalent cations like Ca<sup>+</sup> and Mg<sup>+</sup> is necessary in the connate water to give an additional production with LSW, since these ions have an important role in the interaction between clay minerals and surface active components in crude oil.

However, Cissokho et al.<sup>[31]</sup> showed through their study that the composition of the invading brine was not a sensitive factor for the outcrop sandstone. The 100% monovalent cation LSW (NaCl solution) did also give additional oil recovery.

Austad et al.<sup>[34]</sup> explained the reduction in  $Mg^{2+}$  and  $Ca^{2+}$  ions as Lager et al. observed could be caused by precipitation of  $Mg(OH)_2(s)$  and  $Ca(OH)_2(s)$  as a result of a local pH increase due to desorption of cations in the injected LS brine, and not necessarily an MIE process.

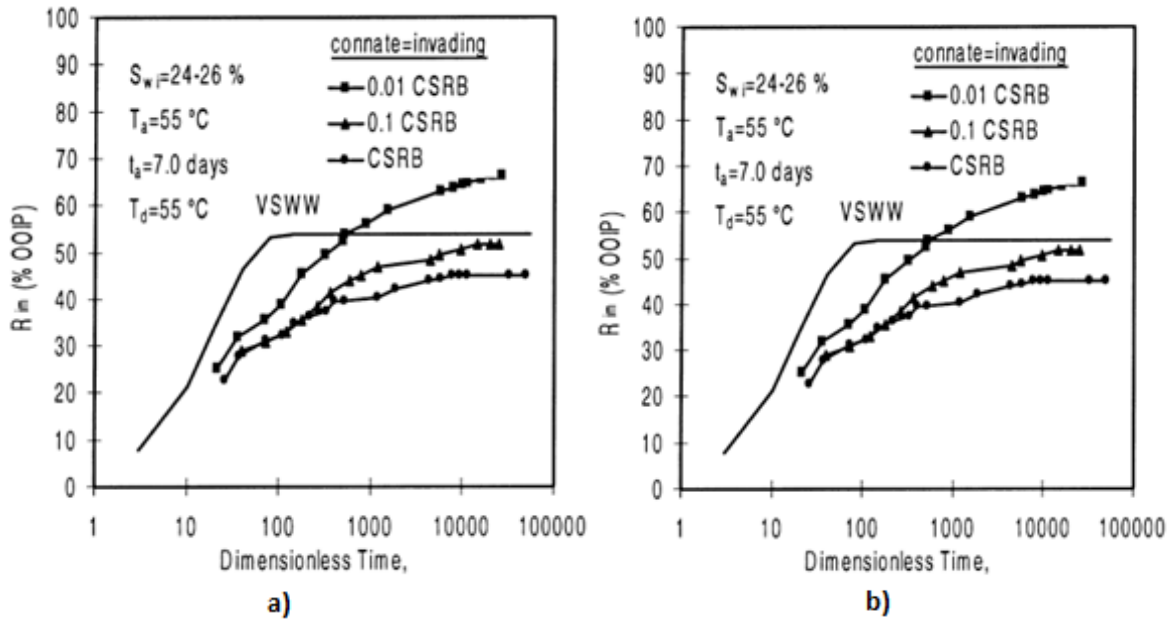
### 3.2.4 Double Layer Expansion

Lingthelm et al.<sup>[37]</sup> proposed a LS mechanism related to the thickness of the water-film referred as the double layer thickness between crude oil and reservoir rocks. They proposed that the high salinity brine contains sufficient amount of divalent ions that can screen off the negative charge formed under formation brine pH at oil/water and water/solid interfaces, which will cause a suppression of the electrostatic repulsion force. Further, they suggested by lowering the salinity especially reduction of multivalent cations in the brine solution reduces the screening potential of the cations. This yield expansion of the electrical double layers (the water-films) that surrounds the crude oil and clay particles, and once the repulsive forces exceed the binding forces via multivalent cation bridges, the oil particles may be desorbed from the clay surfaces. The reduction in fraction of rock surface that has been coated by oil increases the oil production, and so does the wetting state toward more water-wetness.

The Double layer effect is explained by bridging effect occurring between two negatively charged interfaces. Direct bond between oil components and negatively charged surfaces have also been proposed.<sup>[30, 34, 27]</sup> Contradicting evidence is also results obtained by adhesion test which shows the water-film to be most stable in HS brines, also in presence of divalent ions.<sup>[2]</sup>

### 3.2.5 Wettability Alteration

Wettability alteration toward more water wetness has also been proposed to be a cause of increased oil recovery with LSW. Morrow et al.<sup>[9]</sup> performed waterflood and imbibition test on Berea cores with CS crude oil and different dilution of CS reservoir brine. Figure 3.4 a) and b) illustrate their results, and as can be seen from the figures, the oil recovery increases markedly with decrease in brine salinity. Based on spontaneous imbibition observations they concluded that water-wetness and oil recovery increased with decrease in salinity.



**Figure 3.4:** The impact of brine composition on a) imbibition and b) waterflood on oil recovery in Berea core sample.<sup>[9]</sup>

Imbibition test is based on immersing the oil field core at initial water saturation,  $S_{wi}$ , in brine under graduated cylinder, and the rate and amount of spontaneous oil displacement by water are measured. Based on recovery amount of oil by spontaneous water imbibition the degree of water-wetness of the system is concluded.<sup>[22]</sup>

Waterflood are based on injection of brine at constant flow rate with apparatus monitoring differential pressure and oil production.<sup>[30]</sup> The results of waterfloods gives a measure for the end point relative permeability of oil and water, which is a measure for the flow properties of the fluids relative to each other in the porous medium,<sup>[1]</sup> and by interpreting relative permeability data wettability conclusions are made.

The trend of increased oil recovery with increased water-wetness seems to contrast the general trend of intermediate-wet conditions to be the most favourable conditions for oil recovery by waterflooding.

In a study performed by Jadhunandan and Morrow<sup>[38]</sup> where the aim of their work was to study the effect of wettability on oil recovery, they found based on over 50 coreflood experiments conducted on Berea sandstone cores with different oil/water composition maximum oil recovery to appear in

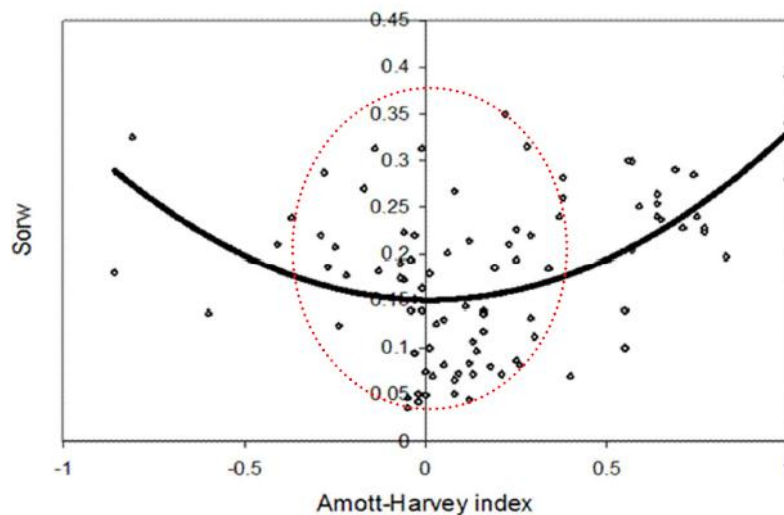


the weakly water-wet side of intermediate-wet state. Amott wettability test was used to measure the average wettability of these cores.

Skauge and Ottesen<sup>[15]</sup> found a similar trend in their study where they reviewed special core analysis data (SCAL) from 30 North Sea sandstone reservoirs, and compared them to find a relationship between wettability measured by Amott test and residual oil saturation after waterflood experiments. Figure 3.5 illustrate the observed trend from the study by Skauge and Ottesen.

The study performed by Ashraf et al.<sup>[39]</sup> showed that this trend is also valid for LS waterflooding in a secondary process. All salinity ranges results showed oil recovery increased as wettability changed from water-wet to intermediate-wet conditions, further change in wettability from intermediate-wet to oil-wet conditions decreased the oil recovery.

Spildo and Gilje<sup>[12]</sup> summarize in their work, some additional previous studies confirming this trend with intermediate-wet state to be the most favourable wettability state for oil recovery.

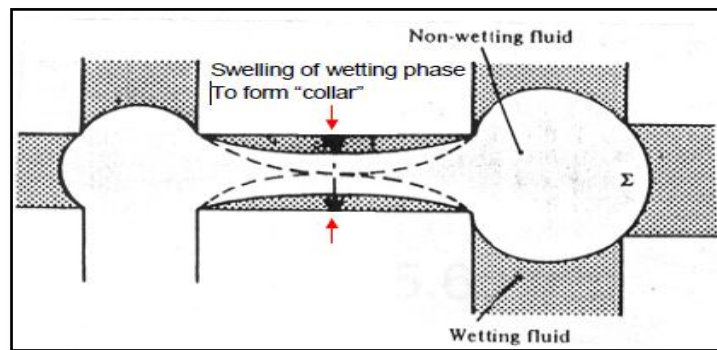


**Figure 3.5:** Residual oil saturation as function of Amott Harvey wettability index for core samples from 30 North Sea reservoirs. The red circle marks out the intermediate-wet region.<sup>[15]</sup>

This trend looks also more realistic with regard to the theoretical explanation for the displacement process taking place in water-wet pores. In water-wet systems water displaces oil through snap-off

displacement, meaning that as oil is imbibed by water in these pores the thickness of the water-film increases, and in restriction areas such as pore throats, the water film swells around the oil and form a collar that will cause the oil to snap-off. This process is shown in Figure 3.6.

The oil left behind is residual oil since it is trapped, and cannot move unless the viscous forces are invoked. As can be seen from the figure, the volume of oil left behind is large and increases as the pore radius increases.<sup>[23]</sup>



**Figure 3.6:** Snap-off displacement of oil by water in water-wet pores result in collars that snap-off the oil.<sup>[23]</sup>

As mentioned in the previous chapter, wettability conclusions based on imbibition test and waterfloods are more characterized as wettability indicators that only provide a rough idea about the wettability state of the system. Even when wettability alteration toward more water-wet state is the case, the regime wettability alteration occurs in will also have an impact. For this reason, Amott-Harvey and USBM test will provide more information about the regime wettability alteration occurs in, and can those explain the cause of increased oil recovery as the system is going toward more water-wet state.

## 4 Fluids/Solid Impact on Wettability Alteration

A general opinion that are now widely accepted as near fact is that wettability alteration is due to the complex interactions occurring in a COBR system, and that such interactions are strongly dependent on oil composition, brine composition and rock mineralogy <sup>[2, 14, 17, 25, 60, 61]</sup> In addition, temperature, pressure and contact time between the phases have also been reported to have a strong influence. <sup>[2, 22, 60]</sup>

This chapter starts with introducing four identified mechanisms by wetting alteration can occur. Even when several other proposed mechanisms can be found in the literature, <sup>[35]</sup> the following mechanisms present in this chapter are more relevant to the experimental study performed in this work. Since each phase has its own impact on interactions leading to the final wetting state of the reservoir rock, the chapter is divided into three different parts concerning the individual impact of the three phases, crude oil, brine and rock. This will provide a background of COBR interactions that will be needed to evaluate the wettability results obtained in this study.

### 4.1 Four Identified Mechanisms by which Wetting can be Altered

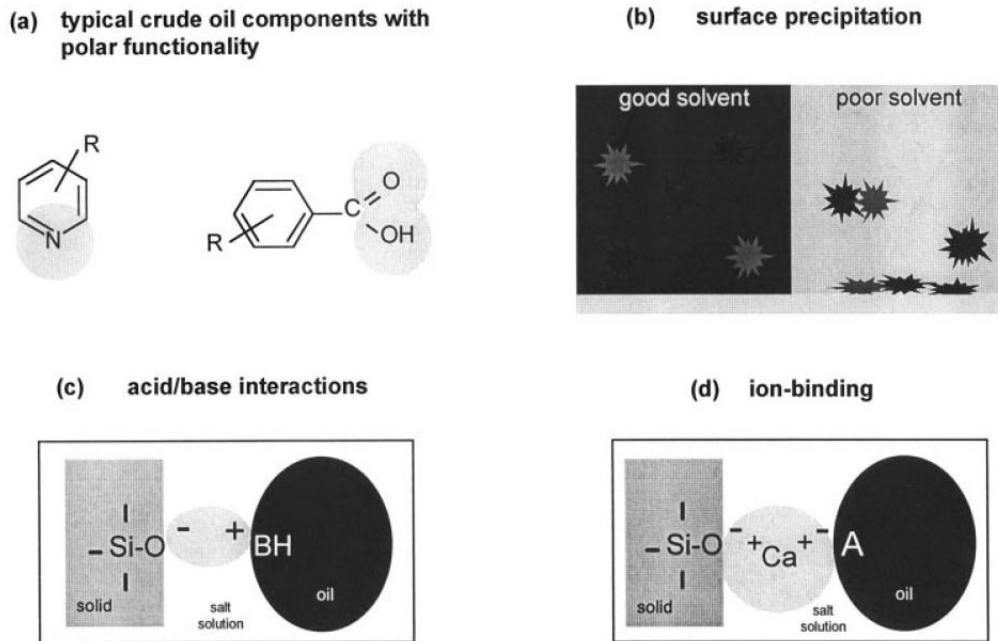
In a study performed by Buckley, <sup>[2]</sup> she investigated the underlying chemistry that controls wettability in fluids/rock system. Based on visual observations of the experiments and by using chemical and physical explanations for the observed results, she identified four mechanisms COBR systems can interact with each other and alter the wettability.

The mechanisms are as follows:

- a) Polar interactions dominating in the absence of water-film between oil and solid.
- b) Deposition or precipitation at the solid surface, dependent mainly on the crude oil solvent character with respect to its asphaltene fraction.
- c) Acid/base interactions at the interface of oil/brine and brine/solid controlling the surface charge, and causing columbic interactions to occur between the two interfaces.
- d) Ion binding between charged species at the interface of oil/brine or brine/solid (or both) and higher valency ions in the brine phase resulting in columbic interactions including the impact of these ions.

Figure 4.1 illustrate the interaction mechanisms a) to d).

In addition to these mechanisms, adsorption of polar organic species in presence of a water-film, a mechanism proposed by Kaminsky and Radke<sup>[41]</sup> should be included.



**Figure 4.1:** Mechanisms of interaction between crude oil components and solid surface.<sup>[2, 40]</sup>

All the above mentioned mechanisms of interactions presented by Buckley alter the wettability due to adsorption or precipitation of crude oil components. Adsorption and precipitation of crude oil components to an initial water-wet rock surface, occur only within the oil/solid contact area<sup>[42]</sup> and can occur in two different ways:<sup>[2, 14]</sup>

1. Adsorption or deposition of components to the rock surface causes water-film to rupture.
2. Water-film rupture cause adsorption of crude oil components.

While the first method allows physisorption and/or precipitation on the rock surface by diffusion through a water-film, the second mechanism allows a direct contact between the oil and rock surface

in absence of a water-film. The latter one is a consequence of disjoining pressure, which is force acting in the water-film between oil/brine and brine/solid interfaces, that controls the stability of the water-film on the rock surface.<sup>[18]</sup> Detailed description of this force is given in Chapter 5 describing the fundamental surface forces in a COBR system. The mechanisms due to this force are c) and d) and are mainly described in Chapter 5, but related to the brine phase and asphaltene components in crude oil, an insight into these mechanisms will be presented in this chapter, but the surface force effects leading to oil adsorption at solid surface by these mechanisms, will be presented in Chapter 5. Since mechanism b) and Kaminsky and Radke's proposed mechanism are mainly related to the oil-phase, these will be discussed under the section describing the importance of oil-phase. Interaction mechanism a) will not be a real situation in a reservoir with regard to the traditional scenario with an initial water-wet reservoir rock. But Buckley<sup>[2]</sup> summarized two proposed ways this type of interaction can be possible:

- 1) Because of specific oil-wet minerals.
- 2) Because the rock is both source and reservoir rock.

However, she mentions that it is unlikely to explain the wetting state of the reservoirs rock by either of these special cases. For this reason, and since no COBR interaction studies have been performed in absence of a water-film in this study, detail description of this mechanism is excluded from this thesis, for more se reference.<sup>[2]</sup>

## 4.2 The Oil Phase

Anderson<sup>[43]</sup> summarized in his research investigated mechanisms for wetting alteration dating back to 1970's. The investigation reported that polar organic components in crude oil, mostly related to resin and asphaltene fractions of crude oils can interact with the rock mineral surface and alter the wettability. These polar compounds did also show both acidic and basic character, and some of them were reported to have sufficient solubility in water, and could thereby diffuse through the water phase and adsorb on the solid surface and cause wetting alteration.

Denekas et al.<sup>[44]</sup> studied the impact of crude oil components on wettability of carbonate and sandstone by coreflooding. Boiling point distillation, solvent extraction and column chromatography were used to separate the different oil samples based on molecular weight, structure and polarity.

Higher boiling point fractions which were also the most polar fractions, appeared to cause wettability alteration from strongly water-wet toward more oil-wet. Sandstone wettability seemed to be sensitive for several of the higher boiling point fractions, while limestone appeared to be sensitive to basic, nitrogenous surfactants.

An interesting study related to asphaltene species in crude oil was performed by Kaminsky and Radke.<sup>[41]</sup> They studied the degree of asphaltene adsorption at solid surface when the two phases were separated by a water-film. The reason behind their study was to address the question of how water-films can have a protective role for asphaltene diffusion from water phase to the solid surface, when asphaltenes have very low solubility in water. This was the explanation given in the literature before them to confirm the water-wet state of reservoirs containing asphaltic crude oil.<sup>[43]</sup>

Kaminsky and Radke's results implied that low solubility asphaltenes were not protected to diffuse through the water-film, and thereby adsorbed on the solid surface. They concluded that although adsorption at the solid surface occurs in presence of water-films, the adsorption by diffusion is not strong enough to reverse the wettability, apparently rupture of the water-film and direct contact between asphaltene species and solid is required to reverse the wettability toward more oil-wet.

Muhammed and Rao<sup>[45]</sup> showed through their investigations by measuring static  $\theta_a$  and  $\theta_r$  angles for pure hydrocarbon and Yates crude oil, that compared with the pure hydrocarbon that showed water-wet  $\theta_a$  and  $\theta_r$  angles, the crude oil showed intermediate-wet  $\theta_a$  and weakly water-wet  $\theta_r$  angles. This type of wetting behaviour is termed hybrid wetting, and Anderson<sup>[43]</sup> reports this wetting alteration to be a result of adsorption of polar compounds from crude oil on the mineral surface.

Work since that time has shown general agreement in that polar organic compounds in crude oil represents the naturally occurring surface active agents in crude oil, and that these compounds can interact with the brine and solid phases and thereby alter the wettability of the solid surface.<sup>[41, 43, 44]</sup> Pure hydrocarbons do not alter the wettability since the interactions are restricted to weak dispersion forces.<sup>[45]</sup> Hence, the focus with respect to wettability alteration is therefore on resin and asphaltene fractions, both which are polar fractions.

### 4.2.1 Crude Oil Composition

Crude oil is a complex mixture of hydrocarbon (HC) components with and without the polar atoms nitrogen, oxygen and sulphur, and metals in particular vanadium, iron, nickel and copper, incorporated in the HC structure in several different ways. Hundreds of components ranging in size from one carbon atom to one hundred or even more constitute this complex mixture. Typical range of each element in conventional crude oil is given in Table 4.1.<sup>[46]</sup>

Conventional petroleum		
Element	symbol	Weight percentage
Carbon	C	83 – 87%
Hydrogen	H	10 – 14%
Nitrogen	N	0,1 – 2%
Oxygen	O	0,05 – 1.5%
Sulphur	S	0,05 – 6%

Metals < 1000 ppm

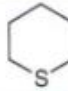
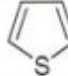
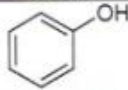
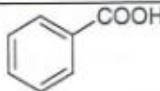

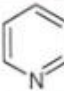
**Table 4.1:** Typical range of each element and metals in conventional petroleum.<sup>[46]</sup>

Beyond the first few members of each homologous series, it is not possible to distinguish between individual species in the crude oil. Since the mixture consist of a large number of molecules which differ in molecular type and weight, it is common to separate the crude oil into different fractions based on chemical and physical properties.<sup>[46]</sup>

One such separation method widely used is SARA (saturates, aromatics, resins and asphaltenes) fractionation method.<sup>[46]</sup> Asphaltene fraction which is the heaviest fraction in crude oil is characterized by its insoluble property in low molecular weight paraffins, such as normal-pentane and normal-heptane. To separate the asphaltene fraction from the crude oil, according to Speight,<sup>[46]</sup> 40 volumes of low-molecular weight paraffin which resin fraction is soluble in, is added to one volume of crude oil. The deasphalted oil is then separated by column chromatographic method based on polarity of the components, with saturates as the least polar fraction followed by aromatics and resins fractions.

## 4.2.2 Polar Organic Compounds in Crude Oil

A polar organic molecule is built up by both a non-polar and a minor polar end. The polar end of the molecule is generally attached to the non-polar HC molecule through functional groups containing NSO hetero atoms.<sup>[46]</sup> Oxygen compounds are generally acidic, and include a large number of carboxylic, phenolic and indolic acids.<sup>[2, 43]</sup> Nitrogen compounds are generally present as basic and non-basic compounds, while sulphur is present as three common functional groups: Thiols, sulfides/disulfides and thiophenes.<sup>[46]</sup> Figure 4.2 presents typical structures of NSO atom compounds present in crude oil.

Name of Compound	Molecular structure
Sulphur Compounds	Sulphides R-S-R'
	Cyclic sulphides 
	Thiophenes 
Oxygen Compounds	Alcohols R-OH
	Phenols 
	Carboxylic acids 
Nitrogen Compounds	Pyrroles (non-basic) 
	Pyridines (basic) 

**Figure 4.2:** Typical structures of polar organic compounds in crude oil.<sup>[14]</sup>



### 4.2.3 Acid/Base Properties of Crude Oil Components

The acid/base and surfactant properties of polar organic species make them to form ions through acid/base dissociation reactions when they come in contact with water. These charged species at oil/brine interface can through (strong) electrostatic forces interact with the opposite charged rock surface.<sup>[45]</sup> The amount of acidic and basic species present in a crude oil is reflected through acid and base numbers that are measures for the total acidic and basic species present in crude oil.<sup>[47]</sup>

In a study performed with 12 North Sea crude oils, Standal et al.<sup>[48]</sup> found a correlation between acid and base numbers, meaning that a low acid number usually corresponded to a low base number or vice versa. However, one crude oil showed a different trend with a relative high acid number compared with the 11 other crude oils, and the difference between acid and base number was also slightly higher for this crude oil, meaning a high acid number compared with base number. Both crude oils used in this study, are from the same field as this highly acidic crude oil, but from two different wells.

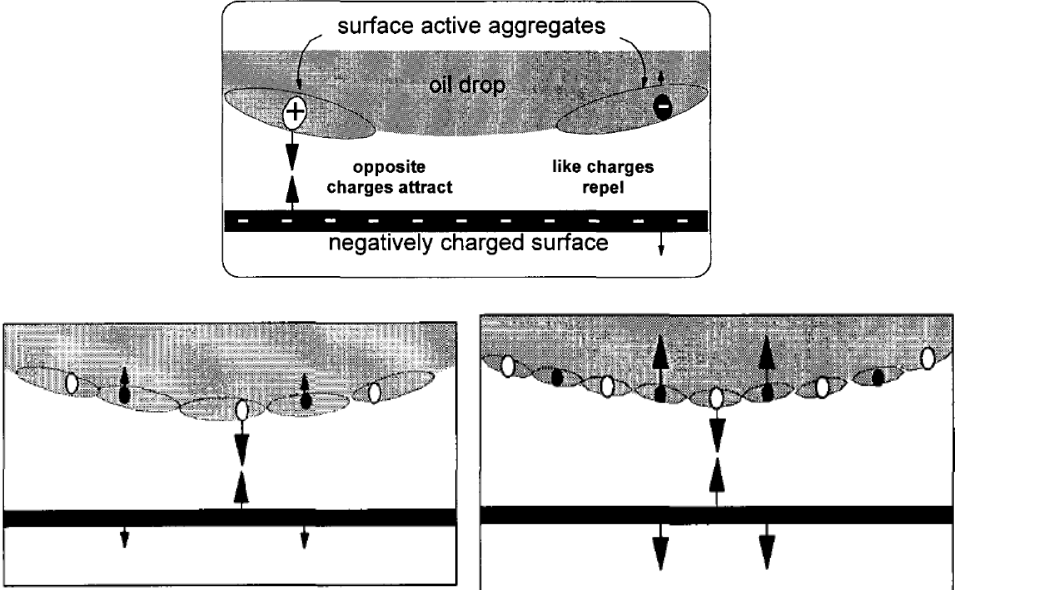
### 4.2.4 Physical Adsorption through Weak Polar Interactions and Precipitation of Asphaltenes

Some of the polar organic species present in crude oil have sufficient solubility in water while some does not.<sup>[2,50]</sup> But generally they have sufficient polarity to accumulate in the interface region between oil and water and act as surfactants, or diffuse through the water phase and adsorb on the solid surface.<sup>[2, 43]</sup> However, commonly the preferred site for these molecules is at the oil-water interface due to the unusual combination of chemical characteristic, which prefers neither oil nor water.<sup>[2]</sup> The molecules in the oil phase, interface or water phase can adsorb at the solid surface through dipol – ionic interactions when the compound is non-ionic and the surface is polar and charged. This type of adsorption is weak compared with pure electrostatic interactions between charged species.<sup>[2]</sup>

The stability of asphaltene molecules and any other polar organic compounds in crude oil depends on the solvent character of crude oil. An excess of light hydrocarbons will destabilize polar organic compounds from crude oil as the polarity of oil decreases.<sup>[46]</sup>

When asphaltene molecules which are poly-aromatic macromolecules in crude oil, exist in a crude oil with an excess of light hydrocarbons, the macromolecules tend to aggregate into micelles. They will act as particles suspended in a lyophobic colloidal system, and as flocculation occurs they precipitate from the solution.<sup>[51]</sup>

In a COBR system the precipitated material can accumulate at oil/brine interface if the asphaltene molecule has some degree of polarity, or diffuse through the water phase and deposit at the rock surface.<sup>[2, 41, 52]</sup> Figure 4.3 a) and b) illustrate asphaltene interactions with the solid surface from the crude oil/brine interface as proposed by Buckley.<sup>[2, 52]</sup> As the aggregate size increases due to decrease in solvency or decrease in temperature, the interaction between opposite charged aggregates and solid surface are stronger compared with the repulsive contribution. In the opposite case when the aggregate size decreases the surface charge density increases. As a result, the surface charges come closer and interactions between neighbouring aggregates become stronger, in other words the attractive and repulsive forces balance one another.



a) Large aggregates allow locally attractive interactions. The repulsive forces are weak. b) Small aggregates contribute net attraction/repulsion to balance one another.

**Figure 4.3:** The columbic interaction between charged asphaltene aggregates at crude oil/brine interface with the solid surface.<sup>[2, 52]</sup>

Organic liquids mixed with a specific crude oil can be classified as solvents or precipitants on the basis of their effects on the solubility and aggregate size of asphaltenes. The effect of precipitants was discussed about above. Saturates are normally classified as precipitants while aromatics such as toluene, limonenes, dipentene are classified as good solvents for the stability of asphaltenes in crude oils, but this stability will also be influenced by the entire crude oil mixture. [2, 52]

The addition of solvents has been reported to influence the crude oil stability either by decreasing the amount of precipitant required to initiate precipitation of asphaltenes, or increase the amount precipitant needed. Thus, since crude oil itself is a mixture of precipitants and solvents, dilution of crude oil with a solvent can affect the stability of the original crude oil dependent on the diluting solvent and the amount of precipitants present in the particular crude oil. [2, 52]

### **4.3 The Brine Phase**

The composition of the aqueous phase is one of the main variables in this thesis and has been varied with regard to both salinity and pH. Mechanism c) and d) of interactions described in the beginning of this chapter are adsorption occurring from the oil/brine interface. These types of oil/solid interactions are strongly dependent on the presence of brine phase. In the absence of water, neither the polar components nor the solid surfaces are charged.<sup>[12]</sup> The charge at the interface depends on the brine composition.<sup>[2, 60]</sup> Dependent on the interface charge, columbic interactions occurring between oil and solid can stabilize or destabilize the water-film separating oil and solid.<sup>[18]</sup>

The impact of brine phase in fluids/solid interactions is discussed with regard to acid/base dissociation reactions occurring at crude oil/brine interface, and with regard to the increased complexity of the interface interactions in presence of divalent/multivalent ions present in the brine phase. The salinity impact on magnitude of the net charge at the oil/brine interface will be discussed in Chapter 5.

### 4.3.1 Acid/Base Reactions at Crude Oil/Brine Interface

The dissociation reactions of the acidic and basic species in crude oil are strongly dependent on the pH of the solution,<sup>[17]</sup> which is a measure for the acidity of water and defined as the negative logarithm of hydronium ion concentration.<sup>[33]</sup>

$$pH = -\log_{10}[H_3O^+] \quad (4.1)$$

At low pH values, the net interface charge will be positive while at higher pH values negative.<sup>[2, 17]</sup> This phenomenon can be explained by simple acid base reactions with respect to Le chatelier's principle.<sup>[33]</sup>

Equation 4.2 presents a weak acid/base reaction in water for acid groups like carboxylic acids.<sup>[17]</sup>



Where  $AH$  represents the nonionic form of the acid groups and  $A^-$  is the ionized form of the acid groups.

Equation 4.3 presents a weak acid/base reaction in water for base groups like pyridine or quinoline.<sup>[17]</sup>



Where  $BH^+$  represents the ionized form of the base groups and  $B$  is the nonionic form of them.

The degree of dissociation of acids and bases is expressed in term of dissociation constant also known as ionization constant. This constant expresses the concentration ratio of the molecules in non-ionic form to ionic form at the state of equilibrium, and is given as follows for Equation 4.2:<sup>[17]</sup>

$$Ka = \frac{[A^-][H_3O^+]}{[HA]} \quad (4.4)$$

Where square brackets represent the concentration of each species,  $\left[\frac{mol}{l}\right]$ .

In order to see the direct relationship of  $Ka$  to  $pH$  in one equation,  $Ka$  is often present as a logarithmic constant,  $pKa$  equal to  $-\log_{10}Ka$ .<sup>[50, 84]</sup> Equation 4.4 can now be written as:

$$Pka = pH - \log \frac{[A^-]}{[HA]} \quad (4.5)$$

According to Equation 4.5, an increase in  $pH$  of the solution means a reduction in the concentration of  $H_3O^+$  ions, such that  $Pka < pH$ . Thus, a corresponding increase in  $A^-$  ions is required to maintain the equilibrium state of the reaction in Equation 4.2. Consequently the equilibrium shifts toward right in Equation 4.2. For the basic groups of components the situation is similar and Equation 4.5 will now be defined as:

$$Pka = pH - \log \frac{[B]}{[BH^+]} \quad (4.6)$$

When  $pH$  decreases such that  $Pka > pH$ , the concentration of  $H_3O^+$  ions increases and a corresponding increase in  $BH^+$  ions is required to keep the system in equilibrium, for this reason Equation 4.3 shifts toward left.

In crude oil different types of acids and bases are presented and the strength of them will vary<sup>[50, 43]</sup>. The stronger the acid/base the higher the dissociation constant is.<sup>[33]</sup> According to Equations 4.5 and 4.6 this means, the stronger the acid the lower the  $Pka$  value is, hence the acid will be present in ionized form over a wide range of  $pH$ . For the basic groups, the stronger the base the higher the  $kb$  value is, but since the reaction in Equation 3.3 is presented with respect to  $ka$  value according to Equation 4.7<sup>[33]</sup>

$$Ka = \frac{kw}{kb} \quad (4.7)$$

the stronger the base the higher is the  $Pka$  value, and the ionized form of the molecule will be presented in a wide range of  $pH$ .

This indicates that over a wide range of conditions, positive and negative charges can co-exist at the interface and give the interface a zwitter ionic character dependent on the components available for ionization, and the composition of the aqueous phase.<sup>[2, 40]</sup> Even when the net charge is same as the

charge at the solid surface, adsorption can occur because of interaction with discrete oppositely charged sites.<sup>[40]</sup>

#### 4.3.2 Interaction with Divalent/Multivalent Ions present in the Brine Phase

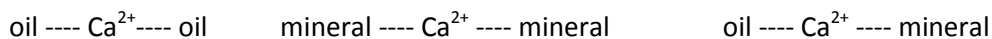
The bridging effect of divalent cations especially  $\text{Ca}^{2+}$  was mentioned previously in Chapter 3, but a more detailed description of the effect of these cations are given below.

Multivalent metal ions reported enhancing the complexity are  $\text{Ca}^{2+}$ ,  $\text{Mg}^{2+}$ ,  $\text{Cu}^{2+}$ ,  $\text{Ni}^{2+}$  and  $\text{Fe}^{3+}$ .<sup>[43]</sup> Present of these ions can mask the simple acid/base interaction between oil/brine and brine/solid interfaces.<sup>[2, 40]</sup>

Two important mechanisms of these multivalent ions which enhance the wettability alteration toward more oil-wet are: ( $\text{Ca}^{2+}$  used as example)

1) Bridging effect:<sup>[40, 42, 43]</sup>

Several interactions are possible when  $\text{Ca}^{2+}$  are present such as,



The first two interactions can limit wettability alteration, whereas the last one can promote it.

By ionic interaction with the opposite charged oil/brine interface, these ions can force the surfactants to bind to the solid surface, or the ions can adsorb at the solid surface and cause it to attract opposite charged surfactants at the oil/brine interface. Hence, if divalent cations are strongly bind to either or both interfaces (bridging between), they may become positively charged and impact the pure acid/base interaction of the system.<sup>[40]</sup> Investigations have reported that monovalent ions such as  $\text{Na}^+$  can cover the rock surface without destroying the pure acid/base interactions.<sup>[2]</sup>

In a work performed by Jadunandan and Morrow<sup>[38]</sup> the corefloods results with  $\text{NaCl}$  and  $\text{CaCl}_2$  solutions showed the rate and extent of spontaneous imbibition for Moutray crude oil with a high acid number and low base number, decreased with increasing calcium ion concentration, while for a basic North Sea crude oil the changes in calcium ion concentration had little effect. Wettability conclusion toward more oil-wet state in presence of  $\text{Ca}^{2+}$  ions in the solution was concluded based on

Amott wettability test. Buckley<sup>[2]</sup> explained the strong dependence of calcium ion concentration for Moutray crude oil could be due to the acidic nature of the crude oil.

## 2) “Salting out” effect:

The increase in preference for the oil phase or the solid surface with increasing brine salinity is called the “salting out effect”<sup>[53]</sup> and the opposite effect with increased solubility of polar organic species in water is called “salting in effect”.<sup>[54]</sup> In contact with water, polar organic species will be solvated by the formation of water structure created by hydrogen bonds around the hydrophobic part.

The organic species are in that way characterized as structure makers. Inorganic ions ( $\text{Ca}^{2+}$ ,  $\text{Mg}^{2+}$ ,  $\text{Na}^+$ ) tends to break up the water structure around the organic molecules, and then decrease the solubility of these in the water phase. These are therefore characterized as structure breakers. The relative strength of divalent ions as structure breakers are reflected in their hydration energy. Therefore, divalent ions have much stronger effect on the solubility of organic material in water.<sup>[54]</sup> For this reason, the “salting out effect” will increase the preference of the organic material for the oil phase or the solid surface, and thereby increase probability of wettability alteration toward more oil-wet.<sup>[53]</sup>

## 4.4 The Solid Phase

Mechanisms c) and d) and b), (b, if the interaction is dipol – ionic interaction) are influenced by the charge at the solid surface. Since crude oils used in this study are from North Sea sandstone reservoirs, measurements have been conducted with “sandstone” as solid surface.

The mineral quartz ( $\text{SiO}_2$ ) is the most common mineral type in sandstone reservoirs in addition to feldspar and clay minerals.<sup>[14]</sup> Compared with the bulk mineralogy, a variety of minerals may be present at the surface of the pores. In sandstone reservoirs, different clay minerals are attached to the sandstone grains as coating due to their large surface area.<sup>[14, 82]</sup> Clay minerals have a basic building stone of structural layers of silicon oxygen tetrahedron,  $\text{SiO}_4^{-4}$  sheets, and aluminium octahedral,  $\text{Al}(\text{OH})_6^{-3}$  sheets.<sup>[85]</sup> The building sheets of the basal surface and the edge surface can vary dependent on clay minerals. E.g. kaolin clay have basal surface building stone of  $\text{SiO}_4^{-4}$  sheets and edge building stone of  $\text{Al}(\text{OH})_6^{-3}$  sheets.

In clay minerals hydrolysis of broken  $\equiv SiO^-$  and  $=Al-OH$  along the surface of the clay lattice can cause the clay mineral charges to be pH dependent. The reactions are similar for those when quartz is exposed to water and are shown below.  $Al_2O_3$  have a point of zero charge (PZC) at pH 8.5, which is the point where the surface charge is zero. Above this point the surface is dominated by acidic species and are negative charged and below this point dominated by basic species and is positive charged.  $SiO_2$  has a PZC at pH 2. <sup>[14, 81]</sup> For this reason, clay minerals e.g. Kaolin clay can have positive charged  $= AlOH_2^+$  edges and negative charged  $\equiv SiO^-$  surface co-existing in a wide range of brine pH.

Mineral Surface used for Contact Angle Measurement:

Due to the large hysteresis observed when using a reservoir rock with surface roughness and heterogeneity which can significantly affect the measurements, smooth solid surfaces made of the main dominating mineral in the representing reservoir rock are normally used as the solid surface in contact angle measurements. <sup>[14, 22]</sup> For this reason quartz ( $SiO_2$ ) crystalline slides are normally used to model sandstone for contact angle measurements.

Quartz hydroxylate upon exposure to water <sup>[55]</sup> and form silanol ( $SiOH$ ) groups. <sup>[56]</sup> Dependent on the pH of the aqueous phase, the hydroxide functional groups at the surface can through ionization act as acids or bases which contribute to the surface charge at the brine/solid interface. Equations 4.8 and 4.9 present the acid and base reaction for the silanol groups: <sup>[14]</sup>



Due to the PZC at pH 2,  $\equiv SiOH$  and  $\equiv SiO^-$  will be the surface active sites in a wide range of pH. <sup>[14]</sup>



## 5 Fundamental Surface Forces

### 5.1 The Stability of the Water-film

The change in energy per unit area with change in distance as two interfaces is brought from a larger separation to a finite thickness is expressed as a force per unit area, named disjoining pressure,  $\Pi$ :

This force tends to disjoin or separate the oil/brine and brine/solid interfaces approaching each other, and is a result of intermolecular or interionic forces. Van der Waal forces and electrostatic forces were first introduced to describe the stability of lyophobic colloidal (solvent fearing) systems explained through DLVO. Later it was realized that these forces could also be used to explain the stability of the water-films between oil and solid in an oil reservoir, as these interactions also appear in colloidal dimensions.<sup>[18]</sup>

In addition to these forces, short range forces collectively called structural forces are also involved in describing the stability of the water-film (1-100 nm).<sup>[17, 18]</sup>

Equation 5.1 defines the total disjoining pressure as function of the three above mentioned forces.<sup>[57]</sup>

$$\Pi_{total} = \Pi_{Van\ der\ Waals} + \Pi_{electrical} + \Pi_{structural} \quad (5.1)$$

Equation 5.3 defines disjoining pressure related to the capillary pressure,  $P_c$ , which is the difference in phase pressure across the interface between two immiscible fluids at equilibrium condition, as defined by Young Laplace Equation 5.2.<sup>[23]</sup> When the interface between oil and water is parallel with the rock surface, the additional pressure in the water film has to be accounted for, and as long as  $P_c > P_c^{cri}$  where  $P_c^{cri}$  is the critical capillary pressure corresponding to the local maximum disjoining pressure (critical disjoining pressure), the water-film at the pore surface between oil/brine and brine/solid interfaces will remain stable.<sup>[23, 24]</sup> Since critical disjoining pressure is a function of the composition of the fluids in-situ, and the curvature of the interface, there can be a wide range of pressures in which film rupture occurs in a porous network dependent on the interactions between all these factors. This leads to selective film collapse in a porous network and is explained to be the reason for the different intermediate-wet classes defined in Chapter 2.<sup>[2, 24]</sup>

$$P_c = P_o - P_w = \sigma_{ow} \left( \frac{1}{R_1} + \frac{1}{R_2} \right) \quad (5.2)$$

$$P_c > P_c^{cri} = \Pi(h_{max}) + \sigma_{ow} \left( \frac{1}{R_1} + \frac{1}{R_2} \right) \quad (5.3)$$

Where the symbols represents:  $P_c$ : Capillary pressure,  $P_c^{cri}$ : Critical capillary pressure,  $\Pi$ : Disjoining pressure,  $P_o$ : Bulk oil pressure,  $P_w$ : Bulk water pressure,  $\sigma_{ow}$ : Interfacial tension between oil and water and  $R_1$  and  $R_2$ : Radii of curvatures at the relevant location of pore surface.

## 5.2 Disjoining Pressure - Contribution Forces

### 5.2.1 Van der Waal Interactions

Attractive van der Waal forces exist between all types of molecules and atoms, and are described as forces independent of ionic strength and the ions present in the aqueous medium, but the strength of the forces is dependent on distance between the interactions. Three types of van der Waal interactions exist: <sup>[19]</sup>

- 1) Dipole – Dipole interactions
- 2) Dipole – Induced dipole interactions
- 3) Induced dipole – Induced dipole interactions.

For macroscopic objects as colloids, van der Waal interactions between two particles (e.g. oil and solid) are calculated from the summation pair of interaction between all molecules in one object with all molecules in the other object. The attractive interaction energy is given as function of Hamaker constant  $A$ , which is a material constant representing the strength of van der Waal interactions between macroscopic bodies, and is an experimental measurable parameter. <sup>[58]</sup>

Van der Waal contribution of disjoining pressure is negative and cause water-film likely to rupture. <sup>[18]</sup>

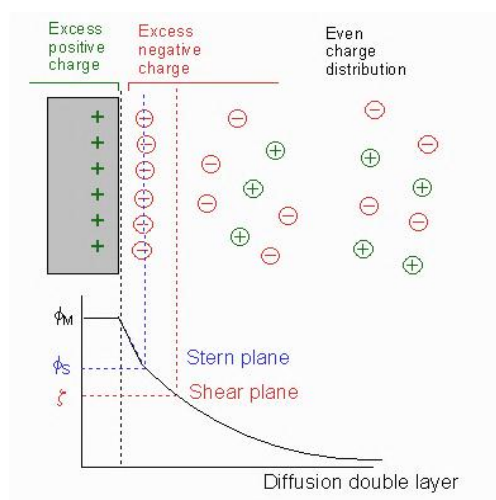
## 5.2.2 Electrostatic Interactions between Electrical Double Layers

The thickness of the water-film is primarily dependent on the presence of electrical double layer repulsion that results from charges being of the same sign at both interfaces. The range of repulsion depends directly on the ionic strength and pH of the aqueous phase.<sup>[2]</sup>

The example given below illustrates double layer interactions between two similar particles dispersed in water. The situation is similar for the interaction between crude oil and the rock surface dependent on the net charge at each interface.

The majority of colloidal particles will in contact with polar medium as water get an enrichment of surface charge as a consequence of ionization, ionic adsorption and ionic dissolution.<sup>[59]</sup> This charge distribution at the particle surface attracts charges with opposite sign (counter-ions) and repulses those with equal sign (co-ions) in the aqueous medium. As a consequence of the charge accumulation and the thermal movements of the ions, an electrical double layer is formed.

This double layer consists of two parts as illustrated in Figure 5.1. A stationary inner layer with particle surface (+) and counter-ions near the surface in the stern layer (-), and a diffuse layer with a higher concentration of counter ions nearest the stationary part, arranged under the influence of electrical forces and thermal movements. The double layer is arranged as the net charge is neutralized. Consequently an electric potential,  $\psi_0$ , due to the unlike charge distribution of co-ions at each side of the interface will develop. The electrical potential referred as surface potential decreases with increasing distance from the surface, and reaches zero at an imaginary boundary of the double layer.<sup>[19, 83]</sup>



**Figure 5.1:** A schematic illustration of the electrical double layer structure for positive charged solid surface, and the corresponding electrostatic potential curve.<sup>[83]</sup>

When two particles within a lyophobic colloidal system e.g. oil particles in water moves within the system, the interaction between them can be attractive or repulsive dependent on the thickness of the diffuse layer known as Debye length,  $\kappa^{-1}$ .<sup>[19]</sup>

Kappa,  $\kappa$ , is defined to be proportional with the ionic strength of an electrolyte solution which is a measure for the concentration of all ions present in the solution and is given as:<sup>[19]</sup>

$$I = \frac{1}{2} \sum Z_i^2 c_i \quad (5.4)$$

Where

I = ionic strength

$Z_i$  = the valency of the ionic species i

$c_i$  = molar concentration of ionic species i

This means  $\kappa^{-1}$  decrease with increasing ionic strength.

Two particles start to interact with each other at a distance equal to  $2\kappa^{-1}$ , and as they come closer the double layer interaction starts. As the counter-ion concentration near the shear plane increases for both charged particles, the two particles will due to the increase of similar charges as they come closer repulse each other. When the Debye length is screened due to high saline water, the two particles starts to interact with each other at very close distance, and as a result coagulation and flocculation occurs and the system gets destabilized.<sup>[58]</sup>

### 5.2.3 Structural Forces

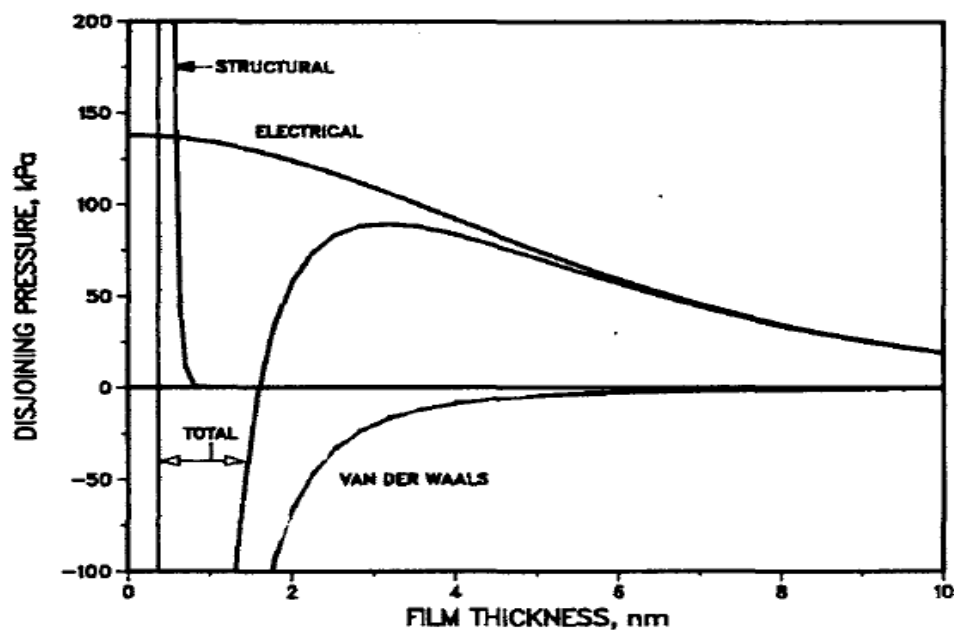
When the distance between oil/brine and brine/solid interfaces are separated by a distance of few molecular diameters, the short range interactions appearing in the system is described by short range forces. These forces are repulsive forces and are called solvation, structural or hydration forces (hydrogen bonds) when the medium is water, and are a result of the intermolecular structure of the water.<sup>[17, 18, 57]</sup>

## 5.2.4 Schematic Illustration of Disjoining Pressure – Summary of Force Contribution

A negative disjoining pressure attracts the two interfaces while a positive disjoining pressure repels the interfaces.<sup>[18]</sup> Figure 5.2 illustrates how the different forces contribute to net disjoining pressure.

When the distance between the interfaces or the thickness of the water-film referred to as the double layer is sufficient, the electrical double layer forces dominate at all distances as a result of similar surface charges at the brine/solid and oil/brine interfaces. Consequently, repulsive electrostatic forces will keep the disjoining pressure high, and maintain a water-wet rock surface.<sup>[2, 17, 18, 60, 61]</sup>

The strength of this repulsive force increases as the thickness of the double layer decreases as observed from Figure 5.2. The reduction in the thickness can be a consequence of salt and pH effects that can reduce the range of repulsion.<sup>[2, 17, 60, 61]</sup> However, at a distance equal to critical disjoining pressure, at the peak of the graph in Figure 5.2, the positive contribution of electrical double layer forces is destroyed, and van der Waals forces in addition to strong attractive electrostatic forces if present will govern the interaction, and the film is likely to rupture.<sup>[14, 18]</sup> This happens at distances below  $\Pi_{cri}$ . When an increase in salinity screens the Debye length, the electrostatic forces will be shielded, and thereby less important, but the stability of the water film can be maintained if structural forces are invoked.<sup>[17, 18]</sup> As can be seen from the figure, this force has a positive contribution to disjoining pressure at short distances. As a result of this force, the water-film still remains at the solid surface.



**Figure 5.2:** Schematic illustration of the individual force contributions to  $\Pi$ , and  $\Pi$  as a function of film thickness.<sup>[18]</sup>

### 5.3 Zeta Potential Measurement

The existence of electrical charges on the surface of particles causes them to show some specific effects, collectively defined as electro kinetic effects. One such effect is electrophoresis, which is the movement of the particles relative to the liquid they are suspended or emulsified in, under the influence of an applied electrical field. This velocity is experimental measureable, and with known electrophoretic mobility, zeta potential,  $\zeta$ , can be measured. The zeta potential is the potential at the surface of shear presented in Figure 5.1, which is an imaginary surface separating the stationary part from the moving part in an electrical double layer. The magnitude of this potential gives a measure for the net charge present at the particle surface (oil/brine and brine/solid interfaces) which is also a measure for the stability of the system. The dividing line between stable and unstable systems is generally taken at either + 30 mV or – 30 mV, and the sign ahead of the numbers represents the net charge.<sup>[62]</sup> Since zeta potential is a part of the double layer, the magnitude of this parameter is also strongly dependent on pH and salinity of the aqueous phase.<sup>[2, 62]</sup>

All crude oils reported in the literature show the same trend with respect to zeta potential measurements with net negative zeta potential value at high emulsion pH, and net positive value at low emulsion pH.<sup>[2, 60, 62, 63, 64]</sup> The absolute magnitude of the potential depends on the salinity of the aqueous phase within a given pH range.<sup>[2, 60, 61, 62]</sup> The same trend is observed for sandstone building minerals, like quartz, mica, and clay minerals such as kaolinite, montmorillonite and illite.<sup>[17, 65]</sup>

The transition from net positive to net negative charge for crude oils occurs after the isoelectric point (IEP) is reached. The IEP for crude oils are reported to be the point where negative charged acidic species and positive charged basic species are equally distributed and neutralise the oil surface, and thereby contributes to zero zeta potential. This point is reported to be the point where the colloidal system is least stable<sup>[62]</sup>

#### Salinity Dependency of Zeta Potential – Crude Oils

Figures 5.3 a) and b), present the results of a recently study performed by Nasralla et.al,<sup>[60]</sup> which presents the salinity dependence of zeta potential in a close to neutral pH for two crude oils emulsified in different brine salinities. Contact angle measurements conducted for the same oil/brine system with mica sheets, resulted in more water-wet behaviour as the salinity of the water reduced. Figure 5.4 a) and b) present the results of contact angle measurements conducted at 1000 psi and

100°C. However, an exception was the contact angle measured with sea water which showed the weakest water-wet behaviour, even when the salinity of formation brine was higher.

This trend was explained could be due to the high difference in sulphate ion concentration in sea-water compared with formation brine, but could also be related to the ratio of monovalent to divalent ions. As can be seen from the figures, crude oil A and B shows different behaviour with regard to both zeta potential and contact angle measurements. Changes in contact angle toward more water-wet behaviour, and higher negative charge as the salinity of the brine phase is reduced, is less with crude oil B compared with crude oil A. This evidence the impact of crude oil type and composition on the electro kinetic charges, but also that there is a relationship between surface charge and wettability alteration.

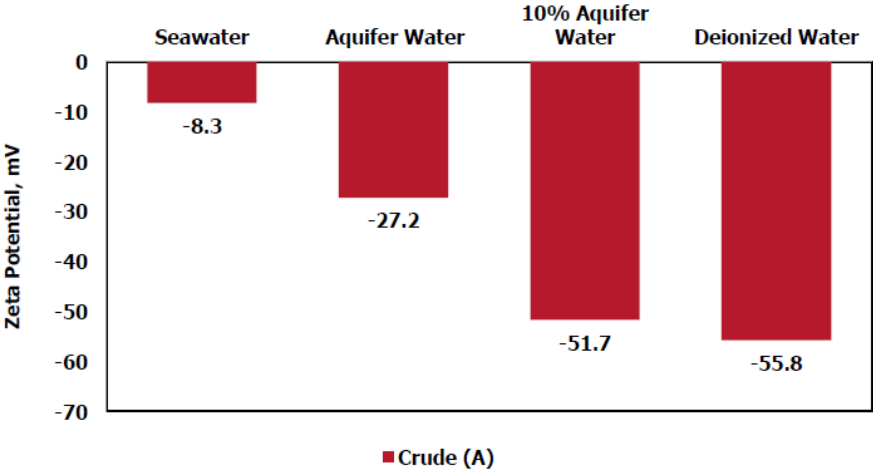


Figure 5.3.a) Impact of brine salinity on zeta potential value for crude oil A.<sup>[60]</sup>

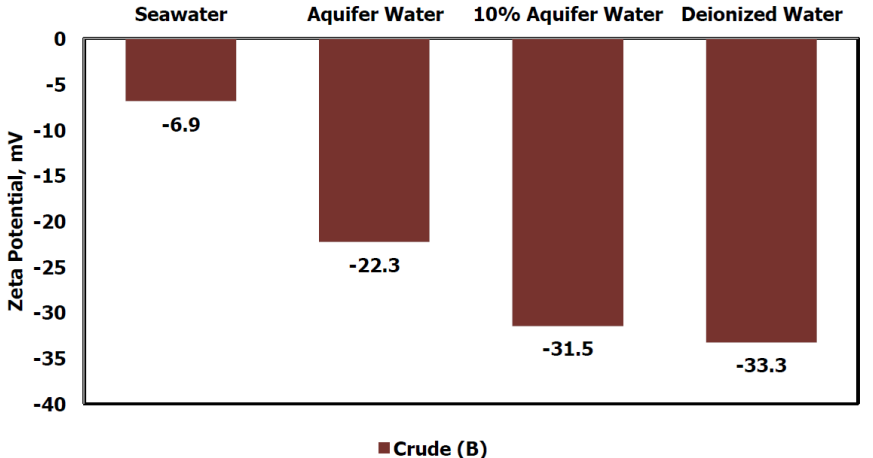
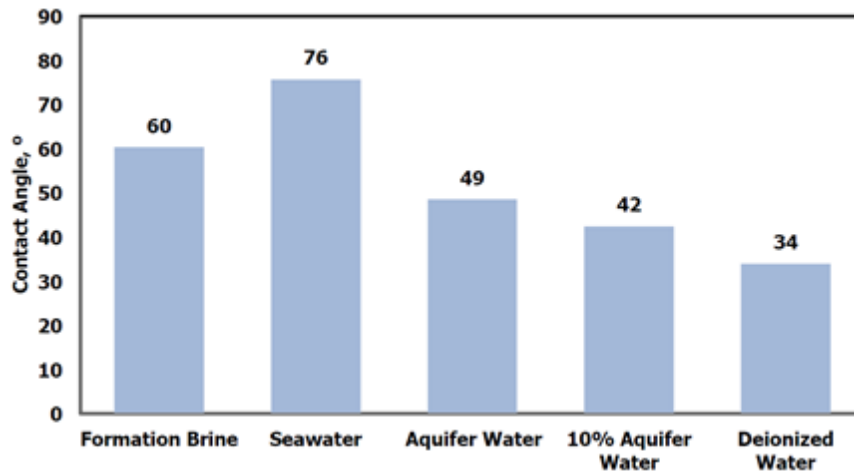
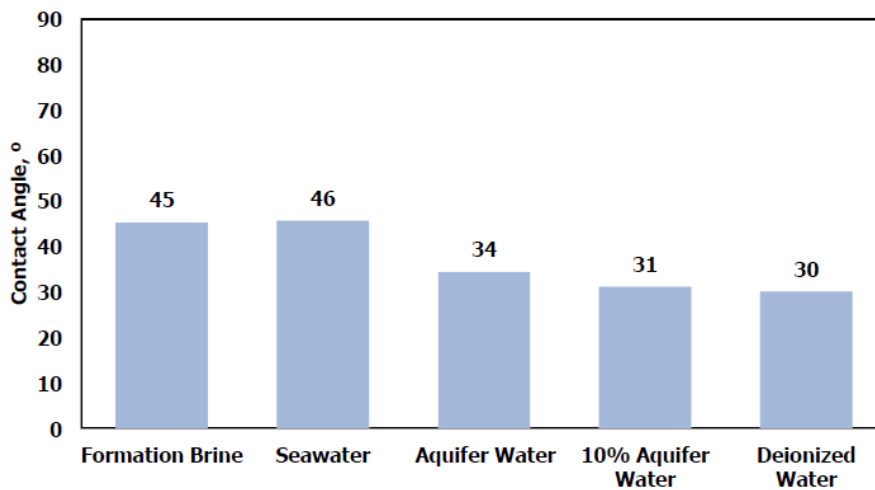


Figure 5.3 b) Impact of brine salinity on zeta potential value for crude oil B.<sup>[60]</sup>



**Figure 5.4 a)** Contact angle of crude oil A versus different brine salinity.<sup>[60]</sup>



**Figure 5.4 b)** Contact angle of crude oil B versus different brine salinity.<sup>[60]</sup>

In addition to contact angle measurements performed at fixed temperature, they studied the effect of changes in temperature on contact angle values and found a trend where contact angle increased with increase in temperature for both crude oils. However, stable contact angle values by increasing temperature<sup>[65]</sup> and increasing contact angle with increase in temperature and thereafter decreasing contact angle with further increase in temperature, have also been reported in the literature.<sup>[74]</sup>

One year later, the same team of Nasralla et al.<sup>[61]</sup> studied the effect of divalent and monovalent ions on zeta potential and contact angle measurements.  $\text{CaCl}_2$  and  $\text{NaCl}$  solutions with same concentration were used. The  $\text{CaCl}_2$  brine produced less negative charge at the oil/brine interface compared with the  $\text{NaCl}$  solution, and contact angle measurements on mica sheets showed more

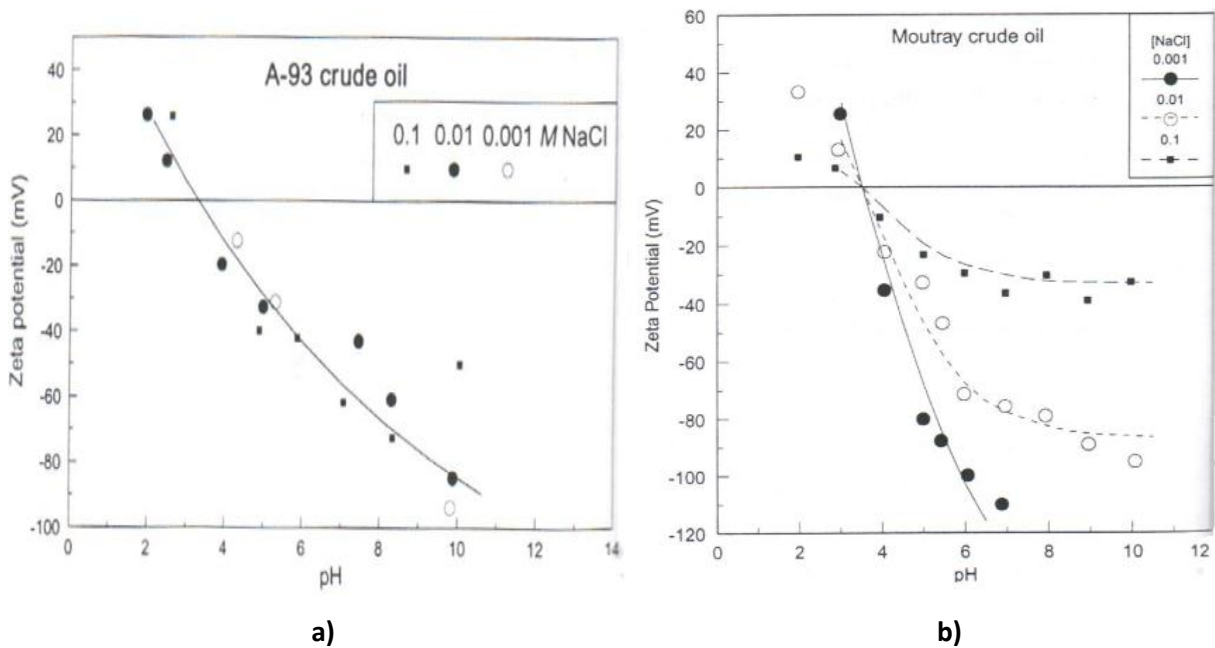


water-wet state for NaCl solution. Contact angle measurements were conducted at 500 psi and 100°C.

pH Dependency of Zeta Potential – Crude Oils

Figure 5.5 a) and b) illustrates zeta potential dependence on manipulated aqueous pH values for emulsions of Moutray crude oil and A-93 crude oil in brines of varying ionic strength. [2]

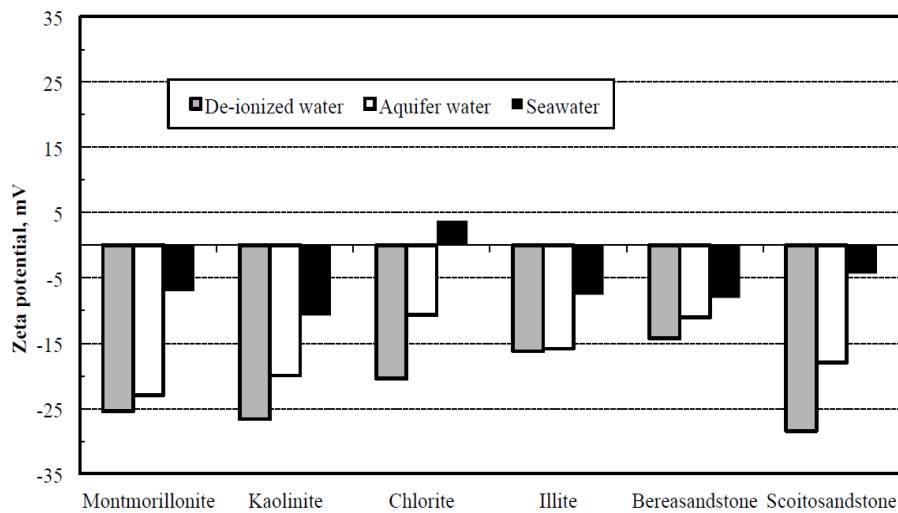
In the figures, the symbols represents the measured data while the dashed lines represents relationship of zeta potential to pH predicted by the ionisable site group (ISG) model. The ISG model is a mathematical tool used to provide an adequate description of the electrical property of crude oil/brine interface with changes in pH, by considering number of ionisable sites, acid/base constants and bulk concentration of the ions in solution. [2]



**Figure 5.5:** Zeta potential data for a) A-93 crude oil and b) Moutray crude oil as function of pH in various brine salinity, measured by Buckley [2]

### Salinity Dependency of Zeta Potential – Solid Surface

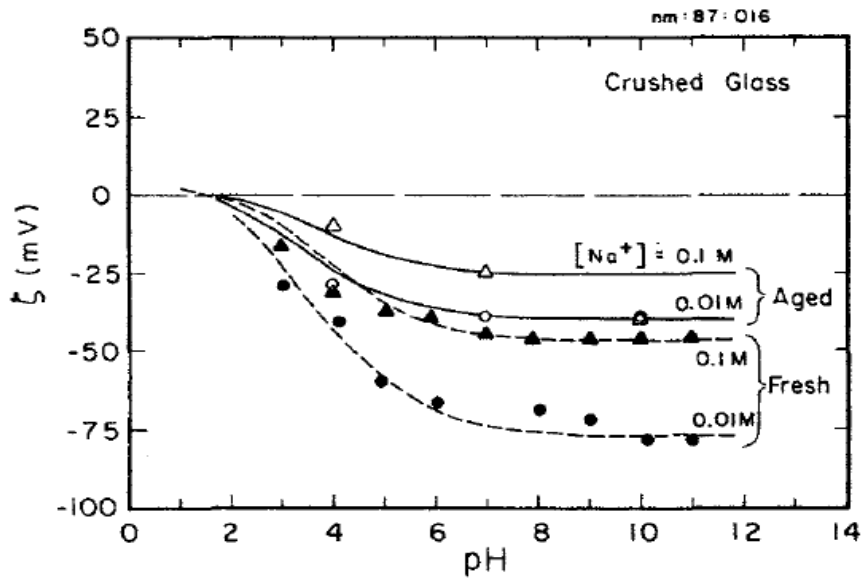
Alotaibi et al.<sup>[65]</sup> measured zeta potential as function of the same brine compositions as Nasrella et al.<sup>[60]</sup> used in their study, but now for different types of clay minerals and two types of sandstone suspensions. The same trend as for crude oils, with decreasing zeta potential as the brine salinity increased was observed. Figure 5.6 presents the results of their study. Farooq et al.<sup>[66]</sup> studied the effect of brine ionic valency ( $\text{Na}^+$ ,  $\text{Ca}^{2+}$  and  $\text{Mg}^{2+}$ ) on zeta potential magnitude for different minerals including silica, kaolinite and Berea sandstone. For the minerals it was found that  $\text{Ca}^{2+}$  and  $\text{Mg}^{2+}$  reduced the zeta potential values more than  $\text{Na}^+$  ions.



**Figure 5.6:** Zeta potential results for different clay minerals and two sandstones in various brine salinity.<sup>[65]</sup>

### pH Dependency of Zeta Potential – Solid Surface

The zeta potential dependency on modified pH for crushed silica glass ( $\text{SiO}_2$ ) in brines with varying salinity was measured by Buckley et al.,<sup>[17]</sup> and is presented in Figure 5.7 for both fresh and aged dispersions. The zeta potential decrease more at low concentration of NaCl, compared with high concentration at the same pH value, and the reduction is higher for the fresh suspension (1 hour aged) compared with the aged one (2-weeks aged).



**Figure 5.7:** Zeta potential as function of pH for different NaCl concentrations for crushed silica glass. Lines represent data predicted by the ISG model. <sup>[17]</sup>

## 5.4 Adhesion

In COBR system adhesion is defined as the preference the oil phase has for the rock surface initially covered by a water-film. <sup>[2, 25]</sup> To study the adhesion behaviour of crude oils, Buckley et al. <sup>[17]</sup> developed a simple test named adhesion test.

### 5.4.1 Adhesion Test

Adhesion test is a simple and less time consuming test used to study the range of impact on stability of the water -film by a specific crude oil, in a system consisting of a smooth solid mineral surface, one specific aqueous solution, and a set of dilutions of this aqueous phase at manipulated pH values. The standard test uses NaCl and dilution of this as the brine phase, but the main test procedure is the same independent of aqueous medium, and is as follows:

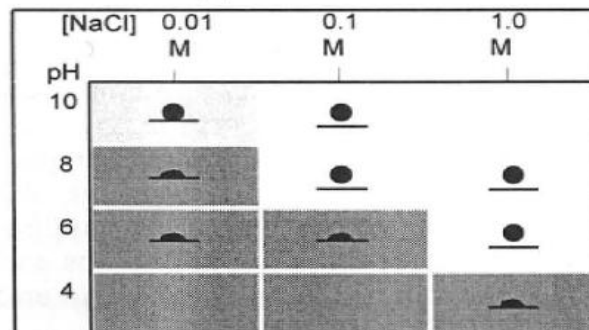
An oil droplet contacts a smooth glass surface placed in a test cell under brine for a standard time of 2 minutes. Upon withdrawal, one of two extremes of cases is usually observed. The oil droplet detaches from the solid surface, referred as non-adhesion, or the interface boundary remains pinned at the three phase line of contact, referred as adhesion. Since the test is repeated for a range of brine concentrations, a map of adhesive and non-adhesive behaviour as function of brine concentration

and pH can be constructed. An intermediate behaviour between adhesion and non-adhesion has also been reported to be observed, in this case the oil drop cling to the surface initially, but then detaches under the influence of their own buoyancy. This type of adhesion behaviour is named temporary adhesion.<sup>[2, 25]</sup>

Early standard adhesion studies performed by Buckley and Morrow<sup>[67]</sup> with 22 different crude oils, showed adhesion at low pH and non-adhesion at high pH, but the cut-off pH from adhesion to non-adhesion within the different salinity regions depended on the specific crude oil character.

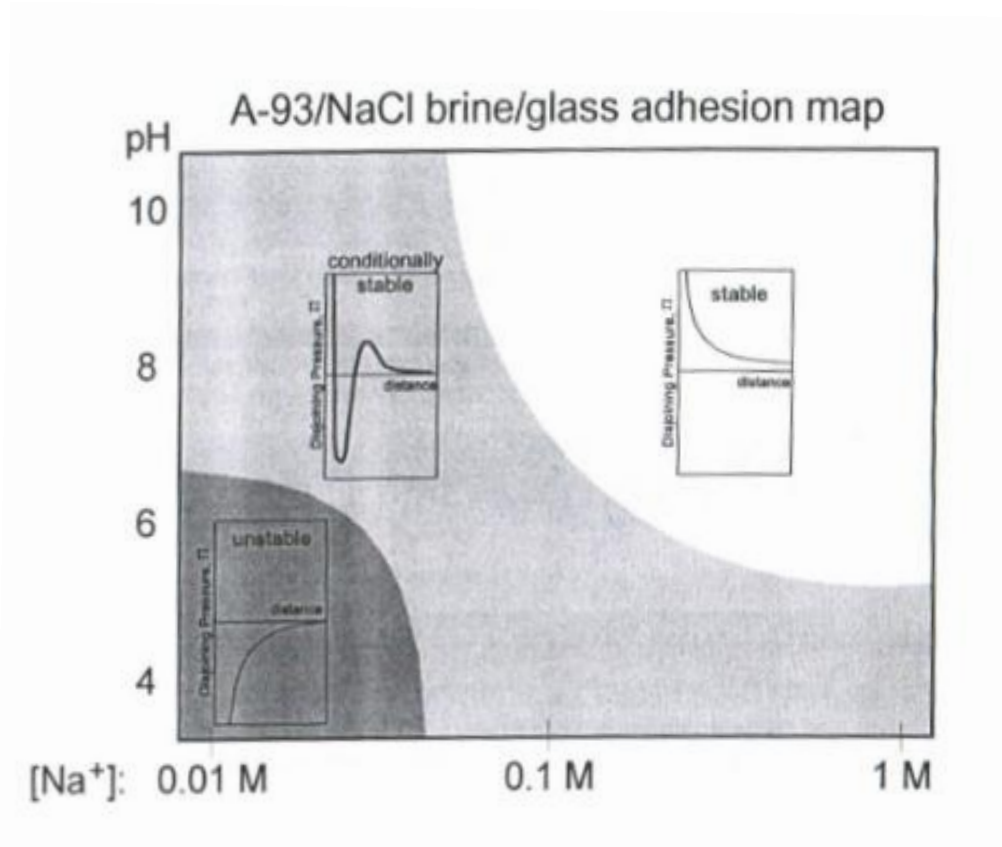
This test is an experimental evidence for the different adhesion behaviour of crude oils than predicted by DLVO calculations. Adhesion is observed with higher pH solutions and lower ionic strength than predicted by DLVO calculations, and at high salinity regions the stability of the system with non-adhesive behaviour is explained by structural forces.<sup>[17, 18]</sup>

Figure 5.8 shows a standard adhesion map for A-93 crude oil/NaCl brine/glass system at 25°C, where the behaviour deviating from DLVO calculations is observable.



**Figure 5.8:** Standard adhesion map for A-93 crude oil at 25°C.<sup>[2]</sup>

The adhesion map can also be present in terms of disjoining pressure with regard to the stability of the water-film, based on adhesion/non-adhesion behaviour. Figure 5.9 illustrate this map separated into three regions based on disjoining pressure property for the test results of A-93 crude oil at 25°C.



**Figure 5.9:** The adhesion test results for A-93 crude oil at 25°C, illustrated in terms of disjoining pressure in an adhesion map. [2]

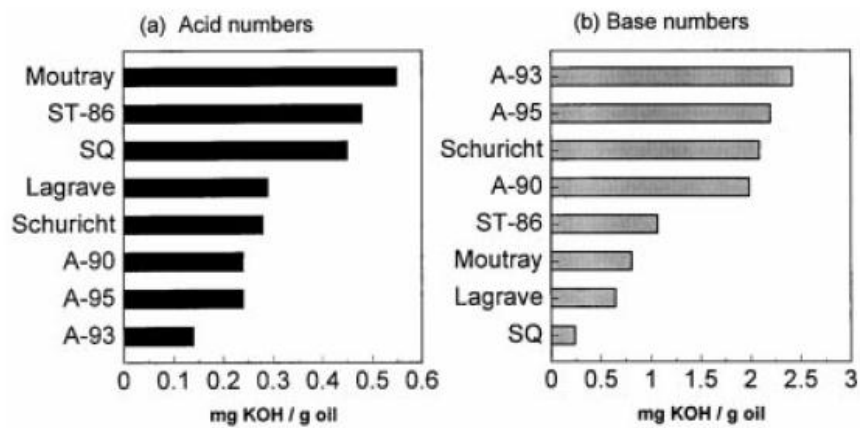
Adhesion occurs in the region where disjoining pressure is negative, meaning if the water-film is unstable and breaks, adhesion occurs. Non-adhesion occurs where the disjoining pressure is positive, thus in the region of stable water-film. In the region marked conditionally stable, disjoining pressure might be negative or positive dependent on the value of critical disjoining pressure, illustrated as the peak value in Figure 5.2 in Section 5.2.4 , which might be influenced by external variables as e.g. capillary pressure, temperature and solvent character of crude oil. [2, 52]

An explanation given in the literature for adhesion at silica surfaces occurring at higher pH values than predicted by DLVO calculations is related to the high base/acid ratio in crude oils.

Standal et.al. [48] found in their study with quartz surfaces a relationship between acid/base numbers and transition zone between adhesion/non-adhesion. As the base/acid ratio of crude oils decreased, cut-off pH from adhesion to non-adhesion also decreased.

This relationship also seems to explain the observed trend for A-93 crude oil. Figure 5.10 presents acid/base numbers for several crude oils including A-93, and illustrate the high base/acid ratio for

this crude oil.<sup>[2]</sup> Moutray crude oil has a high acid number compared with base number, thereby a low base/acid ratio. As can be expected, cut-off pH for this oil has been reported to be as follows: 0,01M NaCl-pH 5, 0,1 M NaCl-pH 6 and 1,0 M NaCl-pH 5.<sup>[67]</sup>



**Figure 5.10:** Acid and base numbers for different crude oils, including A-93 and Moutray crude oils.<sup>[2]</sup>

#### 5.4.2 Relationship between Adhesion /non -Adhesion and Contact Angles

Investigations with regard to contact angles in standard adhesion tests (NaCl solution) reports that oil drop maintains a low water receding angle during enlargement of the drop. In the case of adhesion, the advancing angle during withdrawal of oil drop is very high compared with the advancing angle in the case of non-adhesion, and when the liquid bridge ruptures, the area over which oil drop remains attached to the solid surface is generally strongly oil-wet. Thus, a standard adhesion test can simply distinguish between low and high advancing cases, with only regard to adhesive and non-adhesive behaviour of crude oils.<sup>[25]</sup>

#### 5.4.3 Adhesion in Mixed Brine

Buckley<sup>[2]</sup> performed adhesion test for A-93 crude oil in presence of reservoir brine and reported the adhesion trend to be non-adhesive for both 25°C and 80°C. This indicates different adhesion behaviours of crude oils in presence of mixed brines. For the same crude oil she observed the impact of divalent ions in a longer exposure adsorption test also developed by Buckley et.al.<sup>[42]</sup>

Detail description of this test is beyond the scope of this thesis as it has not been used in this study, but a brief summary of the procedure is as follows: Prior to contact angle measurement, the mineral surface is aged in a specific brine and thereafter aged in a specific crude oil for several days.

The mineral surface is then washed with a good solvent to remove the crude oil from the surface, before contact angle measurements are conducted with the cleaned mineral surface immersed in a light HC phase, with water droplet being placed on the solid surface. The strongest adsorbed crude oil species during the aging process are responsible for the high contact angles being measured.<sup>[2]</sup>

## 5.5 Oil/Water Interfacial Tension

The oil/brine interaction is described in terms of interfacial tension (IFT), a force acting in the boundary region between oil and water. The boundary layer separating oil and water is often only a few molecules diameters thick and sometimes only one molecule layer thick, and therefore considered as an area with zero thickness. The force acting in this region tends to reduce the area of this region due to an imbalance in the intermolecular forces that acts at this interface, compared with similar molecules in either of the bulk phases which experience balanced and equal attractive forces in all directions. The force per unit length that tend to reduce the interface area is termed surface tension (ST), when the boundary is between gas/solid or gas/liquid and IFT when the boundary is between liquid/liquid, liquid/solid or solid/solid.<sup>[58]</sup>

Equation 5.5 defines ST/IFT, and the common unit is dynes/cm or mN/m.<sup>[58]</sup>

$$\sigma = \frac{dF}{dx} \quad (5.5)$$

The stronger the intermolecular interactions between the molecules at the interface region and the bulk phases are, the higher the ST/IFT are. But a reduction in the strength of this interaction will reduce ST/IFT, and can be obtained by the presence of surfactants present in the interface region.<sup>[68]</sup>

In crude oil/brine systems, changes in IFT as function of pH provides another indication with zeta potential measurements, that acidic and basic species are active at crude oil/brine interface.

The interfacial tension value does not only depend on the polar organic species present in the interface region between oil/brine and the composition of the aqueous phase, but also on the length

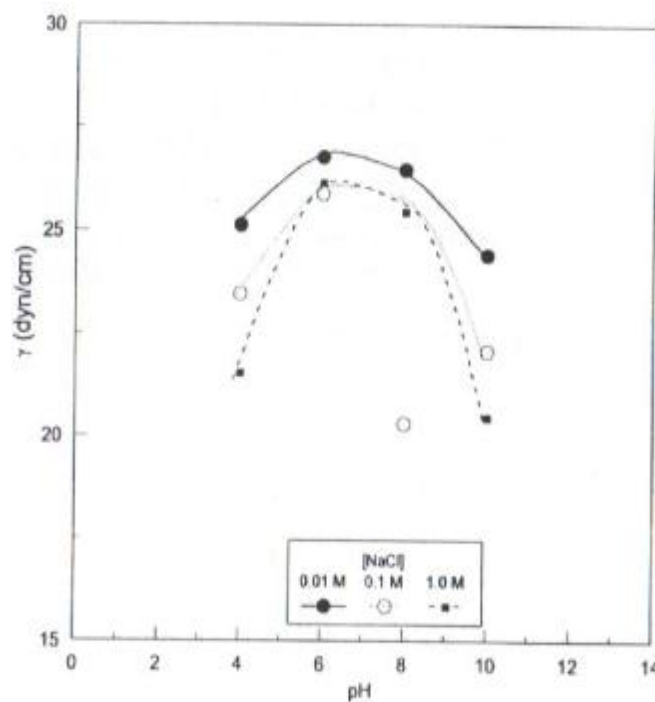
of time the phases are in contact before measurements are conducted, temperature and pressure has sufficient impact on the results. [64]

Buckley<sup>[2]</sup> measured IFT as function of pH and various NaCl concentrations for A-93 crude oil, and found IFT to be highest near neutral pH and lowest at low or high pH ranges, as illustrated in Figure 5.11. As can be seen from the figure, IFT curve is higher for the lowest NaCl (0,01M) concentration at a given pH value, compared with high salinity NaCl solution (1,0 M).

For Moutray crude oil, she observed another trend in IFT as function of pH for 0,01M NaCl brine.

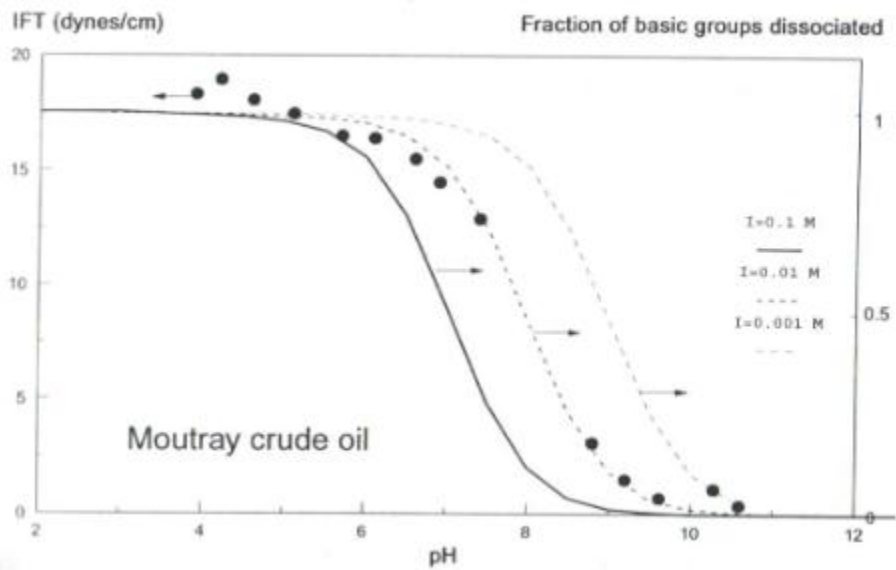
In this case, the IFT was nearly constant at low pH values and decreased with increase in pH.

Figure 5.12 illustrate this trend. Similar trend was observed for ST-86 crude oil. This indicates that the ionic form of the acidic species acts as surfactants that reduce the interfacial tension as dissociation of them take place while pH is increased. The acid/base numbers for these crude oils were presented in Figure 5.10, these numbers together with the IFT curves presented in Figure 5.11 and 5.12 indicates that crude oils with high acid number and high base number to show different IFT trends.



**Figure 5.11:** Interfacial tension as function of pH in various brine salinity for A-93 crude oil. Lines represent data predicted by ISG model. [2]





**Figure 5.12:** Interfacial tension as function of pH in various brine salinity for Moutray crude oil. Lines represent data predicted by ISG model. [2]

Standal et al. [48] found a similar relationship for 3 North Sea crude oils with 0,1M NaCl solution, where the IFT was highest for the oil with highest base number, and lowest for the oil with low acid number at pH 5 to 10. Contact angle measurements performed on quartz glass slides also showed a more water-wet behaviour with high acid number and more oil-wet behaviour with high base number.

### 5.5.1 Salinity Effect on IFT

Without taking into account any modified change in pH of the brine phase, but looking at the salinity effect (neutral pH) on IFT, interesting results and slightly different results have been reported. Some of these most recently results are discussed below.

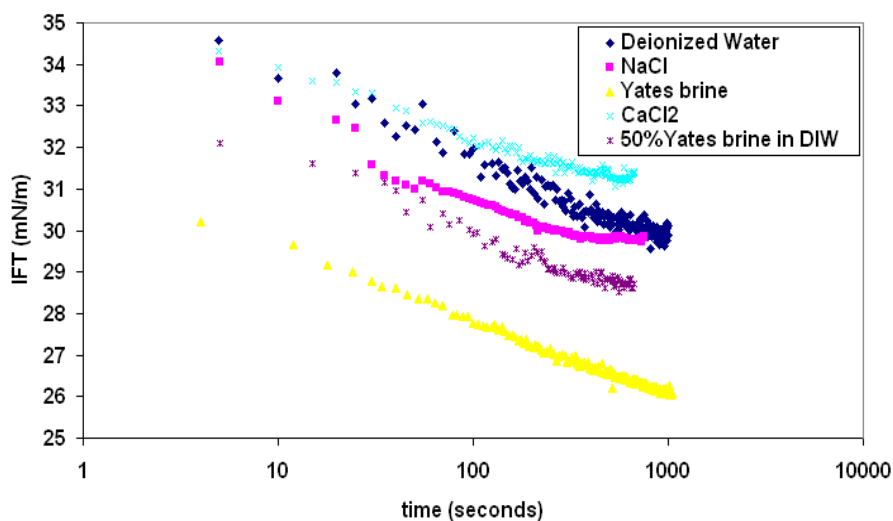
Abdel-Wali [69] studied the impact of salinity and polar organic compound on interfacial tension by varying the concentration of the organic compound in crude oil and the salinity of the brine phase. Oleic acid represented the polar compound, and the brine salinity was varied between 0 – 200,000 ppm NaCl. At a specific acid concentration and salinity of 40,000 ppm, IFT minimum was reached. The oleic acid was acting as an anionic surfactant. Increasing the salinity further increased the IFT.

He concluded this to be a result of the reduced solubility of acid in the water phase, as salt increased (“Salting out” effect).

Standal et.al.<sup>[50]</sup> found a similar relationship with decrease in IFT as the ionic form of the acid became surface active. The increase in ionic form of the molecule was also proportional with the preference for the water phase. IFT was lower for oil/0,5 M NaCl solution, compared with the IFT for the oil/distilled water at same concentration of the acidic component dissolved in isooctane modelling the oil phase. This was the observation even when the preference for the water phase was measured to decrease with increasing salinity.

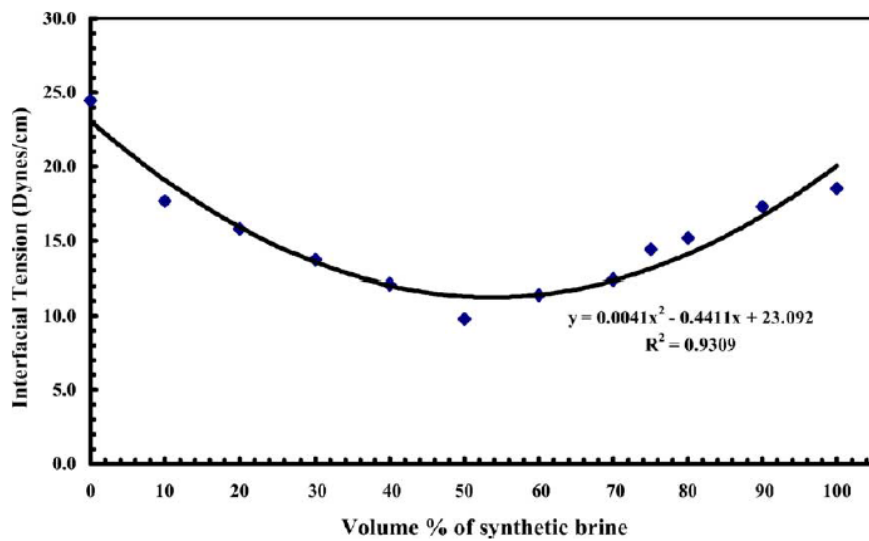
IFT studies with formation brines and synthetic reservoir brines have been performed by Xu,<sup>[68]</sup> Vijapurapu and Rao,<sup>[70]</sup> and Yousef et al.<sup>[49]</sup>

Xu measured the IFT between Yates crude oil and aqueous solutions represented by Yates formation brine, diluted formation brine with 50% distilled water, NaCl solution, CaCl<sub>2</sub> solution and pure deionized water. The dilution of the brine phase increased the IFT, compared with the original brine results. IFT between crude oil and deionized water was even higher. The IFT in the divalent ions solution was higher than for the monovalent system. Figure 5.13 presents the IFT results as function of time. Pendant drop method was used to conduct the measurements, and with this method it is possible to measure the IFT changes as function of time, since a software program called drop shape analysis (DSA) connected to a camera, continuously record the pendant oil drop form in a test cell and thereby contributes the software program to monitor changes in IFT.



**Figure 5.13:** Interfacial tension between Yates crude oil with different brines, performed at ambient conditions<sup>[68]</sup>

Vijapurapu and Rao<sup>[70]</sup> observed a similar trend in their study with Yates crude oil, Yates formation brine and diluted formation brine with 50% distilled water at ambient conditions. But they investigated a wider salinity area, and found that IFT reduced initially when diluting the formation brine with deionized water up to twice dilution, but further reduction increased the IFT. Similar trend was observed in the study conducted with synthetic reservoir brine to see if it behaved in the same way as the reservoir brine. Figure 5.14 presents their results obtained for the synthetic reservoir brine system.



**Figure 5.14:** IFT measurements for Yates crude oil and synthetic reservoir brine/diluted brine system at ambient conditions.<sup>[70]</sup>

Yousef et al.<sup>[49]</sup> observed an opposite trend than observed in the study by Xu, Vijapurapu and Rao. In their work, IFT studies were performed with a carbonate crude oil and different brines including synthetic field connate water, seawater and different diluted versions of seawater. They observed a general trend whereas the salinity decreased, the IFT decreased. Reduction from connate brine to sea water was  $\sim 5$  mN/m, further dilution of the sea water with factors of 2, 10 and 20 reduced the IFT with  $\sim 2$  mN/m between the dilutions, while less reduction was observed with the 100 times diluted sea water.

In a study performed by Hamouda and Karoussi,<sup>[71]</sup> IFT measurement between 0,005 M stearic acid in decane and 0,1 M concentration of sodium sulphate or magnesium chloride was performed to study the effect of these ions in saline water. Their results showed IFT in presence of magnesium ions to show lower IFT value than for the system with sulphate ions present in the water or for distilled

water, respectively. This trend was also observable in a wide range of temperatures, which showed decrease in IFT as the temperature increased. (From 40.1 at 28°C and 35.7 mN/m at 70°C)

## 6 Experimental Work

This chapter provides a detail description of the experimental work. The chapter is divided into two sections. The first section describes the fluids, solid and chemicals used in the experiments, while the second section describes the experimental equipment and apparatus used for the different measurement, including description of the method, procedure, experimental set up and problems associated or observed with the method. All the measurements have been conducted at ambient condition (20-23 °C, ~ 1 atm).

### 6.1 Fluids, Solid and Chemicals

#### 6.1.1 Crude Oils

Two North Sea crude oils produced from the same field but different wells named A-12 and Exp-12 were the main crude oils used in this study. Acid number and viscosity data for these crude oils were obtained from previously measured data at our laboratory.

A third crude oil named crude oil A from the same field, but a different well was analysed by Bøe<sup>[47]</sup> who measured both acid and base numbers and performed analysis of crude oil composition by SARA fractionation method for this crude oil. Table 6.1 presents acid and base numbers and viscosity data at ambient conditions for the different crude oils, and Table 6.2 presents the SARA fractionation data in weight percentage (wt%) for crude oil A.

Crude oil	Acid number* [mg KOH /g oil]	Base number* [mg KOH /g oil]	Viscosity, $\mu$ [mPa.s]
A-12*	$3.61 \pm 0.04$		$72.10 \pm 0.10$
Exp – 12	$2.96 \pm 0.05$		$24.10 \pm 0.10$
A	$2.84 \pm 0.01$	$0.95 \pm 0.01$	

**Table 6.1:** Acid/base numbers and viscosity data for crude oils A12, Exp-12 and A.

\* A12 - filtered crude oil. \* Acid number = mg base required to neutralize 1 g acid in crude oil.

\* Base number = mg base in 1 g crude oil.<sup>[47]</sup>

Saturated [wt%]	Aromatics [wt%]	Resins [wt%]	Asphaltenes [wt%]
55.0	38.0	6.2	0.7

**Table 6.2:** SARA fractionation data for crude oil A.<sup>[47]</sup>

Crude oil Exp-12 was diluted with the chemicals Xylene and Iododecane. The main crude oil mixture used in coreflooding experiments consists of 60% crude oil, 20% Xylene and 20% Iododecane in volume percentage. To study the individual effect of Xylene and Iododecane, Exp-12 crude was in addition to the combined mixture, mixed in three different portions selected to be 5%, 10% and 20% with Xylene for itself and Iododecane for itself. The mixtures were prepared based on weight.

The individual mixtures were made in smaller quantities and put on stir for 15-20 minutes after they were made, while the main mixture was made in a larger quantity and put on stir for 1 day to obtain uniformly mixed oil. Table 6.3 lists the mixed crude oils used in this study, and the shortened name of these crude oils that will be used when presenting and discussing the experimental results in Chapter 7.

Crude oil + solvent	Volume percentage [%]	Name	Organic liquid property
Exp-12 + Xylene X = Xylene	5% X + 95% Oil	Exp-X-5	Aromatic HC = Benzene ring with two methyl substituents $C_6H_4(CH_3)_2$
	10% X + 90% Oil	Exp-X-10	
	20% X + 80% Oil	Exp-X-20	
Exp-12 + Iododecane I = Iododecane	5% I + 95% Oil	Exp-I-5	Iodine + Alkan = Decane with one Hydrogen atom substituted with Iodine $(CH_3)(CH_2)_8CH_2I$
	10% I + 90% Oil	Exp-I-10	
	20% I + 80% Oil	EXP-I-20	
Exp-12 + Xylene + Iododecane	20% X + 20% I + 60% Oil	EXP-12-D (D = Diluted)	

**Table 6.3:** Crude oil mixtures with Xylene and Iododecane.

To prevent contact with light that can cause photochemical reactions, and oxygen that can alter surface properties of the crude oils, the crude oil bottles were sealed with thermoplastic film and placed in a dark environment.

The crude oils used for LSW studies were Exp-12 , A12- and Exp-12-D, while the different portion of the individually Xylene added and Iododecane added crude oils were only studied in presence of HSW.

### 6.1.2 Brines

SSW and dilutions of this have been used as the brine phases for the measurements.

The composition of the SSW used in this study is typical to that of the North Sea water, where the poisonous chemicals like Barium and Strontium is eliminated. Table 6.4 lists the chemical composition of SSW. The different salts listed in the table were dissolved in distilled water to make the SSW with TDS about 44500 ppm. The SSW was then put on stir for one day after it was made to obtain a uniformly mixed salt solution, followed by filtering of it by using a 0,45 $\mu$ m vacuum filter from Pall Corporation, in order to remove impurities from the brine.

Salt	Mass [g]	Concentration of salt [ppm]	Manufacturer
NaCl	124.45	25999	Sigma-Aldrich
Na <sub>2</sub> SO <sub>4</sub>	8.63	1803	Sigma-Aldrich
NaHCO <sub>3</sub>	55.62	11620	Fluka-Chemika
KCl	0.96	201	Fluka-Chemika
CaCl <sub>2</sub> ·2H <sub>2</sub> O	20.28	4237	Sigma-Aldrich
MgCl <sub>2</sub> ·6H <sub>2</sub> O	3.34	698	Fluka-Chemika
H <sub>2</sub> O – Distilled water	4786.72	0	
Total	5000.00	44558	

**Table 6.4:** *Composition of high salinity water (SSW), in total 5 kg.*

SSW was diluted by factors of 2, 10 and 100. The dilution was made based on weight. The amounts of TDS in these brines are displayed in Table 6.5.

Volume percentage [%]	Concentration of salt [ppm]
1% SSW – 99% distilled water	446
10% SSW – 90% distilled water	4456
50% SSW – 50% distilled water	22279

**Table 6.5:** *Diluted SSW composition and concentration.*

With respect to the definition of LSW as water containing no more than 6000 ppm, 1% and 10% SSW brines can be defined as the LSW's used in this study.

### 6.1.3 Solid

Microscope glass slides (20 ×48 mm) with the main dominating mineral quartz (SiO<sub>2</sub>) from the manufacturer Menzel-Gläser (Germany), were used as solid surface for contact angle measurements and adhesion test. The chemical composition of the glass slides is given in Table 6.6.

Chemicals	SiO <sub>2</sub>	Na <sub>2</sub> O	K <sub>2</sub> O	CaO	MgO	Al <sub>2</sub> O <sub>3</sub>	Fe <sub>2</sub> O <sub>3</sub>	SO <sub>3</sub>
Content [weight%]	72.20	14.30	1.20	6.40	4.30	1.20	0.03	0.30

**Table 6.6:** *Chemical composition of microscope glass slides used for adhesion test and contact angle measurements.<sup>[77]</sup>*

Washing procedures of these glass slides are of great importance as even small impurities can indicate incorrect measurement, and reduce the reproducibility of the measurements. To achieve good reproducibility it is important to wash and treat all the glass slides in similar manner.<sup>[2]</sup>

A standard washing procedure for glass slides being used in adhesion test has been developed by Buckley<sup>[2]</sup> and is described below. The quality of the normal washing procedure with detergent and



water was compared with the washing procedure proposed by Buckley, by comparing contact angle measurement data for a set of COBR systems.

#### Standard Washing Procedure for Glass Slides<sup>[2]</sup>

1. The procedure starts with cleaning of the glass slides for at least 15 minutes with ultrasonic vibration in a solution of 9 parts H<sub>2</sub>O<sub>2</sub>, 30% and 1 part NH<sub>4</sub>OH, 20%.
2. The glass slides are then removed from the cleaning solution and washed with distilled water.
3. Thereafter, the slides are soaked in measurement brine for some days before measurements are conducted.

#### Normal Washing Procedure for Glass Slides

In the normal washing procedure, diluted detergent and a soft cloth brush was used to clean the glass slides. To remove the detergent, the slides were washed under sufficient tap water followed by rinsing with distilled water. Thereafter, the slides were soaked in the measurement brine 1-2 days, as earlier studies in our laboratory have shown to be sufficient aging period before measurements were conducted.

### **6.1.4 Chemicals for pH Adjustment**

The brine composition was in addition to salinity varied with regard to pH for adhesion test, IFT and zeta potential measurements. 1M NaOH base and 1M HCl acid were used to adjust the desired pH values. pH adjustments were made during stirring to ensure a homogenous distribution of the H<sup>+</sup> or OH<sup>-</sup> ions in the solution. The time of pH stabilization varied from 5-10 minutes.

### **6.1.5 Chemicals for Washing Procedures of Equipment**

#### Chemical Wash to Remove Crude Oil

Chemical wash with organic liquid is required to remove crude oil from equipment. As several different crude oil compositions have been used in this study, washing of equipment between each measurement with different crude oils was required. Toluene (C<sub>6</sub>H<sub>5</sub>(CH<sub>3</sub>)) which is a good solvent to remove crude oil was used to wash away crude oil from the equipment, followed by rinsing with

methanol (CH<sub>3</sub>OH) required to remove toluene, and distilled water to remove methanol. As a final procedure the equipment was rinsed well with distilled water.

#### Chemical to Wash Capillary Needle

The capillary needle used for contact angle and IFT measurement had a high affinity for the oil phase, especially for the Xylene added crude oil. For this reason, to make the needle more water-wet prior to measurements with Xylene added crude oils, the capillary needle was for 15 minutes immersed in water dissolved with 1-2 droplets of the detergent Sodosil, and thereafter immersed in hot water to rinse the needle for detergent in new 15 minutes. Finally the needle was washed well with distilled water.

## **6.2 Experimental Apparatus, Equipment and Procedures**

### **6.2.1 IFT Measurements - Drop-Volume Method**

The drop-volume method was used to measure the interfacial tension between a set of crude oils and brines. 3-5 parallels were performed for each combination of oil and aqueous phase.

#### Description

The drop-volume method is based on measuring the volume of oil droplets being formed at the end of an inverted capillary needle, mounted to a micrometer syringe and immersed in brine.

The volume of a droplet is slowly and continuously increased until it becomes large enough to break completely free from the tip. In this method the volume of a droplet is found from the mean volume of a set of droplets, and was in this study chosen to be 10.

By using Harkins-Brown equation, IFT can be measured:<sup>[79]</sup>

$$\sigma = \frac{V \cdot \Delta \rho \cdot g}{2\pi \cdot r \cdot F} \quad (6.1)$$

Where:

$\sigma$  = Interfacial tension between oil and water (mN/m)

V = Volume of the oil droplet (mean value)  $\text{cm}^3$

$\Delta\rho$  = Density difference between the oil phase and the aqueous phase ( $\text{g}/\text{cm}^3$ )

g = Gravity ( $\text{m}/\text{s}^2$ )

r = Radius of the inverted needle (m)

F = Empirical correlation coefficient, dimensionless

Density data is the only external data required to measure IFT according to Harkins-Brown equation. All the other data can be measured internal with the method. The radius of the inverted needle is found by measuring drop volume of pure HC compounds with known oil/water interfacial tension. n-Deane/water with IFT equal to 51.2 mN/m,<sup>[80]</sup> was used in this study.

To convert the micrometer readings ( $\mu\text{m}$ ) into volume ( $\text{m}^3$ ), weight calibration of the micrometer syringe is conducted with a fluid e.g., distilled water as chosen in this study. This gives a value for the gram of liquid that disappears per micrometer the piston inside the syringe is displaced. Weight calibration value multiplied with the micrometer readings gives a measure for the mass, which can then be converted to volume according to Equation 6.2:

$$\rho = \frac{m}{V} \quad (6.2)$$

Where:

$\rho$  = Density of the fluid ( $\text{g}/\text{cm}^3$ )

m = Mass of fluid (g)

V = Volume of fluid ( $\text{cm}^3$ )

The empirical correlation factor is a measure for the residual oil that remains on the tip after an oil droplet has pinched off. This correlation factor is a function of the tip radius and the drop volume as given below:<sup>[79]</sup>

$$F = 0.4293 \cdot \left(\frac{r}{V^{1/3}}\right)^2 - 0.7249 \cdot \left(\frac{r}{V^{1/3}}\right) + 0.9054 \quad (6.3)$$

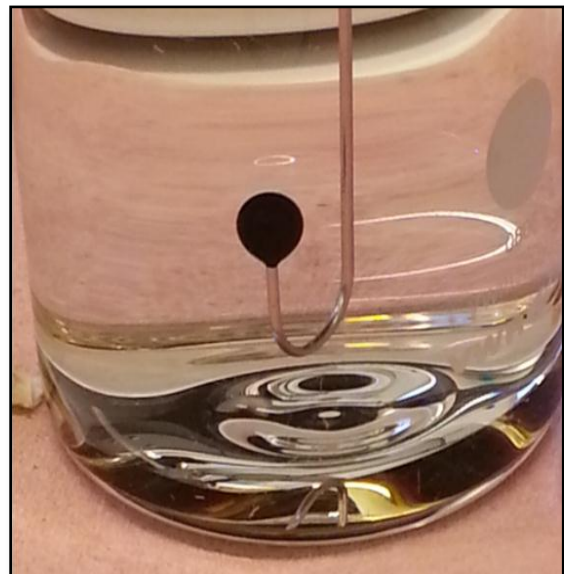
## Experimental Setup and Procedure

Figure 6.1 a) illustrate the experimental setup of the drop-volume method. As can be seen from the figure, a laboratory stand was used to hold the Burkard manufactured 10 mL glass micrometer syringe filled with crude oil. This was required to achieve stable measurements.

Figure 6.1 b) illustrate a close-up picture of an oil droplet being formed at the tip of the needle immersed in brine. As observed from the figures, especially Figure 6.1 a), it is important to mount the syringe as the tip of the needle is deeply immersed in brine. This is to avoid affinity of the oil droplet being formed for the water surface covered by previously broken oil droplets, which remains as film on the surface; otherwise the affinity will make the oil droplet to leave the tip before the maximum volume is reached, and will thereby indicate incorrect volume data.



a)



b)

**Figure 6.1:** *The experimental setup of drop-volume method. Figure 6.1 a) displays the mounting of equipment and 6.1 b) displays a close-up picture of an oil droplet being formed at the tip of the inverted capillary needle*

## The Fluids

Crude oils and brines were not pre-equilibrated prior to IFT measurements.

All the crude oils presented in Section 6.1.1 were investigated for interfacial properties.

The pH adjustment according to the procedure described in Section 6.1.4, was for IFT measurements adjusted at the day of measurement.

## Problems Observed/Associated with the Method

The stainless steel needle had a high affinity for the oil phase (Xylene added crude oils).

To make the needle more water-wet prior to measurement, washing procedure with Sodosil was made according to the procedure given in Section 6.1.5.

Some problems occurred when measuring IFT for high salinity solutions in high pH regions.

The droplets became more deformed with increased affinity for the needle and thereby made the volume measurements more complicated. This can be a consequence of the reduced IFT between crude oil and water in these regions, but also a consequence of the observed precipitate formed in these solutions. Fosse<sup>[78]</sup> has reported changing the inverted capillary with a capillary consisting of a smaller radius, which is believed to increase the drop volume, made the volume measurements rather more complicated.

It is important that no air bubbles are involved when oil is drawn into the syringe.

When air bubbles were involved during the measurements, they caused oil to leak out from the tip of the syringe, and consequently contaminated the brine phase. Leakage was also observed when the screws holding the syringe in place were not tightened enough, but it was important that hard squeezes of the screws also was avoided as the syringe was made of glass.

## The Washing Procedure

The glass syringe and the needle were washed according to the washing procedure given in Section 6.1.5 between the different crude oils, and dried with an air blow gun.

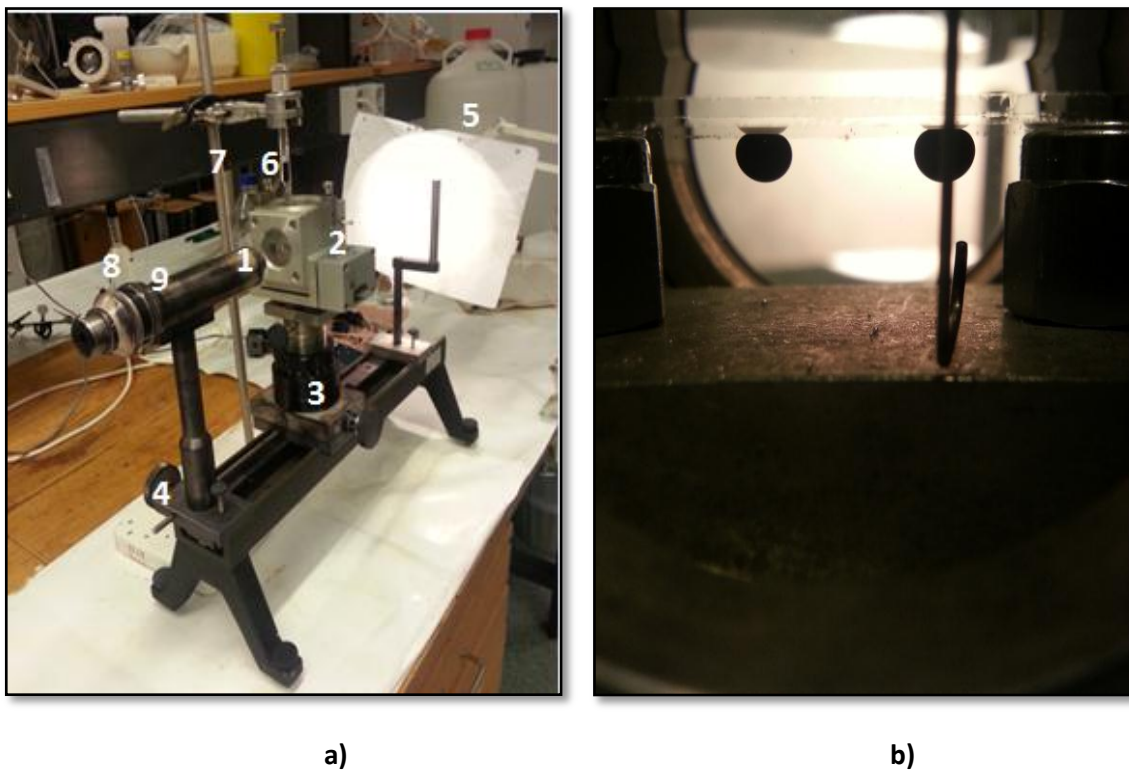
## 6.2.2 Contact Angle Measurements – Sessile Drop Method

Contact angle measurements were performed by the sessile drop method using a NRL Contact Angle Goniometer (CAG) from Ramè-Hart model 100-00, and a 1 mL Hamilton syringe mounted with an inverted capillary needle. The instrumental setup allowed only measurement of static equilibrated receding angles,  $\theta_{e,r}$ , initiated by dynamic water receding angle,  $\theta_r$ . Approximately 3-5 parallels were performed for each combination of oil and aqueous phase.

### Description, Experimental Setup and Procedure

The method is based on direct readings of contact angles of an oil droplet placed on the solid surface immersed in brine, by use of an adjustable lens system with an incorporated degree scale.

Figure 6.2 a) and b) illustrate the experimental setup of this method. Figure 6.2 a), displays the entire experimental setup with goniometer, syringe and the light source. The numbers will be used to refer to the figure when describing the different parts of the instrument and the experimental setup. Figure 6.2 b), displays a close up picture of the droplets placed under the quartz surface immersed in brine in the test chamber.



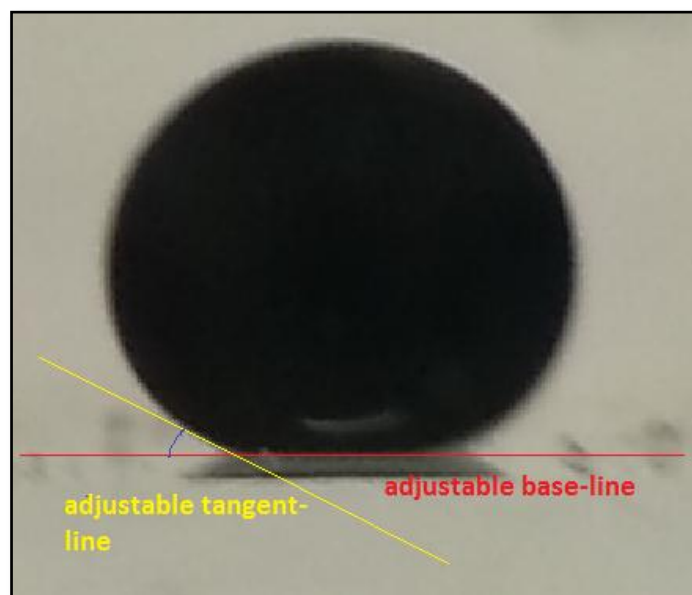
**Figure 6.2:** *The experimental setup of CAG. Figure a) displays the entire set up including all equipment required for contact angle measurements, and figure b) displays a close up picture of the system inside the measurement chamber.*

All the numbers in brackets below are referred to Figure 6.2 a).

The CAG consists mainly of an objective lens (1) and a measurement chamber (2) mounted to the adjustable platform (3). Prior to measurement the chamber was filled with the measurement brine, followed by placement of the quartz surface in the brine. As can be seen from Figure 6.2 b), the glass slide maintains a horizontal position above the chamber surface by using two metal screws.

The platform could be adjusted as the glass plate came visible in the microscope, and with help of the image focus knob (4) and a light source (5), a clear view of the glass plate was obtained.

An oil droplet was then deposited on the mineral surface by using the syringe with the inverted capillary needle (6) mounted to a laboratory stand (7). Focus adjustments could also have been done after deposition of the oil droplet. The base line dial (8) was used to fit the horizontal reference-line or base-line between the oil droplet and the solid surface, and measuring dial (9) was used to fit the tangent line in the three phase point defining the contact angle crude oil and brine creates with the solid surface. Figure 6.3, displays a picture of an oil droplet and the adjustable base-line and tangent-line seen from the CAG microscope point of view. This figure is only an illustration and thereby not representing any real picture of the system seen through the CAG microscope.



**Figure 6.3:** *Illustration of an oil droplet, and the adjustable base-line and tangent-line seen through the goniometer microscope.*

One glass slide was used for two parallels. This provides an opportunity to investigate the wettability state at two different places on the same silica surface. After a static condition of the oil droplet was

obtained, both left and right receding contact angles were measured continuously for 15 minutes and thereafter for each 15 minutes for a period of 1 hour.

### The Fluids

Crude oils and brines were not pre-equilibrated prior to contact angle measurements.

All the crude oils presented in Section 6.1.1 were involved in contact angle measurements.

### The Solid

The glass slides were aged in the measurement brines for 1-2 days before measuring contact angles.

Glasses aged in brine for one day, showed similar results as those aged in brine for two days.

### Problems Observed/Associated with the Method

The CAG instrument used in this study could not be used to measure dynamic  $\theta_a$ ,  $\theta_r$  and static  $\theta_e$ , angles, which are all angles being measured with the sessile drop technique as described in Chapter 2.

Formation of oil droplet had to take place close to the mineral surface as acceleration of oil droplet during detachment of these from the needle made them to roll away from the solid surface during initial contact.

Another problem was related to the position of the measurement chamber. When the position of the chamber surface deviated from a horizontal plane, oil droplets placed under the mineral surface tend to roll away from the surface. For this reason, a bubble level was used to indicate the horizontal position of the surface and was achieved by adjusting the four screws located beneath the cell platform. The levelled position of the platform was sensitive to even small changes in the position of the chamber, and since the chamber had to be washed after each contact angle measurement with two parallels, the set position of the platform changed, and thereby had to be levelled between each measurement.

It was also important to avoid washing the chamber made of metal with hot water, as metals in general have a high thermal conductivity and can thereby impact the measurement temperature.



Right selection of capillary needle was also important. The needle had to be short on the inverted side, as it could be placed vertical between the surface of the chamber and the glass slide as shown in Figure 6.2 b), without always contacting both surfaces. When the height of the inverted side was large, oil droplet had to be placed on the solid surface by holding the syringe in an angle deviating from vertical position, and thereby in a height below the glass surface which in term caused acceleration of droplet that made it to roll away from the surface.

#### The Washing Procedure

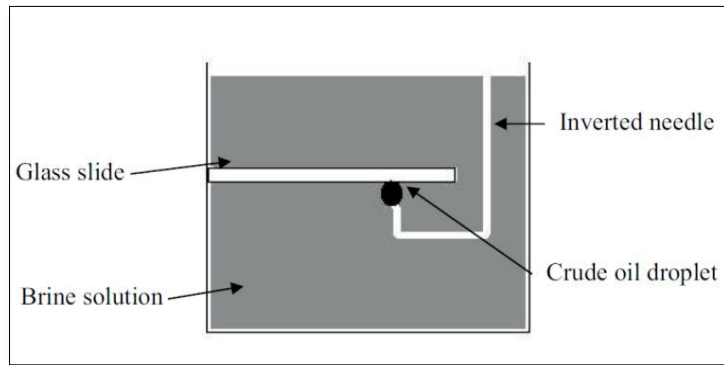
The syringe and the capillary needle were washed according to the washing procedure described in Section 6.1.5, followed by air drying using an air blow gun. The chamber was mainly washed with detergent and water unless oil remaining in the chamber made it necessary to wash it according to the procedure described in Section 6.1.5.

### **6.2.3 Adhesion Test by using Sessile Drop Method**

As discussed in Chapter 5, adhesion test can be used to characterize COBR interactions. In this study, the adhesion behaviour of Exp-12 crude oil as function of the four brine salinities given in Section 6.1.2, and pH values 3, 4, 7 and 10 has been studied. 6-8 parallels were performed for each crude oil/ brine system.

#### Description, Experimental Setup and Procedure

As mentioned in Chapter 2, adhesion test is a further development of the sessile drop method, thus the aperture and equipment used are the same as for contact angle measurements, but the procedure is different. Instead of leaving the oil droplet at the solid surface which was the case when measuring static  $\theta_r$  angles, as described in the section above, the oil droplet being formed is now in contact with the tip of the inverted capillary needle and the mineral surface for a standard period of 2 minutes, as illustrated in Figure 6.4. After 2 minutes, the oil droplet is drawn back into the needle, or can be drawn back by increasing the height of the adjustable chamber platform as was done in this study. At this stage, three different behaviours known as adhesion, non-adhesion and temporary adhesion may be observed. [2, 17, 25]



**Figure 6.4:** *The experimental setup for an adhesion test.*<sup>[3]</sup>

### The Fluids

Adhesion test for Exp-12 crude oil was performed for both equilibrated and non-equilibrated crude oil/brine systems. A 100 mL graduated cylinder was used to equilibrate the two phases with 10 mL crude oil placed in contact with 90 mL brine for approximately one day before measurements were performed. The equilibrated oil used for adhesion test was oil taken from the region close to oil/brine contact where the most chemical reactions occur between the phases.

pH adjustment according to the procedure described in Section 6.1.4, was made 1-2 days before measurements for the non-equilibrated system, and one day before the measurements for the equilibrated system.

### The Solid

The glass slides were aged in the measurement brine 1-2 days before the adhesion test was performed. The brine phase used for aging and measurement brine was the same for the non-equilibrated system, and different for the equilibrated system.

The washing procedure and the observed problems associated with this test are similar as for contact angle measurements.

## 6.2.4 Measurement of Electrophoretic Mobility (Zeta Potential) – Zetasizer

Information about the net charge accumulation at crude oil/brine interface will help to explain the observed wettability results. Malvern zetasizer Nano instrument (model ZS 90) was used to measure electrophoretic mobility, and by application of Henry equation (Equation 6.4) the instrument could measure the corresponding zeta potential of the system.

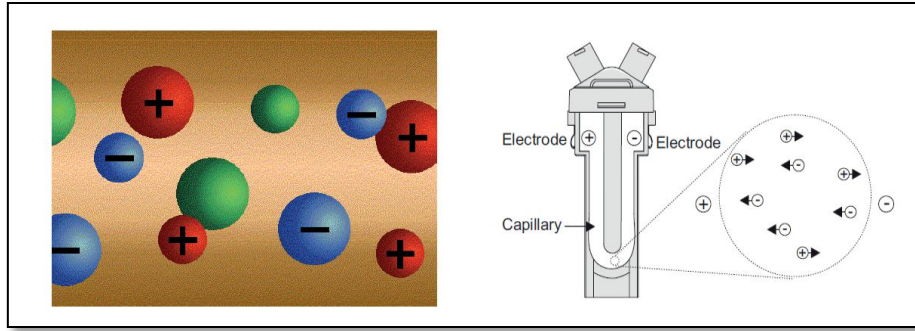
### Description

For zeta potential measurements, Malvern zetasizer uses a capillary cell with electrode at either end where a voltage is applied. As a result of this voltage, the electric field applied across the electrolyte cause charged particles in the electrolyte to be attracted towards the electrode of opposite charge as illustrated in Figure 6.5. In addition to columbic forces, viscous forces acting on the particles try to oppose this movement caused by the electric field, but after a period when equilibrium is reached between the two opposing forces, the particles in the solution will move with a constant velocity commonly referred as electrophoretic mobility. This velocity is dependent on following four factors:

- 1) Strength of electric field or voltage gradient
- 2) Dielectric constant of the medium
- 3) Velocity of the medium
- 4) Zeta potential.

The velocity of the particles is measured based on Laser Doppler Velocimetry technique.

In this technique a laser is used to light up a colloidal particle in movement. When the light source reaches the particle, the light scattering at an angle of  $17^\circ$  is detected. The light scattered at an angle of  $17^\circ$  is combined with the reference beam. This produces a fluctuating intensity signal where the rate of flocculation is proportional to the speed of the particle. A digital signal processor is used to extract the characteristic frequencies in the scattered light, and transmit the measured data to a computer that runs zetasizer software that process the data. <sup>[62]</sup>



**Figure 6.5:** Illustration of the different charged particle movements in an electrolyte solution under an applied electric field. Charges of same sign as the electric field of the same sign moves in the direction of the field. [3, 62]

By application of Henry equation, the software converts the electrophoresis data to zeta potential values. The Henry equation is: [62]

$$U_E = \frac{2\epsilon\zeta f(ka)}{3\mu} \quad (6.4)$$

Where:

$U_E$  = Electrophoretic mobility ( $\mu\text{mcm/Vs}$ )

$\zeta$  = Zeta potential (mV)

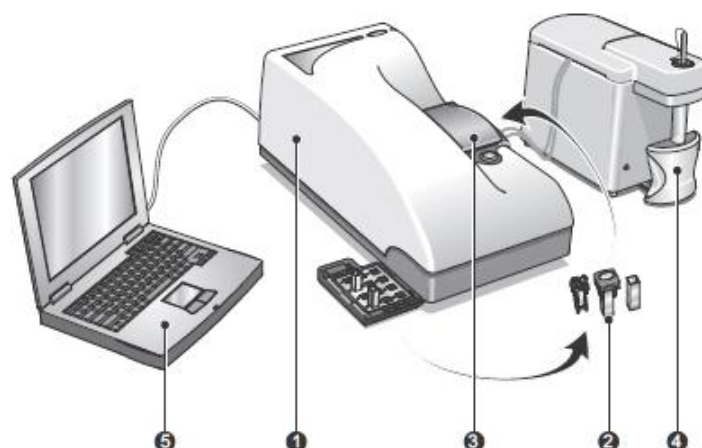
$\epsilon$  = Dielectric constant (dimensionless)

$\mu$  = Viscosity (Pa.s)

$f(Ka)$  = Henry's function

### Experimental Setup and Procedure

Figure 6.6 illustrate the experimental setup of the instrument. The corresponding numbers will be used to refer to the figure. The zetasizer Nano optical (1) is the main component of the zetasizer Nano system, with the incorporated laser system where the measurement cell (2) is inserted to for measurement. The cell area (3) is where the cell or cuvette is placed. A MPT-2 titrator (4) is a part of the system, but not used for zeta potential measurement. The zetasizer Nano optical is connected to a computer (5) that runs the zetasizer software, which controls the optical unit as well as processing and presenting the measured data. [62]



**Figure 6.6:** *The entire experimental setup of Malvern zetasizer.* <sup>[62]</sup>

Prior to measurement the new capillary zeta cell was rinsed with ethanol and distilled water, this was to confirm a clean cell free for impurities before measurements. The sample for measurement was then injected in to the cell by placing the sample syringe in to one of the sample ports shown in Figure 6.5, and then sealed with 2 caps. Two thermal plates were then mounted on the either side of the capillary cell, where the purpose of these plates was to provide temperature stability.

After this procedure was completed, the cell was inserted into the instrument. Before the instrument started running the measurements, the zeta potential software required some sample and measurements parameters to be filled in, e.g. measurement type, sample material, dispersant, measurement temperature, cell type etc. The software also has some build-in settings and options.

For all the measurement the temperature was set to 22°C, with an equilibrium time of 2 minutes.

Five parallels were selected per measurement with minimum 10 runs and maximum 100 runs per parallel. The software automatically determines number of runs required to be performed based on the quality of the results.

For each emulsion two parallels were performed, and two different emulsions were made of the same composition to confirm that same emulsions made separately gave the same result. Thereby totally four parallels were performed each emulsion.

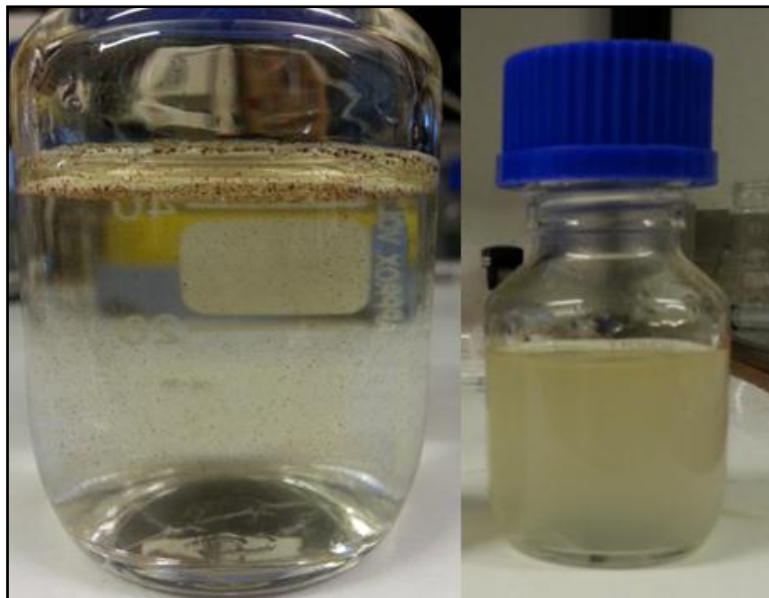
## The Fluids

Measurement of electrophoretic mobility has been performed on emulsified droplets of Exp-12 crude oil in brines of the same compositions as those used for the adhesion test.

pH adjustments of the brine phase used were conducted on the day of measurements according to the procedure described in section 6.1.4. After controlling if the volume of the oil droplets emulsified in brine had impact on the measured zeta potential results, two microliter crude oil droplets were added to 40 mL of the brine phase as a fixed measure to make the emulsions by ultrasonic vibration. The volume test results are presented in Appendix A3.

## Problems Associated/Observed with the Method

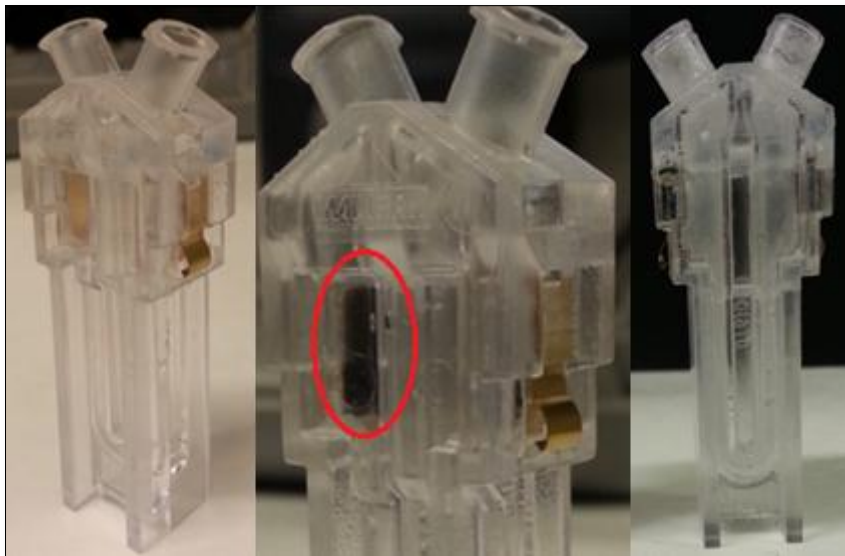
Mixtures that had not been manual shaken before they were put to vibration in the ultrasonic bath resulted in measurement results of poor quality. In the case when they were not shaken, it was observable that the oil accumulated as film droplets at the water surface after subjected to vibration. For this reason a combination of shaking + vibration was required to obtain uniform emulsions as shown in the picture to right in Figure 6.7. The picture to left displays the mixture after manual shaking.



**Figure 6.7:** Pictures of emulsion after manual shaking shown to left, and after shaking + vibration in ultrasonic bath shown to right.

The instrument was insensitive to measure electrophoretic mobility for high saline solutions, one of the reasons given in the user manual for results that does not meet the quality criteria is that the sample is not stable (particle aggregate) during the measurement . This can be considered as the main cause in measurements of high salinity solutions.

Another observation was that inside the cell, the gold plated electrodes seemed to become darker after a set of measurements. One assumption was oil adsorption at these electrodes. For this reason, to confirm the quality of the capillary cell, every day prior to measurement and between the measurements when the results tend to deviate from earlier measurements, or resulted in poor quality, the cell was tested with a standard solution with known zeta potential. The darkening effect of the electrode was confirmed gave incorrect data. This made it possible to quality secures the measured data. It was not possible to confirm if the darkening effect of the electrodes was due to oil adsorption, since washing with toluene destroyed the cell. Figure 6.8 illustrate from left photos of a new cell, cell exposed to impurities at the electrode (circled red) and cell washed with toluene.



**Figure 6.8:** *Capillary zeta cells: From left: a new cell, cell representing the darkening effect of the electrode and a destroyed cell caused by washing with toluene.*

Other factors observed influenced the measurements were formation of bubbles in the cell during injection, therefore injection must be done slowly and free for bubbles.

### The Washing Procedure

The cell was washed with distilled water between the measurements, and flushed through with measurement sample two times before the sample for measurement was injected.

The needle and the syringe were washed according to the washing procedure described in Section 6.1.5.

### **6.2.5 pH Meter**

pH measurements were performed with the waterproof Handheld Hach H160 pH meter shown in Figure 6.9. The procedure for pH adjustment was described in Section 6.1.4.

#### Description and Experimental Setup

This pH meter uses a stainless steel probe with an ion sensitive field effect transistor (ISFET) sensor technology, and is displayed in the picture showing the sensor part of the probe in Figure 6.9.

This ISFET sensor contains several proprietary layers placed selectively on a silicon chip substrate.

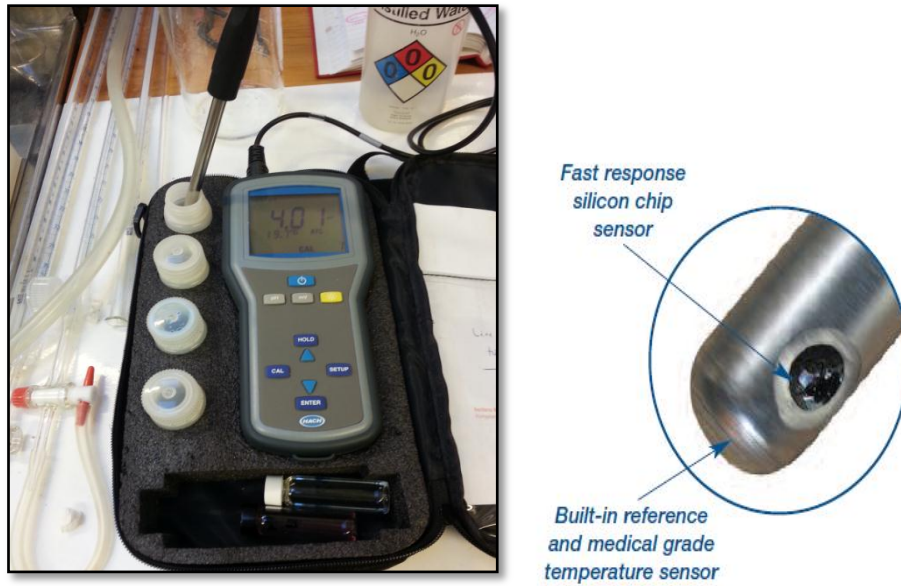
The final layer processes affinity for hydrogen ions in the solution, and only these ions.

The quantity of hydrogen ions at or close to the sensor surface causes an electrical effect that is detected and measured as pH. The probe also contains a sensor that measures the temperature of the solution, and is marked out in Figure 6.9.<sup>[73]</sup> Prior to measurements a three point calibration was performed on the pH meter with standard calibration buffer solution at pH 4, 7, and 10.

#### Washing Procedure

The probe was washed well with distilled water between the measurements and finally after all measurements rinsed with diluted detergent and water by use of a soft cloth brush. It is important to avoid that hard brushes or metal containing washing equipment are used to wash the probe, since the sensor can be permanently damaged with aggressive abrasion of the sensor surface.<sup>[72]</sup>





**Figure 6.9:** Hack H160 pH meter and sensor part of the probe.<sup>[73]</sup>

## 6.2.6 Digital Temperature Meter

Temperature has been shown to be an important factor that influence the measured value of contact angle and IFT as pointed out in Chapter 5.<sup>[60, 65, 71, 74]</sup> For this reason, to perform the measurements at a constant temperature region [20°C - 23°C], temperature in the measurement brine prior to contact angle measurement, adhesion test and IFT measurements were controlled by use of Digitron temperature meter with a stainless steel probe with incorporated sensor system. Figure 6.10 displays the temperature meter. The meter was rinsed with distilled water between the measurements.



**Figure 6.10:** *The Digiton temperature meter*

### **6.2.7 Digital Density Meter**

The instrument DMA 60 density meter with DMA 602 HT measuring cell (oscillator), produced by Anton Paar was used to measure the density of the fluids.

Density measurements were performed for all the fluid presented in Section 6.1.1 and 6.1.2 (including the pH adjusted aqueous solutions). For the brine phase and oil phase, 2 and 3 parallels were performed, respectively.

#### Description

Measurement with this instrument is based on the law of harmonic oscillations. The U formed cell (oscillator rooming 1 mL) is electromagnetically excited to vibrate at its natural frequency when the instrument is switched on. When a sample is introduced into the oscillator, a change in its natural frequency occurs due to a mass change in the oscillator caused by the injected fluid. Thus, the change in frequency depends on the injected fluid. The oscillator is directly connected to a densitometer that counts the frequency changes caused by the fluid injected and is displayed in terms of the period,  $T$ . The instrument allows an option for how many oscillations to happen between each cycle for measurement of the period. The displayed period is a function of mass,

volume, force and elasticity constant of the oscillator system, and the density of the fluid is a function of this period and is given as:<sup>[75]</sup>

$$\rho - \rho^* = \frac{1}{A}(T^2 - T_*^2) \quad (6.5)$$

Where:

A = The apparatus constant

T = Period of the sample

T<sub>\*</sub> = Period of a reference sample

ρ = Density of the sample (g/m<sup>3</sup>)

ρ\* = Density of the reference sample (g/m<sup>3</sup>)

Water was used as the reference sample in this study.

The aperture constant A, can be measured by measuring the period T for two fluids with known density at a given measurement temperature, air and water was used in this study.

The water density equal to 0.997 g/cm<sup>3</sup> at 22°C is literature reported value,<sup>[75]</sup> while air density was measured as function of air pressure and air humidity according to Equation 6.6:<sup>[76]</sup>

$$P_{air} = 0.46464 \cdot \frac{P - 0.08987 \cdot F}{T} \cdot 10^{-3} \quad (6.6)$$

Where:

P = Air pressure (mmHg)

F = Air humidity in (%)

T = Temperature (K)

The system temperature is controlled by a water bath connected to the density meter through a thermostatic casing. The purpose of the water is to circulate near the measuring cell and thereby contribute to a constant measuring temperature. Hetofrig produced water bath was used in this study.

## Experimental Setup and Procedure

After the instrument was turned on the temperature in the measurement cell had to stabilize at 22°C, before calibration with air and distilled water was performed. Number of oscillation was chosen as 100. Figure 6.11 displays the instrumental setup of the density meter. The sample was injected into the U formed cell by injecting with a 2 mL syringe. Before each measurement the tube was flushed through with the measurement sample before the sample for measurement was filled. The period number was noted after the period had stabilized with only the two last decimals of the total six decimals allowed for small variations.



**Figure 6.11:** Hetofrig water bath connected to Anton Paar Density meter

## Problems Associated/Observed with the Method

It was important to avoid bubbles forming in the cell during the injection of the sample, as these made the density meter to display non stabilizing periods.

## Washing Procedure

For oil measurement the cell was washed according to the washing procedure in Section 6.1.5, and flushed through with air to remove water prior to oil injection, and finally rinsed according to the same procedure. For brine measurements the tube was washed with distilled water between the measurements.

## 7 Main Results and Discussion

The following chapter presents the main results and the related discussion to the results obtained in this study. The chapter is structured as after presenting the results of one method, the following discussion relevant to the results of this method, including observations and comparison with previously studies are presented. Exceptions are adhesion test and zeta potential measurements that will be discussed in each other's section. At the end of this chapter a summary of wettability results obtained in this study linked to literature reported data will be presented.

### 7.1 Contact Angle Measurement

All the wettability results obtained in this study are restricted to a negative charged sandstone surface. The wettability results are those expected would have given different results for clay minerals that can have co-existing positive and negative charged surfaces in a wide range of pH.

Contact angle measurements for the crude oils A-12, Exp-12 and Exp-12-D were performed in presence of the four main brine compositions with near neutral pH values listed in Table 7.1.

Contact angle measurement for the individually Xylene and Iododecane added Exp-12 oils were only investigated in presence of 100% SSW.

Volume % SSW	Measured pH
1	6.90 ± 0.1
10	7.23 ± 0.1
50	7.67 ± 0.1
100	7.78 ± 0.1

**Table 7.1:** Measured pH values in the four main brine phases used in this study.

During the deposition of the oil droplet at the quartz surface it displaced the water that initially covered the water-wet surface, and thereby gave receding conditions as discussed in Chapter 2. Thus, the measured contact angles were all static equilibrated receding angles,  $\theta_{e,r}$ . Both left and right contact angles were measured per crude oil droplet placed on the quartz surface, and the

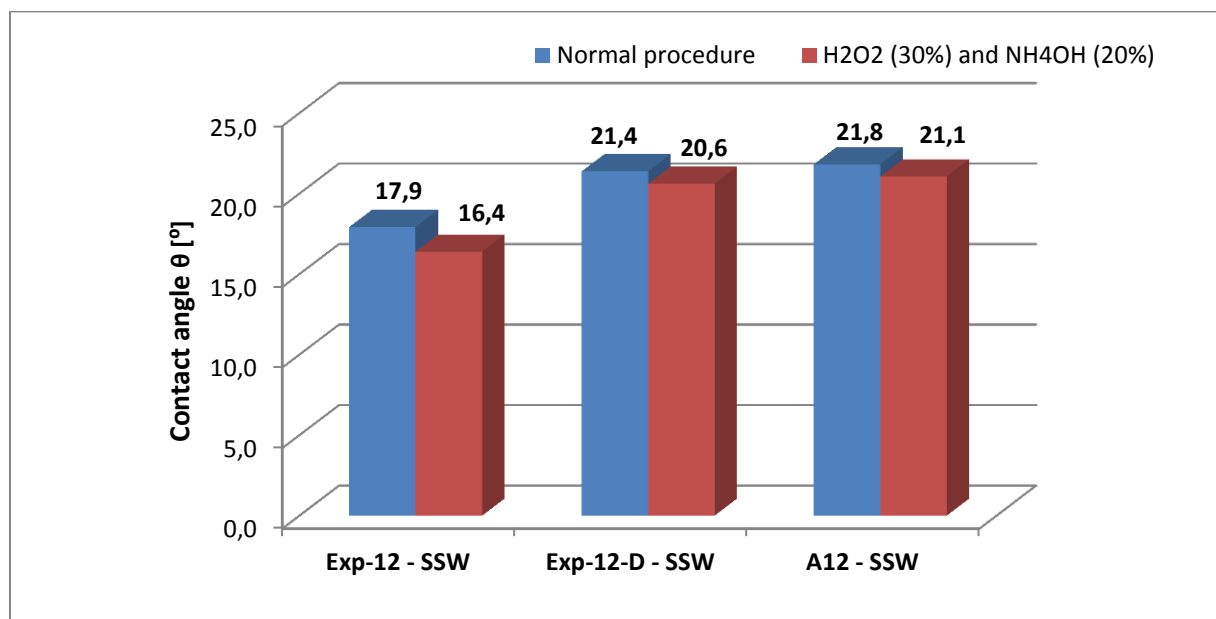
results in this chapter are presented as an average between both angles of the total 3-5 parallels performed. The measured left and right angles and the related uncertainties are listed in Appendix A4.

For the first parallel in each crude oil/brine system the contact angle was monitored in 1 hour. No changes in contact angles were observed during this monitoring period. Earlier studies in our laboratories have shown that these static angles do not change within several days.

The selection of washing procedure of the quartz mineral surface was based on comparison of the contact angle results for the same crude oil/SSW system tested on quartz mineral surfaces, washed according to the procedure proposed by Buckley with H<sub>2</sub>O<sub>2</sub> and NH<sub>4</sub>OH, and normal procedure with diluted detergent and water. These procedures were described in Chapter 6, Section 6.1.3.

Figure 7.1 displays the results of this test. As can be seen from the figure, a systematic trend was observed. The chemical washing procedure showed always a lesser average angle compared with the normal procedure angles for the three crude oils Exp-12, A-12 and Exp-12-D tested.

But since the measured data indicated no surfactant effect of detergent on the mineral surface, and since all the measured data were in the uncertainty region of each other, the normal less time consuming washing procedure was selected to be used as the standard procedure for the further measurements.



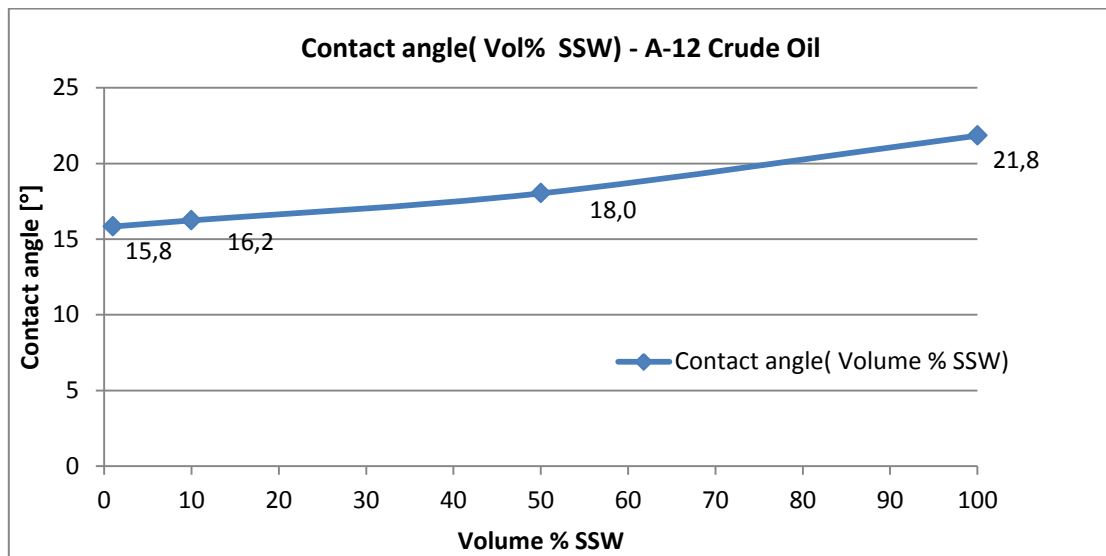
**Figure 7.1:** Comparison test of washing procedures. (See Section 6.1.3)

### 7.1.1 Contact Angle for Crude Oils A-12, Exp-12 and Exp-12-D

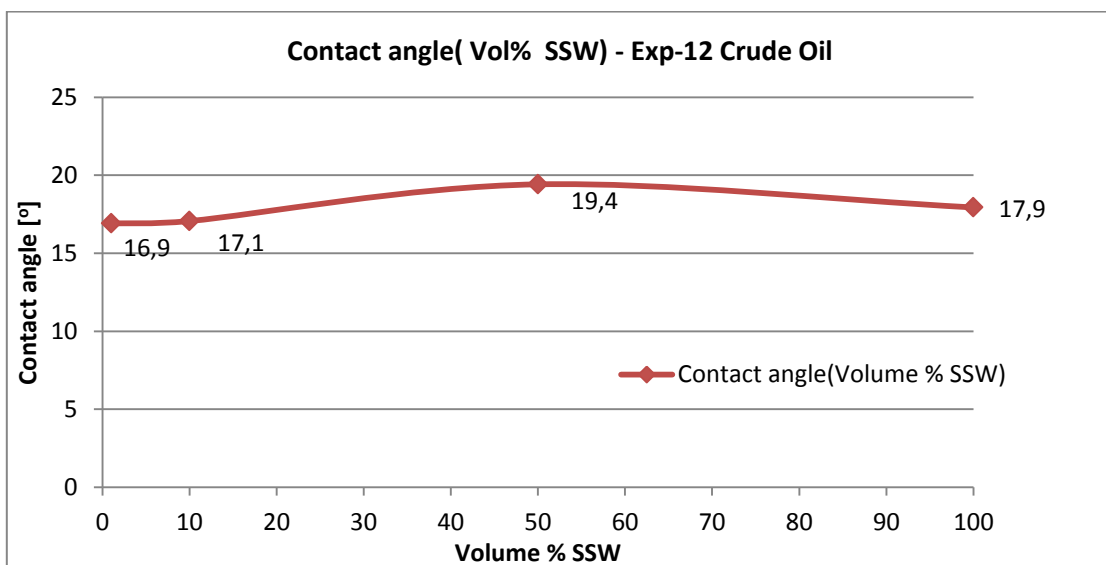
#### Results

The results of the measured contact angles for the three crudes A-12, Exp-12 and Exp-12-D with the four brine compositions listed in Table 7.1 are presented in Figure 7.2 - 7.4, respectively.

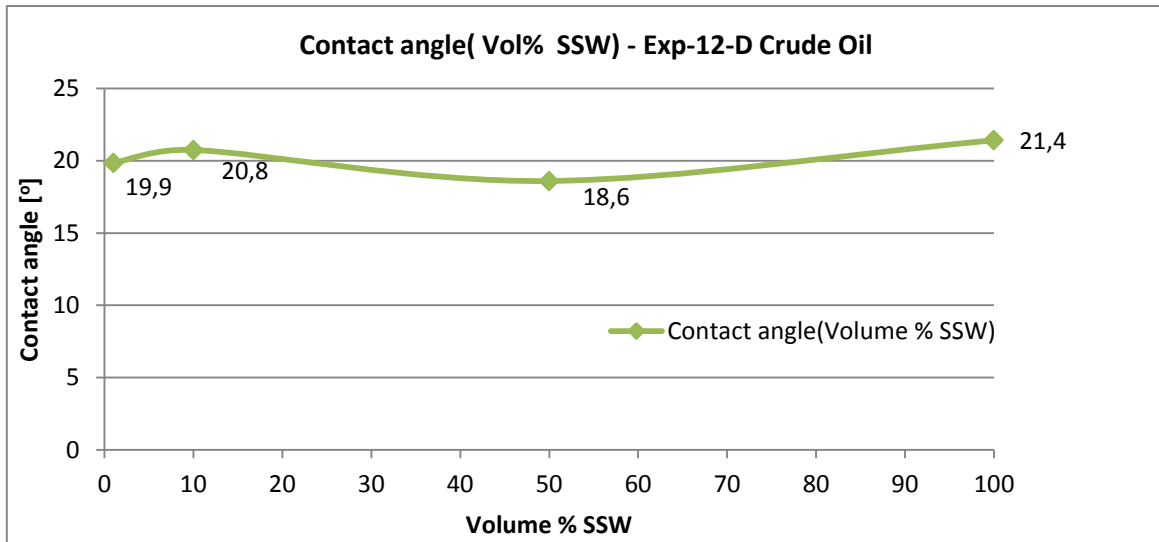
All the measured contact angles were in the strongly water-wet side of wettability.



**Figure 7.2:** Measured average contact angles in a COBR system consisting of A-12 crude oil, the four main brine compositions listed in Table 7.1, and a initially water-wet quartz surface.



**Figure 7.3:** Measured average contact angles in a COBR system consisting of Exp-12 crude oil, the four main brine compositions listed in Table 7.1, and a initially water-wet quartz surface.



**Figure 7.4:** Measured average contact angles in a COBR system consisting of Exp-12-D crude oil, the four main brine compositions listed in Table 7.1, and a initially water-wet quartz surface.

## **Discussion**

### **A-12**

Only the contact angles measured for A-12 crude oil showed a systematic trend with decreasing contact angle with decrease in salinity, as shown in Figure 7.2.

For the 100%, 50% and 10% SSW's, none of the measured contact angles also with respect to the uncertainties were overlapping each other. Only 10% and 1% SSW's seemed to indicate more stabilized angles in the same range of magnitude. The contact angle difference between maximum HSW and minimum LSW was found to be  $\sim 6^\circ$ . According to the hysteresis graph for crude oils presented in Figure 2.2 in Chapter 2, a reduction in  $6^\circ$  in the receding mode can imply a larger reduction in advancing mode. This is due to the flat plateau region in the receding curve and a high slope in the advancing curve. Thus, for an imbibition process (water displaces oil), which is described in terms of  $\theta_a$  angles, this reduction can mean more compared for a drainage process (oil displaces water) described in terms of  $\theta_r$  angles.



### Exp-12

For Exp-12 crude oil no systematic trend was observed. Initially contact angle increased from 100% to 50% SSW with  $\sim 1.5^\circ$ , then decreased again with further reduction in salinity to 10% SSW with  $\sim 2.3^\circ$ , and thereafter seemed to maintain a stable value with further reduction in salinity to 1% SSW as shown in Figure 7.3. 1% and 10% SSW's showed contact angle values very close to each other and to that of 100% SSW. The difference between maximum HSW and minimum LSW was a reduction with  $\sim 1^\circ$ . For this reason, and since both of the LSW's and 50% SSW was in the uncertainty region of the contact angle for 100% SSW, the system seemed to be very little sensitive to reduction in salinity compared with crude oil A-12.

### Exp-12-D

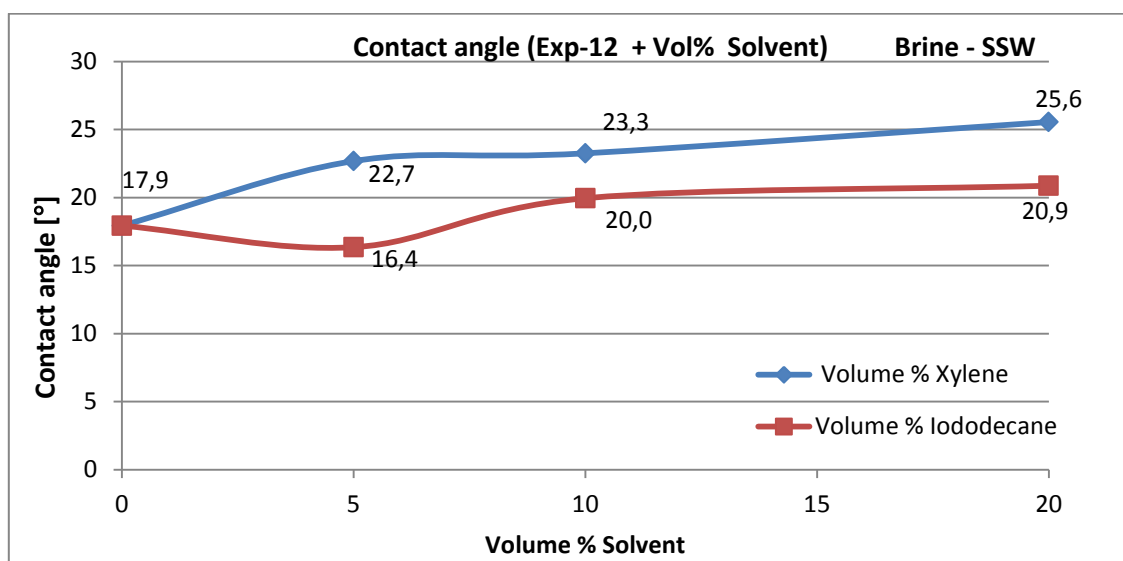
Exp-12-D crude oil, which was the Exp-12 crude mixed with 20% Xylene and 20% Iododecane, showed a wave trend with decreasing and increasing contact angle values with reduction in salinity as displayed in Figure 7.4. Compared with the original crude oil, the contact angle at 100% SSW showed an increase with  $\sim 3.5^\circ$  and the measurements did not overlap with respect to their uncertainties. Meaning a real increase was observable. The same increase compared with the salinity region of the original crude oil was observed in 10% and 1% SSW regions with  $\sim 3.7^\circ$  and  $\sim 3^\circ$ , respectively. Only the 50% SSW showed a decreasing trend with  $\sim 0.8^\circ$ , and it was only for this salinity region the measured angles with respect to their uncertainties were in the region of each other. The overall results indicate that Xylene and/or Iododecane have a small impact on the COBR interactions occurring in this system compared with the original crude oil.

As mentioned in the previous chapter, the CAG system used in this study was not suited for measurement of static  $\theta_{e,a}$  angles or dynamic  $\theta_a$  and  $\theta_r$  angles. But with the strongly water-wet  $\theta_{e,r}$  angle values obtained in this study, a clue about the degree of hysteresis may be obtained by using the general hysteresis graph for crude oils presented in Figure 2.2 Chapter 2. As can be seen from this graph the max hysteresis in contact angle is observed at  $\theta_E$  equal to  $90^\circ$ , and the amount of hysteresis decrease with decrease in  $\theta_E$  angle. In the strongly water-wet region the  $\theta_E$  angle is low, and so are the both the dynamic and static  $\theta_a$  and  $\theta_r$  angles. From this schematic illustration, the degree of hysteresis can be considered to be low for the crude oils investigated in this study at ambient conditions ( $20-23^\circ$ ,  $\sim 1$  atm). To confirm this,  $\theta_a$  angles must be measured under the same conditions.

## 7.1.2 Individual Impact of Xylene and Iododecane on Exp-12 Contact Angle

### Results

The results of contact angle measurements for the different portion of individually Xylene and Iododecane added Exp-12 crude oils in presence of SSW are shown in Figure 7.5.



**Figure 7.5:** Contact angle for individually Xylene and Iododecane added Exp-12 Crude oil.

### Discussion

As observed from the figure, compared with original crude oil in presence of 100% SSW, the chemical added crude oils, despite Exp-I-5, showed an increasing trend in contact angle with increase in chemical added. None of the Xylene added crude oils were in the uncertainty region of Exp-12 crude oil, and for the Iododecane added crude oils only Exp-I-5 seemed to be in this region.

The 20% Xylene added oil showed  $\sim 7.7^\circ$  increase in contact angle compared with the pure crude oil, while the 20% Iododecane added oil showed  $\sim 3^\circ$  increase. These values seem to agree with the observed trend during the measurement. The increasing trend was more observable for the Xylene added crude oils. The Exp-X-20 oil showed a visible decrease in the roundness shape of the oil droplet placed on the mineral surface (seen through the enlarged goniometer view), compared with the pure Exp-12 oil and the Iododecane added crude oils.

The results indicate the observed increase in Exp-12-D crude oil to be a combined effect of Xylene and Iododecane, with a higher influence of Xylene.

One reason for this observed impact of the chemicals can be explained related to the solvent character of the crude oils with respect to its asphaltene components, as described in Chapter 4, Section 4.2.4.

If we consider Exp-12 crude oil to have nearly the same SARA composition as for crude oil A from the same field but different well, the composition contains 55 wt% saturates and 0.7 wt% asphaltenes, in addition to aromatics and resins. Alkanes are normally classified as precipitant for asphaltenes, while aromatic as good solvents.<sup>[2, 52]</sup> Iododecane is not a pure alkane but the main dominating compound in the structure is an alkane.

Buckley<sup>[2,52]</sup> showed through her study that different aromatic liquids even when they are characterised as solvents for asphaltenes can indirectly impact asphaltene stability by either increase or decrease the amount of precipitant required initiating precipitation from the crude oil. Hence, the addition of Xylene can have caused 55 wt% of saturates (alkanes) to be sufficient amount of alkanes to impact the stability of the asphaltenes in the crude. Iododecane could due to the precipitant character of alkanes also have influenced the asphaltene stability and caused small precipitation to occur. Buckley<sup>[2]</sup> further proposed that this precipitated material could either interact with the solid surface from oil/brine interface through acid/base interactions dependent on their polarity and size, or diffuse through the water-film and precipitate at the solid surface.

As can be seen from Figures 7.4 and 7.5, even when the addition of Xylene and Iododecane to Exp-12 increased the contact angle, the increase was still within the strongly water-wet region of wettability with no film collapse. A hypothetical explanation based on Buckley's investigation can be that not strong enough interaction of the precipitated material, which is function of the aggregate size (if any precipitation occurred) from crude oil/brine interface occurred to collapse the water-film.

For the reason that the changes in contact angles with addition of Xylene and Iododecane still was within the strongly water-wet region with no film collapse, and since the increase in contact angle for the combined effect of the chemicals did not impact the original system as the individual effects, Xylene and Iododecane can be classified as a solvent with respect to the entire crude oil.

















## 7.2 Adhesion test

Adhesion test was performed for Exp-12 crude oil with the four brine compositions listed in Table 7.1 with manipulated pH values 3, 4 and 10, in addition to the natural close to neutral pH of the solutions. The results of adhesion test are presented in adhesion maps in Table 7.2 and 7.3 for the equilibrated and non-equilibrated systems. The pH values correspond to the initial adjusted pH values, meaning a pH alteration was observed after the aging and equilibrium processes.

Adhesion results are normally discussed on the basis of electrostatic forces (described in terms of surface charges) that are one of the main contribution forces of disjoining pressure ( $\Pi$ ) that governs the water-film stability between crude oil and rock. For this reason, the results of adhesion test will be discussed based on the zeta potential test results, which was run to study the effect of changing water salinity and pH on the electric charges at crude oil/brine interface. Thus, the related discussion to the results of adhesion test will not be discussed before the results of zeta potential test have been presented and discussed in next section.

















In this section, observations related to adjusted and measured pH in the brine phases, and a comparison of the mixed brine adhesion test performed in this study with the standard adhesion test reported in the literature, with main focus on the wettability results of the adhered droplets will be presented and discussed.

**Adhesion Results for Non-Equilibrated System**

Vol % SSW	1 % SSW	10 % SSW	50 % SSW	100 % SSW
pH				
10				
7				
4				
3				

**Table 7.2:** Adhesion map for Exp-12 crude oil – Non-equilibrated system

**Adhesion Results for Equilibrated System**

Vol % SSW	1 % SSW	10 % SSW	50 % SSW	100 % SSW
pH				
10				
7				
4				
3				

**Table 7.3:** Adhesion map for Exp-12 crude oil – equilibrated system.

## pH Alteration and Observations

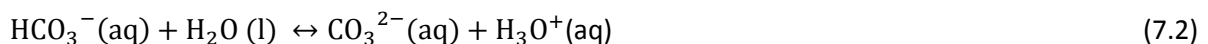
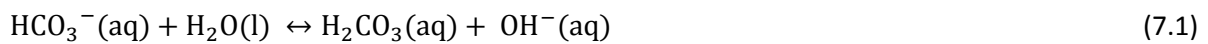
For the aging process of the glass slides and for the 24 hours equilibrium process of crude oil and brine, the test required pH adjustments of the brine phases 1-2 days prior to measurement.

In Appendix A5, one set of the several manipulated pH adjustments made for the equilibrated and non-equilibrated systems measured at the day of pH adjustment and at the day of the test performance are presented.

The measured pH values 1-2 days after pH adjustment in the aging brines with manipulated pH < 7 showed sometimes slightly positive, negative or almost no change in  $\Delta\text{pH}$  which is the difference between the measurement pH and the initial pH. In brines with pH > 7 the measured pH showed always positive  $\Delta\text{pH}$ .

For the aging process with glass the intern buffer process due to natural acid/base reactions occurring in the brine phase, and the hydroxylation process of quartz glass plate in contact with water can explain the observed pH trend.

SSW contains e.g.  $\text{NaHCO}_3$  salt.  $\text{HCO}_3^-$  ions can react with water and initiate following reactions:



Quartz ( $\text{SiO}_2$ ) has a PZC = 2 and the surface charge will above this pH be governed by following equation.<sup>[14]</sup>



According to Le-chatelier's principle, in low pH ranges the natural buffer process will shift the equilibrium in Equation 7.1 toward right and in 7.2 toward left. At the same time, the equilibrium in equation 7.3 will shift to right due to PZC for quartz at pH 2. The different changes observed in pH 3 and 4 regions can be explained is a cause of simultaneous process between uptake and release of  $\text{H}^+$  ions in the brine. In pH 10 region, the higher reduction in pH observed can be explained is due to release of  $\text{H}^+$  ions by both the buffer process and the silica surface.

It was also observed that amount of pH manipulating chemicals, HCL and NaOH droplets added to the brine phase increased with increase in salinity. This can be explained by the increase in concentration of the SSW ions in solution, which makes the ion contribution in the acid/base reactions to become stronger, or in other words makes the buffer effect to become stronger.

For the equilibrated oil/brine system the measured pH in the brine phase showed always positive  $\Delta\text{pH}$  in  $\text{pH} < 7$  solutions and negative  $\Delta\text{pH}$  in  $\text{pH} > 7$  solutions.

In addition to the buffer character of the system, this change in pH can be explained by the acid/base reactions occurring at the interface region between crude oil and brine.

As discussed in Chapter 4, the crude oil contains a number of polar organic species that when exposed to water will be surface activated and create acid/base equilibrium reactions that cause release or uptake of  $\text{H}^+$  ions from the brine phase (see Equation 4.2 and 4.3 in Chapter 4).

This may explain the increase in brine pH at  $\text{pH} < 7$  due to uptake of  $\text{H}^+$  ions by basic species and decrease in pH at  $\text{pH} > 7$  due to release of  $\text{H}^+$  ions by the acidic species.

Thus, a systematic measurement of pH of aqueous phase after contact has been established between crude oil and brine may help to determine when an equilibrium state between the two phases has been reached with pH measurements showing more constant values.

Fosse<sup>[78]</sup> showed in her study with an oil/brine equilibrium period varying from 87 to 365 days, that the changes in pH occurred several days after initial contact, and reported maximum  $\Delta\text{pH}$  in low pH ranges was near +2, and in high pH ranges near -3.5. This indicates that a contact time of 24 hours as chosen in this study is too short period of contact between crude oil and brine to reduce the surface active interactions and obtain a stabilised system.

Another observation in addition to the negative  $\Delta\text{pH}$  for the pH 10 solutions was formation of a white precipitate in the two HS brines. The aged glasses were also covered by this precipitated material as displayed in the picture in Figure 7.6. Based on salt composition of SSW this white material could be formation of the low-solubility salts  $\text{Mg}(\text{OH})_2(\text{s})$  or  $\text{Ca}(\text{OH})_2(\text{s})$  due to the high  $\text{OH}^-$  ion concentration in the brine phase at this pH, or formation of the low solubility salt  $\text{CaCO}_3(\text{s})$  due to a shift in the equilibrium in equation 7.2 toward left, which contributes to more formation of  $\text{CO}_3^{2-}$  ions as a result of the intern buffer system. The precipitation was not observed for the two LS brines 1% and 10% SSW's, and can be explained to be a result of the diluted concentration of the ions in LS brines that contributed to limited precipitation.



**Figure 7.6:** Illustration of the precipitated material in pH 10, 100% SSW, compared with the almost blank pH 10, 10% SSW, and a glass slide covered with the precipitated material.

### **Comparison between the Standard Test and Mixed Brine Test**

In the adhesion test for A-93 crude oil in presence of SSW and dilution of this as brine phase, Buckley<sup>[2]</sup> reported non-adhesive behaviour of the oil in all salinity and pH ranges investigated.

The Exp-12 crude oil used in this study showed different adhesion behaviour than A-93 crude oil in presence of SSW. This indicates that in mixed brine solutions different adhesion behaviours are observed compared with that in monovalent system, which is reported to be more pH dependent.

Both adhesion maps for Exp-12 crude oil showed the transition zone between adhesion and non-adhesion to occur with increase in pH of the solutions, a trend that is consistent with observed adhesion in standard test performed with NaCl brines of varying brine pH.<sup>[2, 40, 52, 67, 77, 78]</sup> With regard to salinity, the non-equilibrated system did not show any clear transition between the two extreme cases as pH 3 solutions gave adhesion at both LS and HS regions. For the equilibrated system a more consistent trend with the standard test showing transition to occur with increase in salinity was observed. Temporary adhesion was not observed in either case.



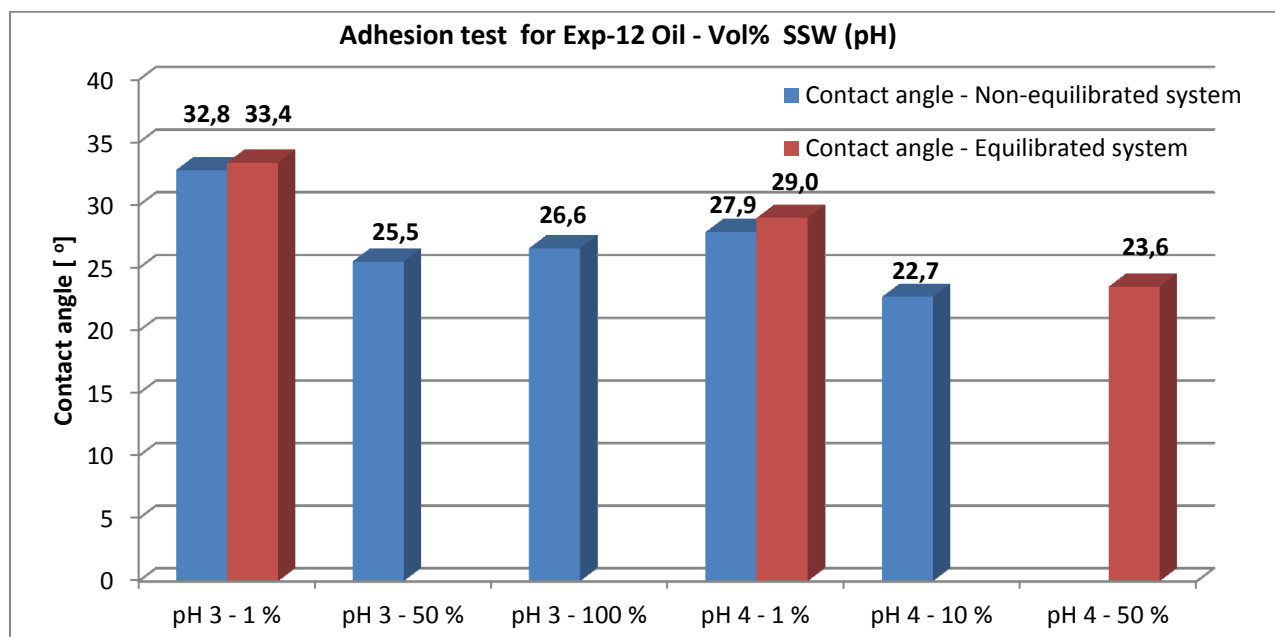
Morrow<sup>[25]</sup> explained the standard adhesion test to be a simple test that distinguish between low and high advancing cases, and thereby strongly water-wet and oil-wet states with only regard to the adhesive and non-adhesive behaviour of crude oils.

In other words, when the liquid bridge ruptures, he reported that the area over which the oil droplet remains attached to the solid surface was generally oil-wet.

## Results

To confirm if this trend was also valid for the mixed brine system used in this study, the associated contact angles for the systems that resulted in adhesion was measured.

Figure 7.7 presents the measured contact angle results for the droplets that adhered to the solid surface in the equilibrated and non-equilibrated systems.



**Figure 7.7:** Contact angle values for the adhesion results with Exp-12 crude oil.

## Discussion

As observed from Figure 7.7, the contact angles related with the adhered droplets showed water-wet contact angles, meaning adhesion has occurred without collapsing the water-film between crude oil and solid surface. Thus, the adhesion behaviour with respect to wettability alteration is not similar to that in the standard test. In pH 4 region were ionization of strongly acidic species with  $Pka < pH$  can occur, the observed wettability results can be explained is due to the unusual high acid number of this crude oil. Crude oils are characterized as oil with sufficient acid content when the acid number  $> 0.2 \text{ mg KOH/ g oil}$ .<sup>[30]</sup> Exp-12 crude oil has an acid number equal to  $2.96 \pm 0.05 \text{ mg KOH / g oil}$ . Standal et al.<sup>[48]</sup> found a relationship for contact angle measured on silica surface where the water-wetness of the system increased with increase in acid number. For this reason, even when attractive electrostatic forces due to ionized basic species, or due to ion binding or cation bridging observed for acidic crude oils with negatively charged acidic species contributes to adhesion, the high concentration of the negative charged acidic species and thereby the strong repulsive contribution can has prevent the water-film to rupture. But in pH 3 region were the surface charge domination is mainly by ionized basic species, the observed water-wet adhesion is difficult to explain.

For this reason, the adhesion map described in terms of disjoining pressure as Buckley presented for A-93 crude oil shown in Figure 5.9 in Chapter 5, will for Exp-12 crude oil be conditionally stable over the entire region were adhesion was observed.

Observed from Figure 7.7, one trend that is similar for both brine phases is the observed reduction in oil-wetness of the system with increased salinity and pH for both equilibrated and non-equilibrated systems. The pH 3, 50% SSW results showed a high variation in the measured data, one explanation for the variations observed can be due to un-succeeded aging process with different wettability state at different places on the solid surface. The equilibrated and non-equilibrated contact angles for the system that resulted in adhesion in both cases showed a systematic trend with equilibrated angles to be a little higher than for the non-equilibrated system, even when the measurements were in the region of each other with respect to their uncertainty. However, this trend can also be explained is a results of the equilibrium process. Even when final equilibrium was not reached, a reduction in the oil/brine interactions can have occurred. Thereby the observed results can be explained is due to more activated basic species that contributed to a stronger attraction (pH 3), and more activated acidic species that contributed to more ion binding effects (pH 4).

### 7.3 Zeta Potential

The increase and decrease in the surface concentration of ionized form of acidic and basic species, and for this reason the net surface charge of crude oils and minerals are governed by brine pH according to Le-chatelier's principle, and brine salinity.

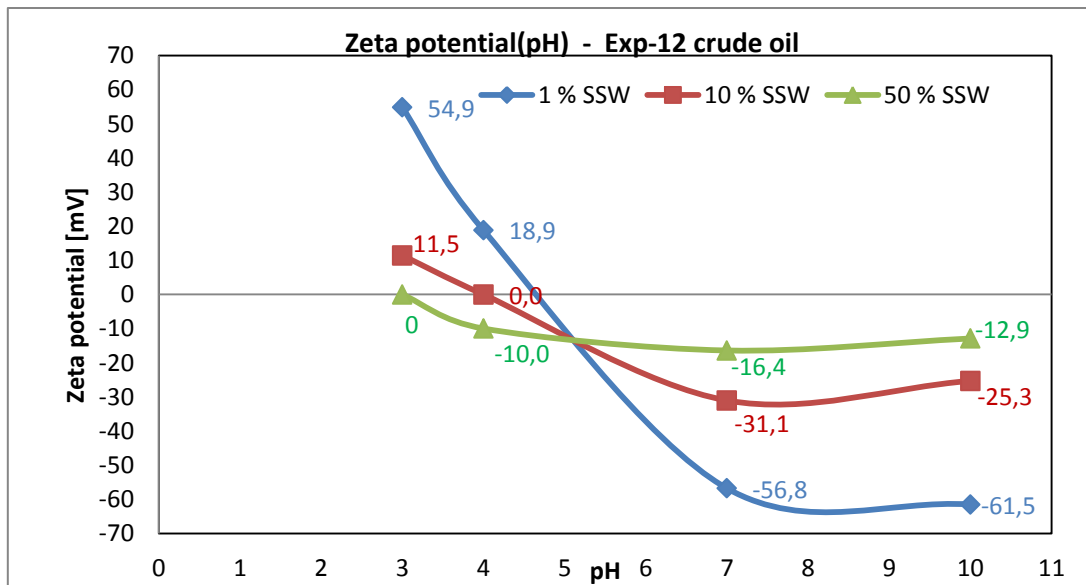
The magnitude of the net charge of crude oils will also depend on the acid and base numbers of the crude oils. This is evident from zeta potential measurement data for Moutray crude oil and A-93 crude oil presented in Figures 5.5 a) and b) in Chapter 5.

Moutray crude oil has a low base/acid ratio compared with the high base/acid ratio of A-93 crude oil.<sup>[2]</sup> At the same pH value and brine composition, net negative charge is higher for Moutray crude oil than A-93 crude oil. (0.1 M solutions show a different trend but can be explained by the unstable trend observed for A-93 data in this region.)

Exp-12 and A-12 crude oils used in this study are more comparable with Moutray crude due to the high acid content. Base number for these crude oils has not been measured, but since acid numbers are very close to crude oil A from the same field it is conceivable that the base number also appear to be in this area. (Data reported in Chapter 6 Section 6.1.1)

### **Results**

Figure 7.8 displays the measured zeta potential for emulsified droplets of Exp-12 crude in the three measurable brine phases, 1%, 10% and 50% SSW's. The results are based on an average of total 4 parallels, where 1 parallel represents 5 instrument measured parallels. The zeta potential measurement data and the corresponding electrophoretic mobility data are presented in Appendix A3. The same brine composition as those used for adhesion test was used in zeta potential measurement.



**Figure 7.8:** Zeta potential results for Exp-12 crude oil emulsified in different brine compositions.

### Discussion

Figure 7.8 shows the magnitude of net negative or positive charge becomes lower as the salinity of the brine phase increases. This can be explained as a result of increasing ion concentration in the solution, +ve or -ve charges, which in turn will screen the electrostatic double layer and contribute to shielding effect of the high negative or positive charges of oil, by high concentration of the opposite charges in brine close to the oil surface. As LSW contains lesser concentration of these ions, and the double layer is expanded the charge at oil/brine interface becomes more dominant.

It has been reported that isoelectric point (IEP) is the point where the colloidal system is least stable.<sup>[62]</sup> In pH 3, 50% SSW and pH 4, 10% SSW, the measured data were very unstable with a flocculating trend shifting between slightly negative, positive or close to zero values, which also several times resulted in measurement error. Several parallels were performed to confirm if this point could be proposed as IEP for Exp-12 at these salinity regions. Based on measurement data of up to 8 – 10 parallels showing an unstable trend, it was expected that IEP for these brine solutions was very close to these pH values, and were therefore set equal to zero.

Thus, the IEP was also different for the different brine salinities. This is an opposite trend than observed for Moutray crude (See Figure 5.5 b, Chapter 5). For this crude, the IEP seemed to cross the zero zeta potential at similar value in all salinity regions.

The observed IEP at pH 3 50% SSW, can be due to a neutralization process as a result of the shielding effect, since activation of ionized acidic species will be limited in this region. At pH 4 10% SSW, the IEP can be due to a combination of shielding effect and activation of ionized acidic species that contributes to a neutralized surface, thus a zero zeta potential.

An interesting observation of this different IEP for Exp-12 crude oil in different brine compositions will be discussed related to the observations of adhesion tests, after the results of adhesion test have been discussed.

Nasralla et al.<sup>[61]</sup> showed in presence of divalent ions the crude oil produced less negative charge compared at the same monovalent brine composition. This trend is as expected since in presence of divalent ions the shielding effect becomes higher as the double layer thickness is also a function of the ion valence, as shown by Equation 5.4 in Chapter 5.

For Exp-12 crude oil this effect is observable when comparing the zeta potential graph with the zeta potential graph for Moutray crude oil shown in Figure 5.5 b in Chapter 5.

Even when Moutray crude oil and Exp-12 crude oil are characterised as acidic crude oils, Exp-12 crude has a much higher acid number than Moutray crude oil,  $2.96 \pm 0.05$  mg KOH/g oil and 0.56 mg KOH /g oil, respectively. From this one can expect the net negative charge with higher pH values as more acidic species ionizes will be higher in magnitude for Exp-12 crude oil compared with Moutray crude oil. But comparing the zeta plots of these two crude oils shows Moutray crude oil to have a higher net negative charge at all salinity regions compared with the magnitude of Exp-12 crude oil, even when the brine salinity is reduced by factors of 100.

As observed from Figure 7.8, in the region between pH 7 and 10 a flattening trend of the zeta potential curves was observable in all salinity regions. In this pH range most of the acidic species e.g. carboxylic acids with  $pK_a \sim 4.70$  will be in the ionized form as a consequence of  $pK_a < pH$ , and equilibrium shift in Equation 7.4 toward right. Even when ionization of acidic species still will occur after pH 7, the effect of more ionization is not observable and can be a result of that all the possible ionizable surface sites are dominated by net negative charge already at pH 7.



### 7.3.1 Adhesion Results Discussed based on Zeta Potential Results

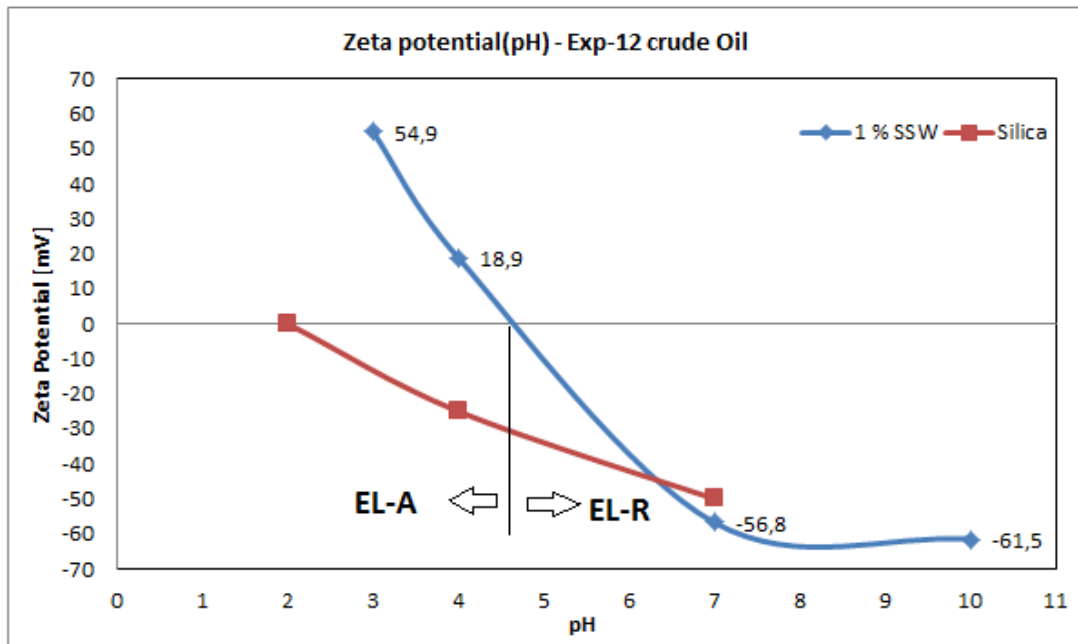
Figures 7.9 - 7.12 displays the individual plots of Exp-12 zeta potential as function of brine pH for the different brine salinities. Based on the zeta potential data for crushed silica glass in NaCl solutions as function of pH, measured by Buckley et al.<sup>[17]</sup> (See Figure 5.7, Chapter 5) the hypothetical zeta potential curve for crushed silica in presence of SSW as function of brine pH has been drawn.

Buckley observed the same reducing trend in the net zeta potential with increase in brine salinity for the crushed silica suspension. Alotaibi et al.<sup>[65]</sup> reported the reducing trend with increase in salinity for clay minerals and sandstones was higher for SSW than aquifer water and deionized water.

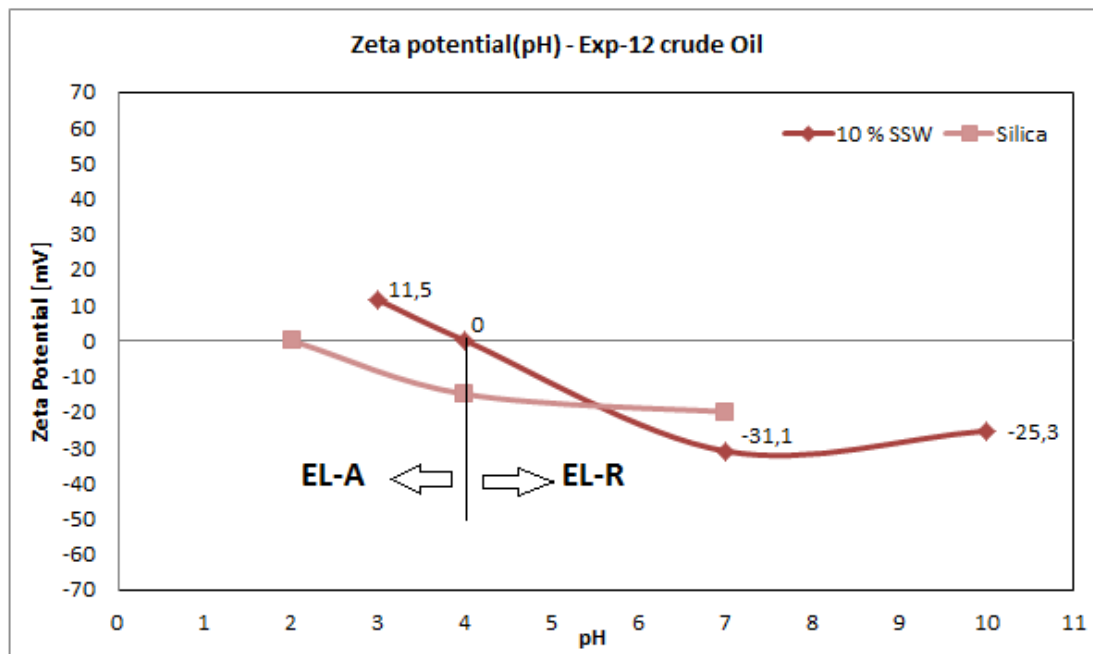
(See Figure 5.6 in Chapter 5)

Since the glass slides used in this study were aged in the measurement brine for 1-2 days, the hypothetical curves has been drawn based on the data for fresh suspension (aged data is for 2 weeks aged suspension). Assuming the same shielding effect for silica glass as for sandstones and clay minerals in presence of divalent ions, the hypothetical zeta potential values has been chosen to be lower than for the monovalent system at a given salinity and pH. The hypothetical values are presented in Appendix A3. The aim of doing this was to see the effect of salinity and pH on the regions of electrostatic attraction and repulsion in the crude oil/brine/silica surface system, and relate this to the observed adhesion behaviour. Even when the silica graph is a hypothetical graph, based on the reported salinity effect on silica surface charge, the real measured data is assumed will have shown approximately similar trend.

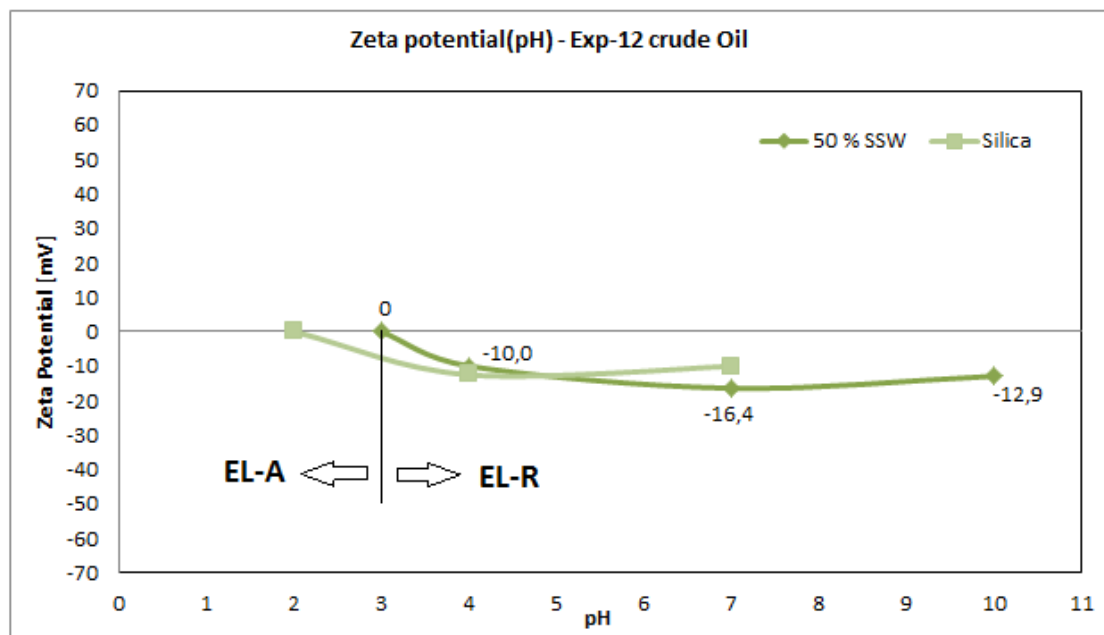
**Hypothetic and Measured Results**



**Figure 7.9:** Zeta potential(pH) for emulsion of Exp-12 crude oil in 1% SSW and a hypothetic zeta curve (pH) for suspension of crushed silica glass in 1% SSW.



**Figure 7.10:** Zeta potential(pH) for emulsion of Exp-12 crude oil in 10% SSW and a hypothetic zeta curve (pH) for suspension of crushed silica glass in 10% SSW.



**Figure 7.11:** Zeta potential (pH) for emulsion of Exp-12 crude oil in 50% SSW and a hypothetical zeta curve for suspension of crushed silica glass in 50% SSW.

### Discussion

In Figures 7.9 - 7.11 the black vertical dividing line from IEP for the crude oil, illustrate the transition region between electrostatic attraction (EI –A) and electrostatic repulsion (EI –R) occurring between crude oil and silica surfaces. As can be seen from the figures the strength of attraction and repulsion decreases with increase in salinity, observed by a decrease in the distance between the graphs.

Figure 7.9 for 1% SSW shows that at pH 3, the oil surface is highly positive charged with zeta potential equal to 54.9 mV, and can be explained by surface charge domination of ionic formed basic species, since  $pK_a > pH$  will apply for all the basic species in this pH range. At pH 4, the surface charge decreased to 18.9 mV and can be explained by surface activation of ionized strong acidic species with low  $pK_a$  values, e.g. 1-Naphtic acid with  $pK_a$  value equal to 3.70,<sup>[50]</sup> which will cause a reduction in net positive charge. The silica surface will become more negative with increase in pH as a result of its PZC equal to 2, and can be expected to have sufficient negative charge at these two pH values to attract the net positive charged crude oil.



Consistent with the measured zeta potential data for crude oil and the graphs presented in Figure 7.9, adhesion was observed for both equilibrated and non-equilibrated 1% SSW system at both pH 3 and 4. At pH 7 and 10 the results showed non-adhesion.

For 10% SSW shown in Figure 7.10, one can expect adhesion to occur with pH 3 solution, since a net positive charge at 11.5 mV was measured for the crude oil and since the region is placed on the attractive side of the graph. However, adhesion was only observed for the non-equilibrated pH 4 solution. This point was also measured to be IEP for the crude oil in this salinity region.

For the equilibrated system, non-adhesive behaviour was observed for the same solution.

The non-adhesive behaviour of the equilibrated system can be due to interface interactions that have activated more ionized acidic species during the equilibrium process that contributed to non-adhesion.

For the 50% SSW system shown in Figure 7.11, the measured pH regions are all within EL-R region with IEP measured at pH 3. According to DLVO calculations one might suggest adhesion to occur at this salinity region as a consequence of a more unstable system with low zeta potential values at -10.0 mV, -16.4 mV and -12.9 mV for the crude oil, and close to equal hypothetical values for the silica surface. These are all far away from the dividing line of -30 mV generally taken as the minimum net charge required characterizing the system as stable.<sup>[62]</sup>

For this salinity region adhesion was observed for the non-equilibrated pH 3 and equilibrated pH 4 solutions. The non-adhesive behaviour of the other pH solutions in the same salinity region, and the non-adhesive behaviour of the equilibrated and non-equilibrated systems for pH 3 and pH 4 respectively, create a doubt if this adhesion behaviour can be explained based on DLVO calculations. Even when the electrostatic force contribution will be shield in this salinity region, the adhesive behaviour is most probably due to interactions between positive charged basic species and negative charged silica surface.

For the 100% SSW brine adhesion was only observed for the non-equilibrated pH 3 solution.

All the other results showed non-adhesion. Buckley explained the stability of the system in presence of high salinity brine to be a cause of short range repulsive forces or hydration forces.<sup>[17]</sup>

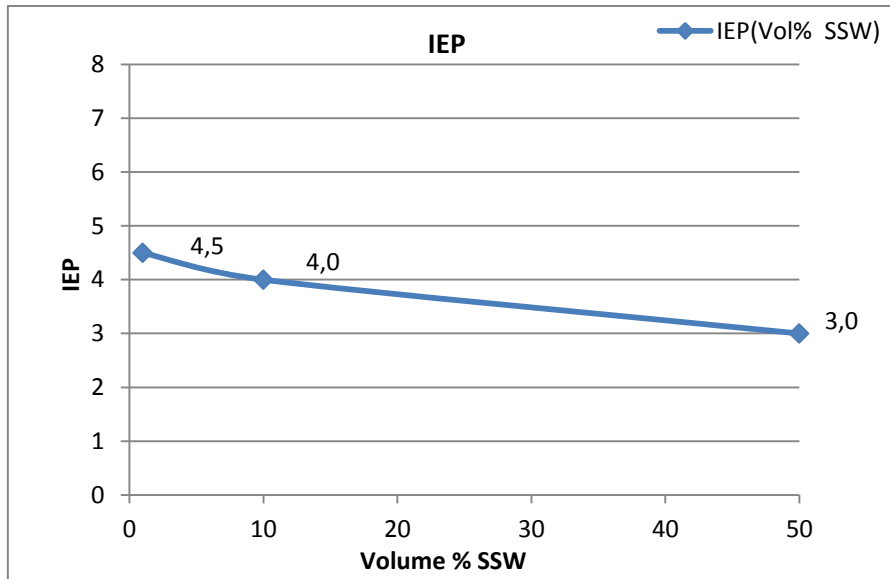
In pH 10 brines especially in the 50% and 100% SSW environments, it was very difficult to form any droplets close to the solid surface. Immediately when the droplet was formed close to the mineral surface, it broke and showed high affinity for the needle. The suggested cause of this observation can be due to the observed precipitate in these solutions and on the glass slides as mentioned previously. This observation is marked with cross in the adhesion maps presented in Table 7.2 and 7.3.

Observations related to the attachment point of the droplet upon withdrawal during the experiments showed a decreasing affinity for the brine covered surface for the results that resulted in non-adhesion. For the droplets that resulted in adhesion, small changes in the position of the attachment point was observed for pH 3, 50% and 100% SSW's in the non-equilibrated system, while the other results showed no change in the attachment point. Further, the observations showed that for pH 3 and 4 1% SSW's, the liquid bridge ruptured much faster than compared with the other results.

These observations are consistent with the magnitude of the attractive electrostatic forces present in Figure 7.9-7.11, and the measured contact angle values shown in Figure 7.7. In the zeta potential graphs, pH 3 brines are in all salinity ranges placed more toward the attractive side of the electrostatic force contribution compared with higher pH solutions, and this was also reflected in contact angle measurements showing less water-wet behaviour to be higher in this region compared with angles in the same salinity region but higher pH values. Even when pH 4 1% SSW was in the same wettability region as pH 3 50% and 100% SSW's with respect to their uncertainties, the stronger rupture observed for pH 4 1% SSW can be due to more dominating positive oil charge compared with screening of these charges in the higher salinity brines and/or due to ion binding effects if this occurred. The overall results indicate reduced oil-wetness with increase in pH and increase in salinity.

#### IEP – Attraction and Repulsion

Based on the results of adhesion test it is clear and evident that in the acidic region the attractive force contribution due to positive charged crude oil surface cause the oil to remain on the negative charged solid surface. This observation linked to the measured IEP for the different brine salinities leads to an interesting relationship. Figure 7.12 displays the measured IEP for Exp-12 in the different brine salinities.

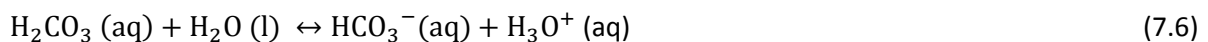


**Figure 7.12:** IEP for EXP-12 as function of brine salinity

As observed from the figure, IEP is higher for 1% SSW compared with 10% and 50% SSW's.

This means, the region of attraction is reached at higher pH values for LS brines compared with the HS brine.

In a reservoir where CO<sub>2</sub> can occur naturally, it can dependent on the reservoir pressure be dissolved in the injected brine and cause a pH reduction. Equation 7.5 and 7.6 shows the reactions that occur.



According to these reactions, the more CO<sub>2</sub> that dissolves in the injected brine, the more is Equation 7.6 shifted toward right due to increased H<sub>2</sub>CO<sub>3</sub>, which will disturb the initial equilibrium that exist between H<sub>2</sub>CO<sub>3</sub> and HCO<sub>3</sub><sup>-</sup> in the brine. Consequently, the pH of the brine phase will decrease.

If we imagine this to happen in a reservoir with Exp-12 crude oil when injecting the different brines, this decrease in pH would initially cause the crude oil to become net positive charged with injection of 1% SSW, due to its high IEP. Thus, instead of contributing the oil to be detached from the solid surface and be produced, the LS brine would have contributed negatively by holding the oil attached to the negative charged solid surface. Injection of the HS brine with IEP at pH 3, would have contributed with electrostatic repulsion until pH 3, thus in a wider pH range.

## 7.4 Interfacial Tension (IFT)

The surfactant character of crude oil species at the interface region between crude oil and brine and the impact on this character by different brine composition was observable through IFT study in this thesis. IFT measurement has been performed for the same fluid systems investigated by contact angle measurement and adhesion test. A total of 3-5 parallels were performed for each crude oil/brine system and the results in this section are presented as an average of the measurements.

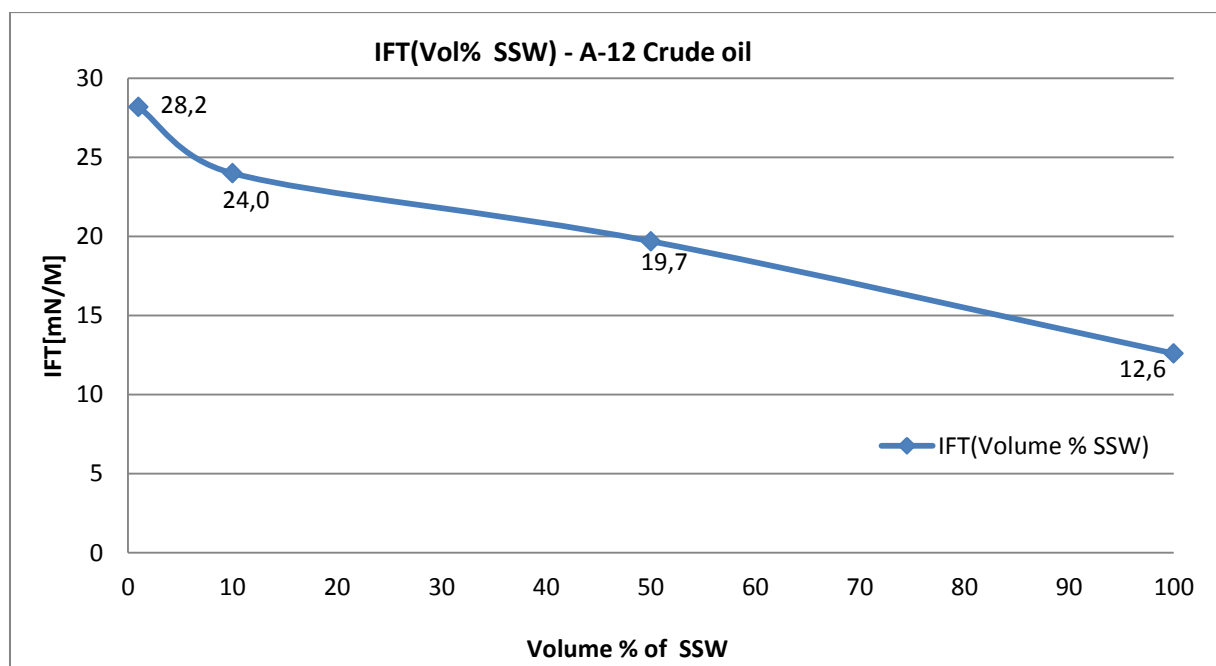
In Appendix A2, the average IFT and the fractional uncertainty of the results are presented.

The results of density measurements for the crude oils and brines used for IFT calculations are presented in Appendix A1.

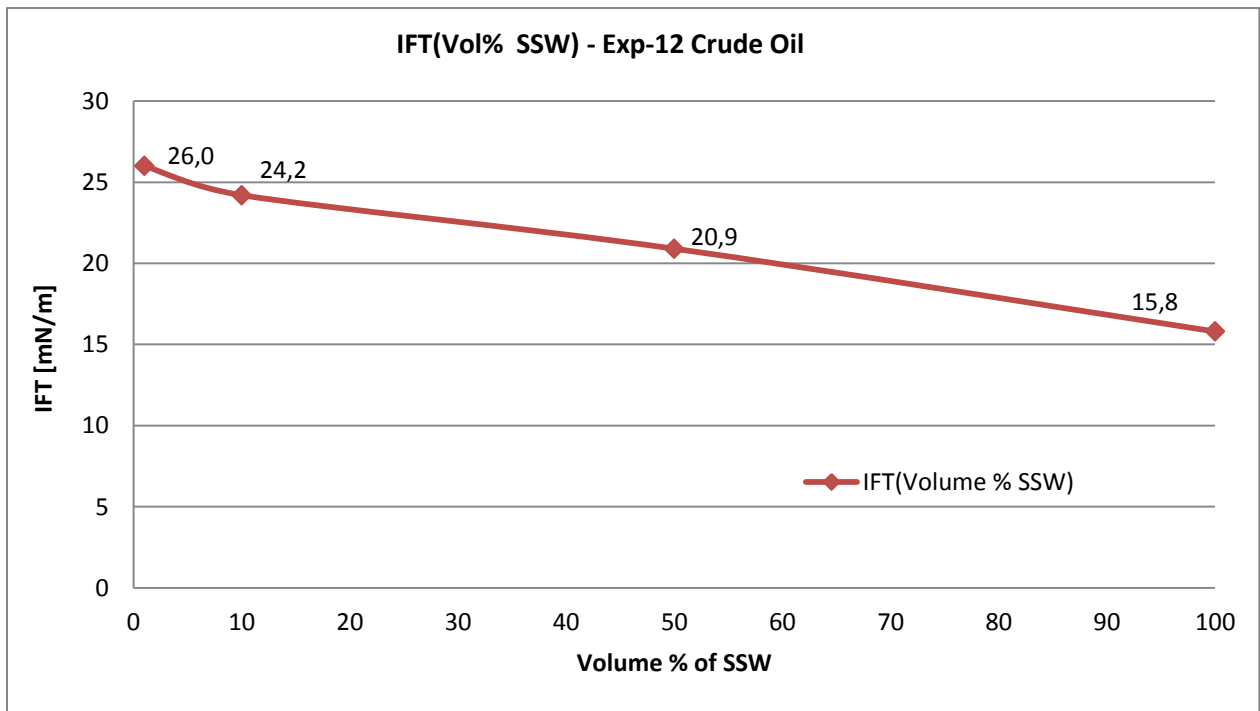
### 7.4.1 IFT – Crude Oils A-12, Exp-12 and Exp-12-D

The general trend observed for the crude oils A-12, Exp-12 and Exp-12-D was as the salinity of the brine phase increased the IFT decreased, meaning altering the fluid/fluid interaction of the original system in presence of 100% SSW, contributed to an unfavourable IFT shift. The IFT results for these crude oils are displayed in Figure 7.13 - 7.15 respectively.

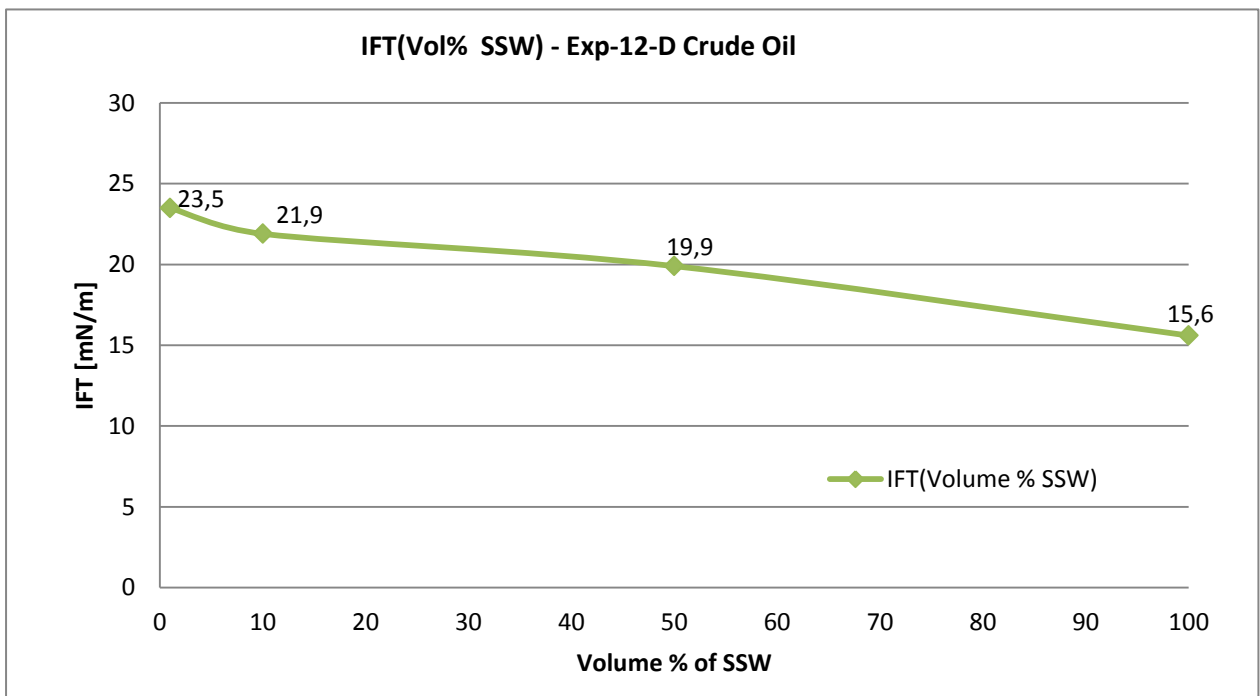
#### Results



**Figure 7.13:** IFT between A-12 crude oil and the four different brine compositions listed in Table 7.1.



**Figure 7.14:** IFT between Exp-12 crude oil and the four different brine compositions listed in Table 7.1.



**Figure 7.15:** IFT between Exp-12-D crude oil and the four different brine compositions listed in Table 7.1.

## Discussion

### A-12 and Exp-12

IFT between A-12 oil and 100% SSW was found to be 12.6 mN/m and between Exp-12 oil and 100% SSW equal to 15.8 mN/m. Both crude oils showed IFT values lesser than the average IFT between crude oil and SSW that are normally found to be between 20 – 30 mN/m. This can be a cause of the highly acidic character of the crude oils. In Chapter 5, Section 5.5, some previous IFT studies were summarized. Among these, the study performed by Standal et al.<sup>[48]</sup> showed the oil with the highest acid number to have lowest IFT in presence of all brine compositions. Buckley<sup>[2]</sup> observed for Moutray crude oil that reduction in IFT in all salinity ranges increased with activation of the acidic species compared with the activation of basic species. From zeta potential measurement for Exp-12 crude oil it was evident that at close to neutral pH the surface charge of the crude was net negative, meaning a surface charge domination of ionized acidic species. Even when salt tends to shield the net negative charges, the effect is still there. Net surface charge for A-12 crude oil is assumed would be slightly higher in this pH range due to its higher acid concentration than Exp-12, which will also impact the magnitude of the net charge (see Table 6.1, Chapter 6).

As observed from Figure 7.13 and 7.14, the IFT starts to increase with decrease in salinity for both crude oils. For A-12 crude the change in brine salinity from 100% to 50% SSW (still HSW) increased the IFT with ~ 7 units, from 50% to 10% SSW with ~ 4 units and further reduction to 1% SSW with ~ 4 units. The difference between maximum HSW and minimum LSW was found to be ~15.6 mN/m.

For Exp-12 crude the reduction in salinity from SSW to 50% SSW increased the IFT with ~ 5 units and further reduction to 10% and 1% SSW with ~3 units and ~2 units, respectively. The difference between maximum HSW and minimum LSW for this crude oil was found to be ~ 10 mN/m.

The results showed the impact of brine dilution was higher for crude oil A-12 compared with Exp-12, even when both crude oils showed unfavourable IFT trend with reduction in salinity.

In presence of high salinity brine the “salting out” effect has been reported to decrease the preference of polar organic species for the water phase.<sup>[54]</sup> It has also been reported that the surface active contribution of acidic and basic species to reduction in IFT is higher from their activity in water phase compared with oil phase.<sup>[50]</sup> It can be easy to conclude that the more acid/base present in water phase the better it is, since species in water phase are reported to contribute to reduction in

IFT. But with respect to the studies of Abdel Wali<sup>[69]</sup> and Standal et al.<sup>[50]</sup> discussed about in Chapter 5, Section 5.5, their results indicates there is a specific relationship required between the concentration of the acidic components present in the interface region between oil and water (active from the water phase) and salinity of the aqueous phase to give a positive IFT contribution.

For Exp-12 and A-12 crude oils the “salting out” effect seems to give the optimum relationship between acid components active from the water phase and the brine salinity.

Vijapurapu and Rao<sup>[70]</sup> showed the reduction in IFT for Yates crude oil and SSW to occur in the region between 100% and 50% SSW's, further reduction increased the IFT. This salinity region has not been investigated in this study and creates a doubt if any other IFT trend could have been observed by investigating a wider salinity area.

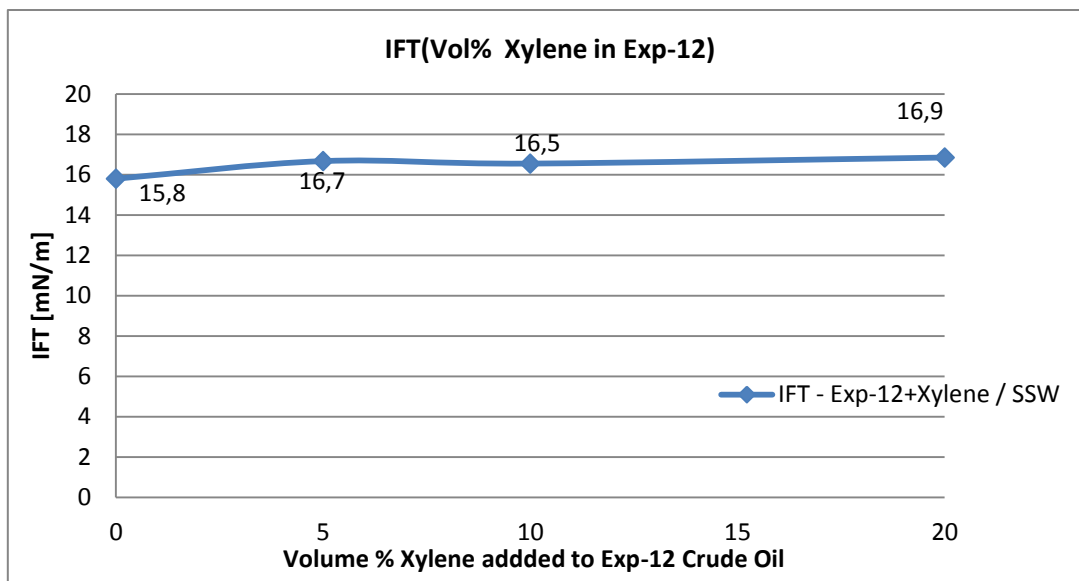
#### Exp-12-D

As visible from Figure 7.15, the IFT results obtained with Exp-12-D crude oil and 100% SSW showed a similar IFT value as the original crude oil, while dilution with factors of 2, 10 and 100 reduced the IFT with  $\sim 1$  mN/m,  $\sim 2$  mN/m and  $\sim 2.5$  mN/m respectively compared with IFT values at the same brine salinities for Exp-12 crude. The difference between maximum HSW and minimum LSW for this crude oil was  $\sim 8$  mN/m compared with  $\sim 10$  mN/m for the original crude oil. The small changes observed creates a doubt that Xylene and/or Iododecane must have impacted the fluid/fluid interaction due to the reduction observed, but since the changes are not as catastrophic the combined effect of Xylene and Iododecane can be considered as maintaining close to similar fluid/fluid interactions as the original system.

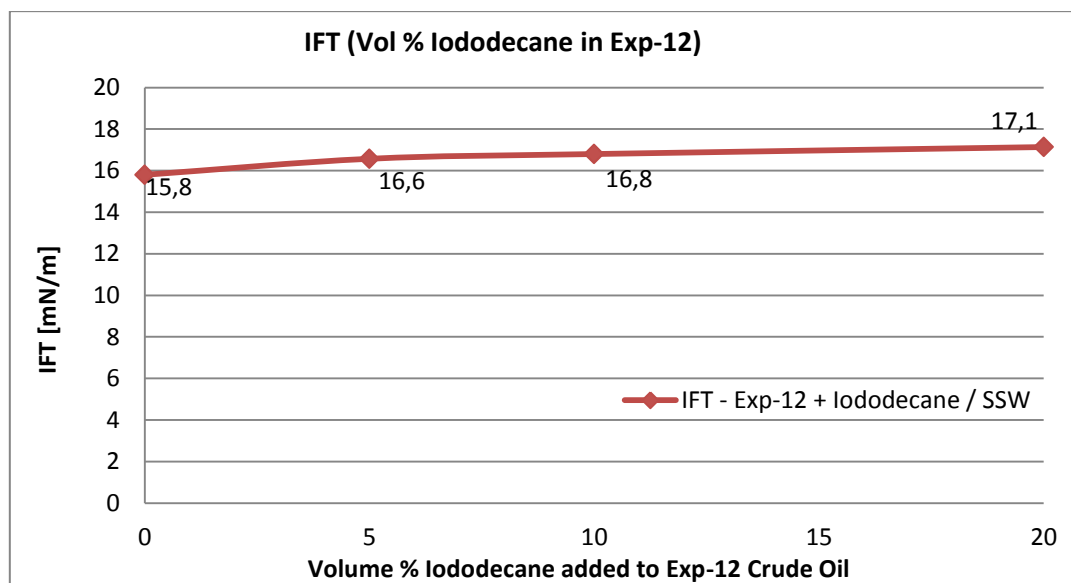
### **7.4.2 Individual Impact of Xylene and Iododecane on Exp-12 IFT**

#### **Results**

The results of IFT measurements between the different portion of individually Xylene and Iododecane added Exp-12 crude oils and 100% SSW are shown in Figure 7.16 and 7.17.



**Figure 7.16:** IFT between SSW and individually Xylene (5%,10% and 20%) added Exp-12 crude oil.



**Figure 7.17** IFT between SSW and individually Iododecane (5%,10% and 20%) added Exp-12 crude oil.

### Discussion

5%, 10% and 20% addition of the chemicals showed a similar trend with an increase in  $\sim 1$  mN/m for all volume percentage of chemical added compared with the original crude oil. The IFT results indicated that none of the chemicals influenced the original IFT more or less than the other, but a more systematic trend in increase was observable for the Iododecane added oil than Xylene.



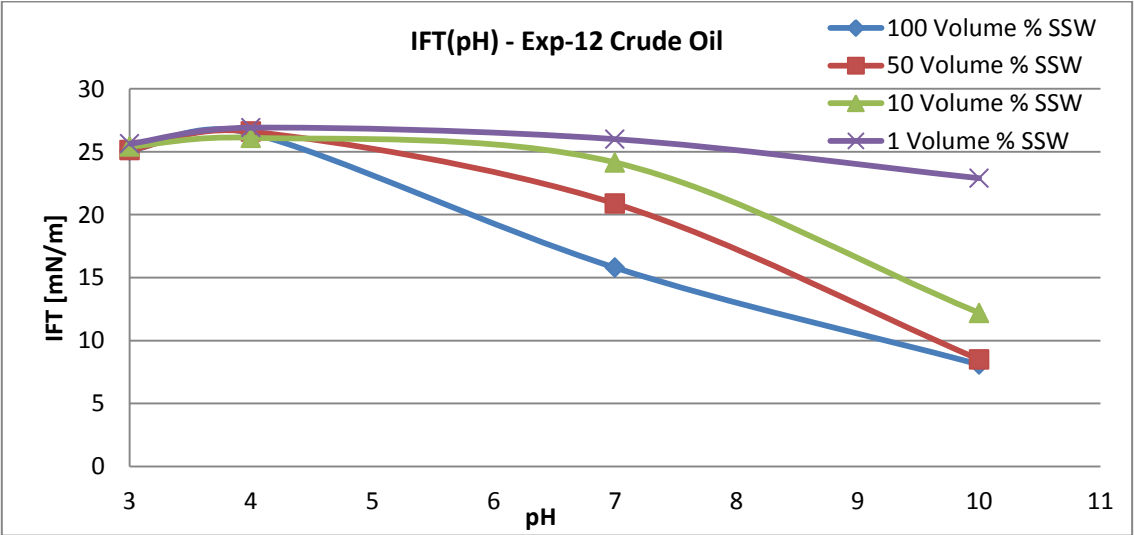
The ~1 mN/m increase in IFT for the 20% Xylene and 20% Iododecane added crude oils was not visible in the combined effect, and in the lower salinity region the impact was rather opposite. Since the uncertainty of the IFT measurements is relatively low the decreasing trend in the combined mixed crude oil is difficult to explain. The overall results indicate that the individual impact of Xylene and Iododecane does not seem to influence the crude oil behaviour more than the combined effect, especially in LS regions.

**7.4.3 IFT as Function of Brine Salinity with varying pH**

When Buckley measured IFT between crude oils and brines of different pH, she found a trend where the IFT curve for the basic crude oil A-93 was highest near neutral pH and decreased as pH either increased or decreased. For the acidic crude she observed the IFT curve to almost be constant at low pH region, and decreased with increase in pH. Similar trend was also found for ST-86 crude oil which was also an acidic crude oil. (See Figures 5.11 and 5.12 in Chapter 5).

**Results**

Consistent with the acidic crude oils, IFT curves for IFT between Exp-12 crude oil and the similar brine compositions as those used for adhesion test showed the same decreasing trend with increase in pH. Figure 7.18 presents the IFT results.



**Figure 7.18:** IFT(pH) between Exp-12 crude oil and the four different brine compositions listed in Table 7.1.

## Discussion

As observable from the figure, the sharpness of the decrease in IFT increase with salinity in all pH ranges. At pH 3 and 4 all the saline brines showed similar trend with constant IFT at  $\sim 25$ - $26$  mN/m and  $\sim 26$ - $27$  mN/m, respectively. This indicates that the surface activated basic species does not give any positive contribution to IFT, but rather increased the IFT between crude oil and brine compared with the neutral brine solutions. The decrease started with surface activation of the ionic form of the acidic species. For the 100% and 50% SSW's in pH 10 region, almost similar IFT's at 8.1 mN/m and 8.6 mN/m were observed. This means a reduction in 12.4 mN/m for the 50% SSW solution and 7.7 mN/m reduction for the 100% SSW from pH 7 to 10. Also for the 10% SSW in this pH range a reduction in 12.0 mN/m was observed compared with the IFT at pH 7. This indicates that more miscible interaction occurred between the brine and oil phase as more acidic species ionized.

As observed from the figure and the measured data, the trend of "salting out" that seemed to be preferred at neutral pH seems to be eliminated in pH 10 region for the different brines, despite for 1% SSW which showed a reduction with  $\sim 2$  mN/m from pH 3 to 10. For the 50% and 100% SSW's the precipitated salt could also have influenced the observed IFT's.

IFT between crude oil and brine has been reported to be time dependent, meaning with increased contact time between the phases different results can be observed due to more stabilised surface reactions. As observed from the study performed by Xu,<sup>[68]</sup>(See Figure 5.13, Chapter 5) the static pendant drop method allowed measurement of the time dependent IFT. Drop-volume method is a dynamic measurement method and does not show any variation with time.

The fluids were not pre-equilibrated prior to measurement. This creates a doubt of how the interfacial tension would have developed with more initial contact time between the phases.

Since IFT between crude oil and brine is an important factor in achieving potential oil recovery, and since the LSW's used in this study shows an increase in IFT compared with HSW's at comparable brine pH, one reason for different production trend observed with LSW sometimes being higher and sometime showing no additional oil recovery, can be a cause of negative IFT contribution with LSW.

## 7.5 Wettability Results and Previous Studies

Table 7.4 summarizes the measured, proposed and literature reported wettability data in presence of LSW and HSW. Measured zeta potential trend for Exp-12 crude oil, and literature reported zeta potential trend for silica surface is also presented in the table. (WW = Water-Wet)

Measurement	LSW	HSW	Measured / Literature
$\theta_r$ Exp-12	~Constant	~Constant	Measured
$\zeta$ potential Exp-12	Higher	Lower	Measured
IEP Exp-12	Higher	Lower	Measured
$\zeta$ potential Silica	Higher	Lower	Literature <sup>[17]</sup>
$\theta_r$ A-12	More WW	Less WW	Measured
Adhesion test	Less WW	More WW	Measured + Literature <sup>[2, 52, 67]</sup>
Proposed LS-mechanisms (Wettability indicators)	More WW	Less WW	Literature <sup>[8, 9, 11, 30]</sup>
Coreflooding Lingthelm (Amott wettability test)	More WW	Less WW	Literature <sup>[37]</sup>

**Table 7.4** Measured, proposed and literature reported wettability trends with LS and HS brines

In Chapter 3, five of the most accepted proposed LS mechanisms assumed contributes to higher oil recovery with LSW were presented. For all the proposed mechanisms, wettability alteration toward more water-wet state was considered as being central in achieving the low salinity effect (LSE).

The results of adhesion test for Exp-12 crude oil showed decreased water-wetness with decrease in salinity in the acidic region of the adhesion map, and non-adhesion behaviour in the neutral and basic region of the adhesion map. The adhesive behaviour deviating from DLVO calculations in higher pH, LSW regions (not observed in this study) are reported to be a result of high base/acid ratio of the

crude oils.<sup>[2, 48]</sup> Based on the trend observed in the acidic region of the adhesion map, and on the trend observed deviating from DLVO calculations in LS region, and in HS regions due to the stability of the water-film in this region, the general adhesion behaviour of crude oils based on an adhesion map are concluded to be more water-wet at HS regions than LS regions.

This means, the result of adhesion test shows an opposite trend of what the proposed LS mechanisms suggest.

Among the 5 proposed mechanisms it was only the mechanism proposed by Lingthelm et al.<sup>[37]</sup> that concluded wettability shift toward more water-wet state with injection of LSW based on Amott-wettability test. None of the other studies included measurement of wettability indices or contact angle measurement to confirm the wettability shift. But when the conclusion of more water-wet state are based on Amott test, USBM test or contact angle measurements, the general trend of adhesion comes also in conflict with the most accepted wettability measurement methods that exist.

Contact angle measurements performed for Exp-12 crude oil showed almost no change in wettability with reduction in salinity, while A-12 crude oil was more sensitive to reduction in salinity.

Nasralla et al.<sup>[60]</sup> measured contact angles for two different crude oils A and B in presence of different brine compositions, and observed reduction in contact angle with reduction in salinity was higher for crude oil A compared with crude oil B (See Figures 5.4 a and b in Chapter 5). This evidence the impact of the type of crude oil and composition on wettability as function of brine salinity.

Their results also showed crude oil A with highest net negative surface charge at a given brine salinity, to be more sensitive to reduction in salinity. One reason for crude oils to have a sufficient high net negative charge at given salinity (also a given pH) seems to be a consequence of the acidic nature of the crude oils. E.g. Moutray crude oil (acidic) had a higher net negative charge at higher pH regions than A-93 crude oil (basic). (See Figure 5.5 a and b, Chapter 5)

The zeta potential for crude oils and silica surface has been reported and measured to be higher in LS regions compared with HS regions due to the shielding effect in HS regions.

Even when adhesion test performed for Exp-12 crude oil showed non-adhesive behaviour in the close to neutral pH in all salinity regions, this behaviour does not need to mean that the system is equally water-wet in all salinity regions, but can rather be due to sufficient negative charges at crude oil and silica surfaces to result in non-adhesion. The contact angles measured in this region seemed to be a function of the net charge at crude oil and mineral surfaces, relative to each other.

At low pH values the net negative charge for silicate surface can be higher than for crude oils due to its PZC at pH 2. But as more the acidic species in the crude oil ionizes after IEP for crude oils are reached, the net negative charge of crude oils can become even higher than for the silicate surface. This is also visible by comparing the zeta potential plots for crushed silicate glass and Moutray crude oil at comparable salinities. (See Figure 5.5b and 5.7, Chapter 5)

For this reason, the constant wettability behaviour of Exp-12 crude oil in all salinity regions can be due to a close to equal net negative charge at both surfaces, and the system is those maintaining a constant repulsion in all regions.

For A-12 crude oil, which is a more acidic crude oil than Exp-12, the more water-wet behaviour with reduction in salinity can be a cause of higher net negative charge at the oil surface compared with the mineral surface at the same pH region, and as the shielding effect is reduced as a consequence of reduction in salinity, and the net surface charge at oil surface becomes more dominant, the strength of repulsion can increase and the system can become more water-wet.

The combined results of adhesion test and contact angle measurements indicate reduction in water-wetness or increase in water-wetness to be governed by pH of the brine phase and acid/base composition of the oil phase. The result also indicates that to achieve a more concrete wettability description, contact angle measurements are more valid than the adhesion test.

For this reason, to confirm a wettability shift with LSW, a complete wettability study including Amott-Harvey, USBM and contact angle test should be included and be consistent with following equations:

$$I_{\text{USBM}} (\text{HS}) < I_{\text{USBM}} (\text{LS}) \quad (7.7)$$

$$I_{\text{AH}} (\text{HS}) < I_{\text{AH}} (\text{LS}) \quad (7.8)$$

$$\theta(\text{HS}) > \theta(\text{LS}) \quad (7.9)$$

A complete wettability study will also give information about the regime wettability alteration occurs in. In the study performed by Lingthelm et al.<sup>[37]</sup> they found the wettability shift to occur from more oil-wet to intermediate wet state. Hence, the observed increase in oil recovery does not need to be a

consequence of production of the previously attached oil as film that is volumetric less in amount compared with oil in larger pores, as the low salinity mechanisms suggest (also Lingthelm et al. proposed), but due to a wettability shift toward a more favourable wettability state.

## 8 Conclusion

- The combined effect of oil dilution with organic solvents to reduce crude oil viscosity and for x-ray contrast does not change physicochemical properties of the crude oil significant.
- For oils tested, there is either almost unchanged or reduced contact angle with reduction in brine salinity.
- Zeta potential measurement showed at a constant pH with reduction in salinity, the electric charge at oil/brine interface increased either negative or positive.  
The measurements also showed shift of isoelectric point to higher pH with decrease in salinity.
- Adhesion mapping showed at low pH values, there are stronger tendencies to alter the wettability toward more oil-wet state with reduction in brine salinity.
- The overall wettability and zeta potential data obtained in this study indicates that a combination of low salinity water and low pH will make it easier to alter the wettability to more oil-wet.
- For the oils examined, the interfacial tension measurements showed the original oil/brine system in presence of high salinity water, with interface domination of ionized acidic species to provide the most favourable conditions.
- The two North Sea crude oils show generally analogous trends with the trends existing in the literature.





## 9 Further Work

Static physicochemical low salinity water studies combined with dynamic coreflood studies will help to provide a better understanding of the mechanisms around low salinity water, which is still not completely understood. The only way to achieve a better understanding is through more research and more data. Some suggested further works of this study are given below:

- Investigate if the data and trends observed in this work are observable for more crude oils with varying composition, especially with respect to their acid and base numbers.
- More research around the isoelectric point is also required. If this trend was observed due to the unusual high acid number of the crude oil remains as a question mark.
- Compare the observed physicochemical data with coreflood experiments that monitors oil recovery as function of time, under the same conditions.
- Perform Amott and USBM test to compare, control and strength the wettability data obtained with contact angle measurements.
- More adhesion test performed with mixed brines and brines composed of different salts than NaCl is required, to achieve a wider understanding for why adhesion behaviour in mixed brine deviates from NaCl tests.
- Conduct zeta potential measurements for crushed silica glass in presence of synthetic sea water and a set of dilution of this.
- Investigate a wider salinity region for the interfacial tension between crude oils and brines, investigated in this study.

## 10 References

1. M. Skarestad and A. Skauge  
[Compendium: Reservoarteknikk2, Ptek 213]  
**“Fluid properties and Recovery methods compendium”**  
[2011]
2. J. S. Buckley  
[Doctoral thesis]  
**“Mechanisms and Consequences of Wettability Alteration by Crude Oils”**  
[1996, Heriot-Watt University Petroleum Engineering]
3. N. Hamidreza  
[Doctoral thesis]  
**“Enzymes for Enhanced Oil Recovery (EOR) “**  
[2011, The University of Bergen]
4. M.B. Alotaibi, SPE; R.M. Azmy, SPE, and H.A. Nasr-El-Din, SPE, Texas A&M University  
[Conference Paper]  
**“A Comprehensive EOR Study Using Low Salinity Water in Sandstone Reservoirs”**  
[2010, Society of Petroleum Engineers]
5. J. S. Solbakken  
[Master thesis]  
**“An Experimental Study of Low Salinity Surfactant Flooding in Low Permeability Berea Sandstone”**  
[2010, Centre for Integrated Petroleum Research (Uni CIPR), University of Bergen]
6. J. C. Martin, Creole Petroleum Corp.  
[Conference Paper]  
**“The Effects of Clay on the Displacement of Heavy Oil by Water”**  
[1959, Society of Petroleum Engineers of AIME]
7. G. G. Bernard, Union Oil Research Center  
[Conference Paper, 1725-MS]  
**“Effect of Floodwater Salinity on Recovery of Oil from Cores Containing Clays”**  
[1967, Society of Petroleum Engineers]
8. G.Q. Tang, SPE and N.R. Morrow, SPE, University of Wyoming  
[Journal Paper, 36680-PA]  
**“Salinity, Temperature, Oil Composition, and Oil Recovery by Waterflooding“**  
[1997, Society of Petroleum Engineers]

9. N. R. Morrow, G.Q. Tang, Marc Valat and Xina Xie, Department of Chemical and Petroleum Engineering, University of Wyoming, Laramie  
[Journal Paper]  
**“Prospects of Improved Oil Recovery Related to Wettability and Brine Composition”**  
[1998, Petroleum Science and Engineering]
10. W. Winoto, SPE; N. Loahardjo, SPE; X. S. Xie, SPE; P. Yin, and N. R. Morrow, SPE, University of Wyoming  
[Conference Paper, 154209-MS]  
**“Secondary and Tertiary Recovery of Crude Oil from Outcrop and Reservoir Rocks by Low Salinity Waterflooding”**  
[2012, Society of Petroleum Engineers]
11. P. L. McGuire, SPE; J.R. Chatham; F.K. Paskvan, SPE; D.M. Sommer, SPE; and F.H. Carini, SPE, BP Exploration (Alaska) Inc  
[Conference Paper, 93903-MS]  
**“Low Salinity Oil Recovery: An Exciting New EOR Opportunity for Alaska’s North Slope”**  
[2005, Society of Petroleum Engineers Inc.]
12. K. Spildo and E. Gilje  
[Report NO: 09/2007]  
**“Technology update: Low Salinity Waterflooding”**  
[2007, CIPR, University of Bergen]
13. K. Skrettingland, Statoil; T. Holt, SPE, Sintef Petroleum Research; and M.T. Tweheyo, SPE, and I.Skjevrak, Statoil  
[SPE 129877]  
**“Snorre Low-Salinity-Water Injection-Coreflooding Experiments and Single-Well Field Pilot”**  
[2010, Society of Petroleum Engineers]
14. S. H. Standal  
[Doctoral thesis]  
**“Wettability of Solid Surfaces Induced by Adsorption of Polar Organic Components in Crude Oil”**  
[1999, Department of Chemistry, University of Bergen]
15. A. Skauge and B. Ottesen, Norsk Hydro ASA and University of Bergen, Reservoir Laboratories, Trondheim  
[SCA2002-12]  
**“A Summary of Experimentally Derived Relative Permeability and Residual Saturation on North Sea Reservoir Cores”**  
[2002, Norsk Hydro ASA and Reslab AS]

16. R. A. Salathiel, SPE-AIME, Esso Production Research.Co.  
[Journal Paper, 4104-PA]  
**“Oil Recovery by Surface Film Drainage in Mixed-Wettability Rocks”**  
[1973, Society of Petroleum Engineers]
17. J. S. Buckley, New Mexico Petroleum Recovery Research Center; K. Takamura, Alberta Research Council; N.R. Morrow, New Mexico Petroleum Recovery Research Center  
[Journal Paper, 16964-PA]  
**“Influence of Electrical Surface Charges on the Wetting Properties of Crude Oils”**  
[1989, Society of Petroleum Engineers]
18. G. J. Hirasaki, SPE, Shell Development Co.  
[Journal Paper, 17367-PA]  
**“Wettability: Fundamentals and Surface Forces”**  
[1991, Society of Petroleum Engineers]
19. J. C. Berg  
[Book]  
**“An Introduction to Interfaces & Colloids. The Bridge to Nanoscience”**  
[2009, World Scientific Publishing Co. Pte. Ltd.]
20. W. G. Anderson, Conoco Inc.  
[Journal Paper, 16471-PA]  
**“Wettability Literature Survey-Part 6: The Effects of Wettability on Waterflooding”**  
[1987, Society of Petroleum Engineers]
21. F. F. Craig  
[Book]  
**“The Reservoir Engineering Aspects of Waterflooding”**  
[1971, The American Institute of Mining, Metallurgical, and Petroleum Engineers Inc.]
22. W. G. Anderson, Conoco Inc.  
[Journal Paper, 13933-PA]  
**“Wettability Literature Survey-Part 2: Wettability Measurement”**  
[1986, Society of Petroleum Engineers]
23. A. Skauge, University of Bergen  
[Lecture note in Ptek 312]  
**“Selected topics in petroleum technology”**  
[2012,CIPR, University of Bergen]

24. A. Skauge, K. Spildo, B. Vik, Centre for Integrated Petroleum Research (CIPR); and L. Høiland, Statoil ASA  
[Journal Paper]  
**“Theoretical and Experimental Evidence of Different Wettability Classes”**  
[2007, Journal of Petroleum Science and Engineering]
25. N. R. Morrow, SPE, New Mexico Petroleum Recovery Research Center, New Mexico Inst. Of Mining and Technology  
[Journal Paper, 21621-PA]  
**“Wettability and Its Effect on Oil Recovery”**  
[1990, Society of Petroleum Engineers]
26. N. R. Morrow, Petroleum Recovery Institute, University of Calgary  
[Journal Paper, 75-04-04]  
**“The Effects of Surface Roughness on Contact: Angle with Special Reference to Petroleum Recovery”**  
[1975, Society of Petroleum Engineers]
27. G. Tang, and N. R. Morrow, Department of Chemical and Petroleum Engineering, University of Wyoming  
[Journal Paper]  
**“Influence of Brine Composition and Fines Migration on Crude Oil/Brine/Rock Interactions and Oil Recovery”**  
[1999, Journal of Petroleum Science and Engineering]
28. A. Skauge  
[Extended Abstract, Symposium: Emerging technology of EOR, Beijing, China]  
**“Microscopic diversion – a new EOR technique”**  
[2008, The International Energy Agency]
29. K. Spildo, SPE; A. Skauge, SPE; and T. Skauge, SPE, CIPR/Uni Research  
[Conference Paper, SPE 129927]  
**“Propagation of Colloidal Dispersion Gels (CDG) in Laboratory Corefloods”**  
[2010, Society of Petroleum Engineers]
30. A. Lager and C. J. J. Black, BP Exploration (Alaska); K. J. Webb, BP Exploration Production Technology; M. Singleton and K. S. Sorbie, Institute of Petroleum Engineering  
[Journal Paper, 2008-v49n1a2]  
**“Low Salinity Oil Recovery – An Experimental Investigation 1”**  
[2008, Society of Petrophysicists & Well Log Analysts]

31. M. Cossikho, H. Bertin, TREFLE-CNRS, University of Bordeaux, France; S. Boussour, Ph. Cordier, G. Hamon, Total, Pau, France  
[Paper]  
**“Low Salinity Oil Recovery on Clayey Sandstone: Experimental Study”**  
[2009]
32. S. Boussour, SPE, Total; M. Cissokho, SPE, U. of Bordeaux-France; P. Cordier, SPE, Total; H. Berlin, SPE, U. of Bordeaux-France; and G. Hamon, SPE, Total  
[Conference Paper, SPE 124277]  
**“Oil Recovery by Low-Salinity Brine Injection: Laboratory Results on Outcrop and Reservoir Cores”**  
[2009, Society of Petroleum Engineers]
33. T. Grønneberg, M.Hannisdal, B. Pedersen and V. Ringnes  
[Book]  
**“Kjemien stemmer 2KJ”**  
[2001, Cappelen]
34. T. Austad, A. RezaeiDoust, and T. Puntervold, University of Stavanger  
[Conference Paper, 129767-MS]  
**“Chemical Mechanism of Low Salinity Water Flooding in Sandstone Reservoirs”**  
[2010, Society of Petroleum Engineers]
35. G. Sposito  
[Book]  
**“The Chemistry of Soils”**  
[1989, Oxford University Press USA]
36. A. Lager, K. J. Webb, and I.R. Collins, BP, EPTG, Pushing Reservoir Limits, Sunbury, UK and D. M. Richmond, BP, BP Exploration (Alaska), Anchorage, AK, USA  
[Conference Paper, 113976-MS]  
**“LoSal Enhanced Oil Recovery: Evidence of Enhanced Oil Recovery at the Reservoir Scale”**  
[2008, Society of Petroleum Engineers]
37. D. J. Ligthelm, SPE, J. Gronsveld, J. P. Hofman, M. J. Brussee, F.. Marcelis, and H.A. van der Linde, Shell International Exploration and Production B.V.  
[Conference Paper, 119835-MS]  
**“Novel Waterflooding Strategy by Manipulation of Injection Brine Composition”**  
[2009, Society of Petroleum Engineers]

38. P. P. Jadhunandan, SPE, Inst. Teknologi Bandung; N. R. Morrow, SPE, New Mexico Petroleum Recovery Research Center  
[Journal Paper, 22597-PA]  
**“Effect of Wettability on Waterflood Recovery for Crude-Oil/Brine/Rock Systems”**  
[1995, Society of Petroleum Engineers]
39. A. Ashraf, N.J. Hadia, and O. Torsæter, Norwegian University of Science and Technology (NTNU), and M.T. Tweheyo, Statoil  
[Conference Paper, 129012-MS]  
**“Laboratory Investigation of Low Salinity Waterflooding as Secondary Recovery Process: Effect of Wettability”**  
[2010, Society of Petroleum Engineers]
40. J. S. Buckley, SPE; Y. Liu, SPE; and S. Monsterleet, New Mexico Petroleum Recovery Research Center, New Mexico Inst. of Mining and Technology  
[Journal Paper, 37230-PA]  
**“Mechanisms of Wetting Alteration by Crude Oils”**  
[1998, Society of Petroleum Engineers]
41. R. Kaminsky and C. J. Radke  
[Journal Paper, 39087-PA]  
**“Asphaltenes, Water Films, and Wettability Reversal”**  
[1997, Society of Petroleum Engineers]
42. Y. Liu, J. S. Buckley, New Mexico Petroleum Recovery Research Center, New Mexico Inst. of Mining and Technology  
[Journal Paper, 28970-PA]  
**“Evolution of Wetting Alteration by Adsorption from Crude Oil”**  
[1997, Society of Petroleum Engineers]
43. W. G. Anderson, Conoco Inc.  
[Journal Paper, 13932-PA]  
**“Wettability Literature Survey - Part 1: Rock/Oil/Brine Interactions and the Effects of Core Handling on Wettability”**  
[1986, Society of Petroleum Engineers]
44. M. O. Denekas and C. C. Mattax, Jersey Production Research Co.; G. T. Davis, Esso Research and Engineering Co.  
[Other, 1276-G]  
**“Effects of Crude Oil Components on Rock Wettability”**  
[1959, Society of Petroleum Engineering]

45. Z. Muhammad, D. N. Rao, Louisiana State University  
[Conference Paper, 65409-MS]  
**“Compositional Dependence of Reservoir Wettability”**  
[2001, Society of Petroleum Engineers]
46. J.G. Speight  
[Book]  
**“The Chemistry and Technology of Petroleum, 4<sup>th</sup> Edition”**  
[2010, CRC Press]
47. S.O. Bøe  
[master thesis]  
**“Syre/base eigenskapar til råolje og deira innverknad på fukting i vann-olje-kvarts system”**  
[1998, Universitetet i Bergen]
48. A. Skauge, Norsk Hydro; S. Standal, S. O. Boe, T. Skauge, A. M. Blokhus, University of Bergen  
[Conference Paper, 56673-MS]  
**“Effects of Organic Acids and Bases, and Oil Composition on Wettability”**  
[1999, Society of Petroleum Engineers]
49. Ali. A. Yousef, Salah Al-Saleh, and Mohammed Al-Jawfi, Saudi Aramco  
[Conference Paper, 154076-MS]  
**“Improved/Enhanced Oil Recovery from Carbonate Reservoirs by Tuning Injection Water Salinity and Ionic Content”**  
[2012, Society of Petroleum Engineers]
50. S. Standal, A.M Blokhus, J. Haavik and T. Barth, Department of Chemistry, University of Bergen; Arne Skauge, Norsk Hydro Research Center  
[Article]  
**“Partition Coefficients and Interfacial Activity for Polar Components in Oil/Water Model Systems”**  
[1999, Elsevier]
51. T. Barth, University of Bergen  
[Lecture note in Kjem 203]  
**“Petroleum Chemistry”**  
[2011, University of Bergen]
52. J.S. Buckley and Yu Liu, New Mexico PRRC; Xina Xie and Norman R. Morrow, U. of Wyoming  
[Journal Paper, 35366-PA]  
**“Asphaltenes and Crude Oil Wetting – The Effect of Oil Composition”**  
[1997, Society of Petroleum Engineers]



53. S. Standal, J. Haavik, and A. M. Blokhus, Department of Chemistry, University of Bergen; A. Skauge, Norsk Hydro Research Centre  
[Article]  
**“Effect of Polar Organic Components on Wettability as Studied by Adsorption and Contact Angles”**  
[1999, Elsevier]
54. A. RezaeiDoust, T. Puntervold, S. Strand and T. Austad, University of Stavanger  
[Article]  
**“Smart Water as Wettability Modifier in Carbonate and Sandstone: A Discussion of Similarities/Differences in the Chemical Mechanisms”**  
[2009, American Chemical Society]
55. G. A. Parks, Department of Applied Earth Science, Stanford University  
[Journal]  
**“Surface and Interfacial Free Energies of Quartz”**  
[1984, The American Geophysical Union]
56. R. D. Kulkarni and P. Somasundaran, Henry Krumb School of Mines, Columbia University  
[Journal]  
**“Effect of Pretreatment on the Electrokinetic Properties of Quartz”**  
[1976, Elsevier]
57. C. Busireddy, Nandina N. Rao, Louisiana State University  
[Conference Paper, 89425-MS]  
**“Application of DLVO Theory to Characterize Spreading in Crude Oil-Brine-Rock Systems”**  
[2004, Society of Petroleum Engineers]
58. T. Skodvin, University of Bergen  
[Lecture note in Kjem 214]  
**“Surface and Colloid Chemistry”**  
[2007, University of Bergen]
59. B. Salopek, D. Krasic and S. Filipovic, Faculty of Mining, Geology and Petroleum Engineering, University of Zagreb  
[Article]  
**“Measurement and Application of Zeta-Potential”**  
[1992, University of Zagreb]
60. R. A. Nasralla, SPE, Mohammed A. Bataweel, SPE, Hisham A. Nasr-El-Din, SPE, Texas A&M University  
[Conference Paper, 146322-MS]  
**“Investigation of Wettability Alteration by Low Salinity Water”**  
[2011, Society of Petroleum Engineers]

61. R. A. Nasralla, SPE, Hisham A. Nasr-El-Din, SPE, Texas A&M University  
[Conference Paper, 154334-MS]  
**“Double-Layer Expansion: Is it a Primary Mechanism of Improved Oil Recovery by Low-Salinity Waterflooding?”**  
[2012, Society of Petroleum Engineers]
62. Malvern Instruments Ltd.  
[Instrument Manual]  
**“Zetasizer Nano User Manual”**  
[2012, Malvern Instrument Ltd.]
63. S. T. Dubey, P. H. Doe, Shell Development Co.  
[Journal Paper, 22598-PA]  
**“Base Number and Wetting Properties of Crude Oils”**  
[1993, Society of Petroleum Engineers]
64. J. S. Buckley, New Mexico Petroleum Recovery Research Center, New Mexico Institute of Mining and Technology  
[Article]  
**“Chemistry of the Crude Oil/Brine Interface”**  
[1994]
65. M. B. Alotaibi, SPE; R. A. Nasralla, SPE; and H. A. Nasr-El-Din, SPE, Texas A&M University  
[Journal Paper, 149942-PA]  
**“Wettability Studies Using Low-Salinity Water in Sandstone Reservoirs”**  
[2011, Society of Petroleum Engineers]
66. U. Farooq, J. Sjøblom and G. Øye, Department of Chemical Engineering, Ugelstad Laboratory, Norwegian University of Science and Technology (NTNU), and Medad T. Tweheyo, StatoilHydro R&D, Research Centre  
[Article]  
**“Surface Characterization of Model, Outcrop, and Reservoir Samples in Low Salinity Aqueous Solutions”**  
[2011, Taylor & Francis]
67. J. S. Buckley, N.R. Morrow, New Mexico Petroleum Research Center  
[Conference Paper, 20263-MS]  
**“Characterization of Crude Oil Wetting Behavior by Adhesion Tests”**  
[1990, Society of Petroleum Engineers Inc.]

68. W. Xu, Louisiana State University, Agricultural and Mechanical College  
[Master thesis]  
**“Experimental Investigation of Dynamic Interface Interactions at Reservoir Conditions”**  
[2005, Louisiana State University]
69. A. A. Abdel-Wali  
[Journal]  
**“Effect of Simple Polar Compounds and Salinity on Interfacial Tension and Wettability of Rock/Oil/Brine System”**  
[1996, King Saud University]
70. C. S. Vijapurapu, and D. N. Rao, The Craft and Hawkins Department of Petroleum Engineering, Louisiana State University  
[Article]  
**“Compositional Effects of Fluids on Spreading, adhesion and Wettability in Porous Media”**  
[2004, Elsevier]
71. A. A. Hamouda and O. Karoussi  
[Article]  
**“Effect of Temperature, Wettability and Relative Permeability on Oil Recovery from Oil-wet Chalk”**  
[2008, Department of Petroleum Engineering and University of Stavanger]
72. HACH  
[User Manual, Edition 1]  
**“Waterproof Handheld H160 and H170”**  
[2009, Hach Company]  
<http://www.hach.com>  
[downloaded 01.06.2013]
73. HACH  
[User Manual, Rev 2]  
**“H-Series Meters and Non-glass Probes”**  
[2012, Hach Company]  
<http://www.hach.com>  
[downloaded 01.06.2013]
74. W. Wang and A. Gupta, University of Oklahoma  
[Conference Paper, 30544-MSS]  
**“Investigation of the Effect of Temperature and Pressure on Wettability Using Modified Pendant Drop Method”**  
[1995, Society of Petroleum Engineers Inc.]

75. DMA – PAAR Digital Density Meters  
[Instruction Manual]  
**“DMA 60 Processing Unit”**  
[Anton PAAR]
76. S. Riisøen, Department of Chemistry, Centre of Integrate petroleum Research (CIPR),  
University of Bergen  
[Master thesis]  
**“Effect of Combined Low Salinity and Surfactant Injection on Oil Recovery in Aged  
Bentheimer Sandstones at Different Temperatures”**  
[2012, University of Bergen]
77. A.E Nymark, Department of Chemistry, University of Bergen  
[Master thesis ]  
**“Fuktegenskaper til kvartsoverflater i systemer med råolje, vann og enzymer”**  
[2010, University of Bergen]
78. B. Fosse, University of Bergen  
[Docthoral thesis ]  
**“Innverknad av Vasskjemi på Statistiske og Dynamiske Grenseflateeigenskapar til Olj- vatn og  
Olj- Vatn- Fast Stoff”**  
[1995, University of Bergen]
79. C. R. Hocott, Humble Oil and Refining Co.  
[Journal Paper, 939184-G]  
**“Interfacial Tension between Water and Oil under Reservoir Conditions”**  
[1939, The American Institute of Mining, Metallurgical, and Petroleum Engineers Inc.]
80. H. Kunh, H. D. Forsterling and D. H. Waldeck  
[book]  
**“Principles of Physical Chemistry”**  
[2009, John Willey & Sons]
81. E. Eslinger and D. Pevear  
[Book]  
**“Clay Minerals for Petroleum Geologists and Engineers”**  
[1988, SEPM Society for Sedimentary Geology]
82. <http://www.attension.com/contact-angle>  
**“Contact Angle”**  
[downloaded 01.06.2013]
83. [http://web.nmsu.edu/~snsnsm/classes/chem435/Lab14/double\\_layer.html](http://web.nmsu.edu/~snsnsm/classes/chem435/Lab14/double_layer.html)  
**“Double Layer Expansion”**  
[downloaded 01.06.2013]

84. <http://www.web-books.com/MoBio/Free/Ch2A4.htm>

**“pH – pKa”**

[downloaded 01.06.2013]

85. <http://www2.nau.edu/~doetqp-p/courses/env320/lec12/Lec12.html>

**“Clay minerals”**

[downloaded 01.06.2013]

## Appendix

The rule of significant digit < 3 in the measured uncertainty has been used to present the measured averages related to the uncertainty.

### A.1 Density Data

Measured density data for brine and oil phases are listed Table A.1.1 and A.1.2. The uncertainty is estimated based on variation in the measured data. The oil phase uncertainty is some higher than for brine phase, and can be a result of measurements performed on different days and under different room temperature that can also impact the measured densities.

Vol% SSW	pH	Density $\left[\frac{\text{g}}{\text{cm}^3}\right]$		Average $\pm$ uncertainty
		Parallel 1	Parallel 2	
100	7	1.0259	1.0270	1.0264 $\pm$ 0.0008
50		1.0130	1.0136	1.0133 $\pm$ 0.0005
10		1.0022	1.0029	1.0025 $\pm$ 0.0005
1		0.9998	1.0004	1.0001 $\pm$ 0.0004
100	3	1.02622	1.02640	1.02630 $\pm$ 0.0001
50		1.012920	1.012945	1.012932 $\pm$ 0.00002
10		1.002235	1.002214	1.002224 $\pm$ 0.00002
1		0.99973	0.99967	0.99969 $\pm$ 0.00005
100	4	1.02600	1.02611	1.02606 $\pm$ 0.00008
50		1.01264	1.01231	1.01247 $\pm$ 0.0002
10		1.0012	1.0016	1.0014 $\pm$ 0.0003
1		0.99931	0.99925	0.99928 $\pm$ 0.00004
100	10	1.02441	1.02434	1.02438 $\pm$ 0.00004
50		1.01111	1.01101	1.01103 $\pm$ 0.00003
10		1.00050	1.00038	1.00044 $\pm$ 0.00008
1		0.99783	0.99799	0.99791 $\pm$ 0.0001

**Table A.1.1:** Brine phase density data with average density and uncertainty.

Oil Phase	Density $\left[\frac{\text{g}}{\text{cm}^3}\right]$			Average Density $\pm$ uncertainty $\left[\frac{\text{g}}{\text{cm}^3}\right]$
	Parallel 1	Parallel 2	Parallel 3	
A12	0.911	0.914	0.926	0.917 $\pm$ 0.008
Exp-12	0.898	0.902	0.904	0.902 $\pm$ 0.003
Exp-12-D	0.94762	0.94752	0.94782	0.94765 $\pm$ 0.0002
Exp-X-5	0.9020	0.9023	0.8981	0.9008 $\pm$ 0.002
Exp-X-10	0.9006	0.9001	0.8967	0.8991 $\pm$ 0.002
Exp-X-20	0.8968	0.8953	0.8930	0.8950 $\pm$ 0.002
Exp-I-5	0.9213	0.9207	0.9178	0.9199 $\pm$ 0.002
Exp-I-10	0.9364	0.9399	0.9391	0.9384 $\pm$ 0.002
Exp-I-20	0.9731	0.9713	0.9741	0.9728 $\pm$ 0.001

**Table A.1.2:** Oil phase density data with average density and uncertainty.

## A.2 IFT Data

Uncertainty calculations for IFT measurements has been calculated using the uncertainty formula A.2.1.

$$\frac{\sigma_{\sigma}}{\sigma} = \frac{\sigma_V}{V} + \frac{\sigma_{\Delta\rho}}{\rho} + \frac{\sigma_r}{r} + \frac{\sigma_F}{F} \quad (\text{A.2.1})$$

Since the calculations showed,  $\frac{\sigma_{\Delta\rho}}{\rho} + \frac{\sigma_V}{V} \gg \frac{\sigma_r}{r} + \frac{\sigma_F}{F}$ , the equation A.2.1 was reduced to equation A.2.2.

$$\frac{\sigma_{\sigma}}{\sigma} \approx \frac{\sigma_{\Delta\rho}}{\rho} + \frac{\sigma_V}{V} \quad (\text{A.2.2})$$

The fractional uncertainty of density and volume had influence on the fractional uncertainty of IFT. The high influence of density was due to the high variation in the measured density data for the oil phase, it also seemed to impact the measured data more than the volume.

The IFT data are displayed in table A.2.1 – A.2.3

SSW	IFT [mN/m] – parallels					Average	$\frac{\sigma_{\sigma}}{\sigma}$ - Average
Oil	1	2	3	4	5		
Exp-X-5	16.7	16.5	16.7	16.7		16.7	0.03
Exp-X-10	16.5	16.7	16.5	16.5		16.5	
EXP-X-20	16.6	17.3	16.7	16.8		16.9	
							0.04
Exp-I-5	16.7	16.5	16.9	16.3	16.5	16.6	
Exp-I-10	16.2	16.8	16.5	17.2	17.0	16.8	
Exp-I-20	17.1	16.8	17.4	17.2		17.1	

**Table A.2.1:** Xylene and Iododecane added Exp-12 crude oil IFT data with average values and fractional uncertainty.

	Vol% SSW	IFT [mN/m] – parallels					Average	$\frac{\sigma_{\sigma}}{\sigma}$ - Average
		1	2	3	4	5		
Exp-12	100	15.5	16.0	15.8	15.7		15.8	0.05
	50	21.1	20.8	21.4	20.5	20.6	20.9	
	10	24.0	24.2	24.0	24.4	24.1	24.2	
	1	25.8	26.0	25.9	26.2		26.0	
Exp-12-D								0.05
	100	15.7	16.0	16.2	15.0	14.9	15.6	
	50	19.6	20.4	20.4	19.4	19.5	19.9	
	10	21.7	21.9	22.0	22.0		21.9	
	1	23.5	23.6	23.7	23.3		23.5	
A-12								0.09
	100	12.5	12.7	12.7			12.6	
	50	19.3	19.7	19.9	19.9		19.7	
	10	23.7	23.9	24.4			24.0	
	1	28.1	28.2	28.3			28	

**Table A.2.2:** Exp-12, Exp-12-D and A-12 IFT data with average values and fractional uncertainty.



Exp-12	Vol% SSW	IFT [mN/m] – parallels					Average	$\frac{\sigma_{\sigma}}{\sigma}$ - Average
pH		1	2	3	4	5		
3	100	25.0	25.1	25.2			25.1	0.05
	50	25.1	25.2	25.1			25.1	
	10	25.3	25.5	25.3	25.4	25.5	25.6	
	1	25.8	26.0	25.9	26.2		25.1	
4								0.03
	100	26.3	26.5	26.4	26.5		26.5	
	50	26.7	26.5	26.6			26.6	
	10	26.1	26.1	26.1			26.1	
10	1	26.9	26.9	27.0			26.9	0.08
	100	8.1	8.1	8.1			8.1	
	50	8.7	8.8	7.9	8.9		8.6	
	10	12.4	12.4	12.1	12.0		12.2	
	1	22.9	23.0	22.8			22.9	

**Table A.2.3:** IFT data between Exp-12 and brines of varying pH, and average values with fractional uncertainty.

### A.3 Zeta Potential Data

Measured zeta potential data and electrophoretic mobility data are displayed in Tables A.3.1 and A.3.2. The drop test data are displayed in Table A.3.3. The uncertainty was measured based on variation in the total 20 parallels performed for zeta potential and electrophoretic mobility measurements, and based on 10 parallels for the test data. Table A.3.4 presents the hypothetical and literature reported zeta potential data for crushed silica glass.

SSW percentage [%]	pH	Zeta Potensial [mV]					
		Solution 1		Solution 2		Average $\pm$ uncertainty	
		1 Parallel = 5 instrument parallel		1 Parallel = 5 instrument parallel			
		1	2	1	2		
1	7	-55.4	-57.2	-56.7	-57.9	$-56.8 \pm 2$	
10		-30.4	-31.7	-30.7	-31.4	$-31.1 \pm 2$	
50		-16.0	-16.1	-16.9	-16.6	$-16.4 \pm 1$	
1	3	53.8	52.8	56.7	56.1	$54.9 \pm 2$	
10		12.0	10.6	10.6	12.6	$11.5 \pm 1$	
50						<b>IEP</b>	
1	4	20.9	18.5	19.2	16.8	$18.9 \pm 2$	
10						<b>IEP</b>	
50		-11	-9	-9	-11	$-10 \pm 3$	
1	10	-65	-60	-60	-61	$-62 \pm 3$	
10		-25.8	-25.0	-25.1	-25.3	$-25.3 \pm 0.9$	
50		-13.0	-12.6	-12.2	-13,7	$-12.9 \pm 1$	

**Table A.3.1:** Zeta potential data for emulsified droplets of Exp-12 crude oil in brines of varying pH and average values with uncertainty.

Vol% SSW	pH	Electrophoretic Mobility [ $\mu\text{mcm/Vs}$ ]				
		Solution 1		Solution 2		Average $\pm$ uncertainty
		1 Parallel = 5 instrumental parallel		1 Parallel = 5 instrumental parallel		
		1	2	1	2	
1	7	-4.23	-4.10	-4.19	-4.28	$-4.20 \pm 0.1$
10		-2.25	-2.34	-2.27	-2.32	$-2.29 \pm 0.1$
50		-1.18	-1.19	-1.25	-1.23	$-1.21 \pm 0.07$
1	3	3.90	3.98	4.19	4.15	$4.05 \pm 0.1$
10		0.89	0.79	0.78	0.93	$0.85 \pm 0.1$
50						IEP
1	4	1.55	1.37	1.42	1.24	$1.39 \pm 0.1$
10						IEP
50		-0.78	-0.66	-0.68	-0.83	$-0.74 \pm 0.2$
1	10	-4.78	-4.46	-4.48	-4.47	$-4.55 \pm 0.2$
10		-1.91	-1.85	-1.85	-1.87	$-1.87 \pm 0.07$
50		-0.96	-0.93	-0.90	-1.01	$-0.95 \pm 0.1$

**Table A.3.2:** Electrophoretic mobility data for emulsified droplets of Exp-12 crude oil in brines of varying pH and average values with uncertainty.

Oil droplet test Zeta Potential [mV]			
Drops	Parallel 1	Parallel 1	Average $\pm$ Uncertainty
1	30.8	28.5	$29.7 \pm 2$
2	29.9	32.7	$31.3 \pm 2$
3	31.0	29.9	$30.5 \pm 1$

**Table A.3.3:** Zeta potential data for oil droplet test with average values and uncertainty.

Silica surface Zeta Potential [mV]				
	Littertaure reported <sup>[17]</sup>		Hypothetic values	
Concentration	pH 4	pH 7	pH 4	pH 7
1%	~-40.0	~-70.0	-20.0	-50.0
10%	~-30.0	~-40.0	-15.0	-20.0
50%	-20.0*	-25.0*	-10.0	-12.5

**Table A.3.4:** Hypothetic and literature reported zeta potential data for silica surface  
\*Hypothetic value

#### A.4 Contact Angle Data

Contact angle data are presented in Table A.4.1 – A.4.6. The average angle and uncertainty was measured based on variation in both left and right angles.

Oil	Contact Angle [°] System: Exp-12 + Xylene/SSW												
	Left					Right					Average Angle ± Uncertainty		
	Parallel										Left	Right	Left and Right
	1	2	3	4	5	1	2	3	4	5			
Exp-X-5	25.8	25.5	21.9	25.0	20.1	22.5	22.0	20.0	23.0	21.0	24 ± 3	21.7 ± 1	22.7 ± 2
Exp-X-10	23.0	24.2	22.0			25.3	23.0	22.0			23.1 ± 1	23.4 ± 2	23.3 ± 1
Exp-X-20	27.0	26.0	25.0	23.0		24.0	26.9	25.5	27.0		25.3 ± 2	25.9 ± 1	25.6 ± 1

**Table A.4.1:** Contact angle data for Xylene added crude oils and average angles with uncertainty.

Oil	Contact Angle [°] System: Exp-12 + Iododecane/SSW											
	Left Angle				Right Angle				Average Angle ± Uncertainty			
	Parallel								Left	Right	Left and Right	
	1	2	3	4	1	2	3	4				
Exp-I-5	15.0	16.0	17.0		14.0	17.0	19.0		16.0 ± 1	17 ± 3	16.4 ± 2	
Exp-I-10	19.8	19.0	19.8		18.8	18.4	23.9		19.5 ± 0.5	20 ± 3	20.0 ± 2	
Exp-I-20	20.9	20.0	24.1		20.3	19.9	20.0		21.7 ± 2	20.1 ± 0.2	20.9 ± 2	

**Table A.4.2:** Contact angle data for Iododecane added crude oils and average angles with uncertainty.

Vol% SSW	Oil	Contact Angle [°]												
		Left Angle					Right Angle					Average Angle ± Uncertainty		
		Parallel										Left	Right	Left and Right
		1	2	3	4	5	1	2	3	4	5			
1	A-12	16.0	15.0	15.0			17.0	17.0	15.0			15.3 ± 0.6	16.3 ± 1	15.8 ± 1
10	A-12	16.2	16.0	15.9	17.3	17.0	15.0	17.0	15.0	15.0	18.0	16.5 ± 0.6	16.0 ± 1	16.2 ± 1
50	A-12	17.9	17.3	18.5	19.5		17.0	17.0	19.0	18.0		18.3 ± 0.9	17.8 ± 1	18.0 ± 0.9
100	A-12	23.2	22.0	22.3	21.9		21.0	22.1	23.2	19.0		22.4 ± 0.6	21.3 ± 2	21.8 ± 1
1	Exp-12	16.9	16.0	19.0			17.2	15.5	16.9			17.3 ± 2	16.5 ± 0.9	16.9 ± 1
10	Exp-12	16.3	18.0	16.8			17.3	18.0	16.0			17.0 ± 0.9	17.1 ± 1	17.1 ± 0.8
50	Exp-12	17.5	21.0	22.0	21.3	16.3	20.0	18.3	17.9	21.9	18.0	20 ± 3	19.2 ± 2	19.4 ± 2
100	Exp-12	15.5	16.0	20.3	20.9		15.8	16.0	18.0	21.0		18 ± 3	17.7 ± 2	17.9 ± 2
1	Exp-12-D	21.3	18.0	21.8			18.0	18.0	22.0			20.4 ± 2	19.3 ± 2	19.9 ± 2
10	Exp-12-D	23.5	19.1	19.3			24.8	18.0	19.8			20.6 ± 2	21 ± 4	21 ± 3
50	Exp-12-D	20.2	17.0	17.0			17.9	21.0	18.5			18.1 ± 2	19.1 ± 2	18.6 ± 2
100	Exp-12-D	23.3	23.0	20.1	21.3	24.0	21.0	20.0	19.0	20.0	22.5	22.3 ± 2	20.5 ± 1	21.4 ± 2

**Table A.4.3:** Contact angle data for A-12, Exp-12 and Exp-12-D crude oil with average angles and uncertainty.

pH	Vol% SSW	Contact Angle [°] Adhesion test (Non-Equilibrated system)												
		Left Angle					Right Angle					Average Angle ± Uncertainty		
		Parallel										Left	Right	Left and Right
		1	2	3	4	5	1	2	3	4	5			
3	1	31.8	33.0	33.8	35.0	32.0	32.3	33.0	33.5	34.0	30.0	33.1 ± 1	32.6 ± 2	32.8 ± 1
3	50	29.8	27.6	21.0	22.3		27.0	29.0	24.7	23.0		25 ± 4	26 ± 3	26 ± 3
3	100	25.7	24.8	23.5	28.5	27.9	28.5	26.0	24.5	28.0	28.6	26.1 ± 2	27.1 ± 2	26.6 ± 2
4	1	26.0	25.3	26.5	30.2	30.0	27.5	26.5	28.0	29.4	29.5	27.6 ± 2	28.2 ± 1	27.9 ± 2
4	10	23.9	21.0	23.3	22.8	22.0	25.3	22.3	22.1	22.5	22.3	22.6 ± 1	22.9 ± 1	22.7 ± 1

**Table A.4.4:** Contact angle adhesion test for Exp-12 oil non-equilibrated system, with average angles and uncertainty

pH	Vol% SSW	Contact Angle [°] - Adhesion test (Equilibrated system)												
		Left					Right					Average ± uncertainty		
		Parallel										Left	Right	Left and Right
		1	2	3	4	5	1	2	3	4	5			
3	1	33.5	35.0	33.5			32.9	35.0	30.6			34.0 ± 1	32.8 ± 2	33.4 ± 2
4	1	28.5	28.0	28.5			31.0	29.1	29.0			28.3 ± 0.3	29.7 ± 1	29.0 ± 1
4	50	25.0	24.0	22.0			23.2	25.1	22.0			23.7 ± 2	23.4 ± 2	23.6 ± 1

**Table A.4.5:** Contact angle adhesion test for Exp-12 oil equilibrated system, with average angles and uncertainty



Oil	Contact angle [°] Buckley washing procedure test System: Oil/SSW												
	Left					Right					Average ± uncertainty		
	Parallel										Left	Right	Left and Right
	1	2	3	4	5	1	2	3	4	5			
Exp-12-D	20.9	21.0	22.8			18.0	19.1	22.0			21.6 ± 1	19.7 ± 2	20.6 ± 2
Exp-12	16.0	17.0	16.0			15.0	16.3	18.0			16.3 ± 0.6	16.4 ± 2	16.4 ± 1
A-12	19.5	22.3	22.8	18.3		20.1	23.0	23.0	20.1		20.7 ± 2	21.6 ± 2	21.1 ± 2

**Table A.4.6:** Contact angle washing procedure test

**A.5 pH Data** - pH meter uncertainty  $\pm 0.1$

Vol% SSW	pH	Modified pH	Measured pH 24h equilibrated o/w system	Measured pH Water phase with 24h equilibrated glass	Measured pH Water phase with 48h equilibrated glass	$\Delta$ pH o/w system	$\Delta$ pH 24 h equilibrated glass	$\Delta$ pH 48 h equilibrated glass
1	<b>3</b>	3.03	3.31	2.86	2.93	0.28	-0.17	-0.10
10		3.04	3.17	2.91	3.02	0.13	-0.13	-0.02
50		3.03	3.16	2.85	2.95	0.13	-0.18	-0.08
100		3.04	3.28	2.89	2.99	0.24	-0.15	-0.05
1	<b>4</b>	4.00	4.16	3.99	4.05	0.16	-0.01	0.05
10		3.99	4.69	3.89	3.98	0.70	-0.10	-0.01
50		4.03	4.39	4.21	4.18	0.36	0.18	0.15
100		4.00	4.54	4.02	4.15	0.54	0.02	0.15
1	<b>7</b>	6.90	6.64	6.67	6.77	-0.26	-0.23	-0.13
10		7.23	6.95	7.18	6.96	-0.28	-0.05	-0.27
50		7.67	7.42	7.76	7.70	-0.25	0.09	0.03
100		7.78	7.65	7.80	7.74	-0.13	0.02	-0.04
1	<b>10</b>	10.06	8.46	8.67	7.29	-1.60	-1.39	-2.77
10		10.09	9.10	9.71	9.72	-0.99	-0.38	-0.37
50		10.16	8.95	9.29	9.03	-1.21	-0.87	-1.13
100		10.12	8.96	8.87	8.63	-1.16	-1.25	-1.49

**Table A.5.1:** One set of manipulated pH values and measured pH in the brine phase after equilibrium/aging processes with oil and glass.

